ABSTRACT

Title of Dissertation:	CHROMATIN CONTROL OF PAPILLOMAVIRUS INFECTION
	Samuel Porter, Doctor of Philosophy, 2020
Dissertation directed by:	Dr. Alison McBride, DNA Tumor Virus Section, Laboratory of Viral Diseases, National Institute of Allergy and Infectious Diseases, National Institutes of Health

The genomes of papillomaviruses are packaged into chromatin throughout the entire viral lifecycle. A peculiar feature of papillomaviruses genome organization is that the viral DNA is associated with host histones even inside the virion particle. However, little is known about the nature of the epigenome within papillomavirions, or its biological impact on early infection. Here, we use three approaches to study the epigenome of papillomavirions. Papillomaviruses can be assembled in packaging cells by expression of the capsid proteins in the presence of the viral genome. We have optimized and manipulated this process to generate viruses with replicated and genetically modified virion DNA and have used these "quasivirions" to evaluate early infection of primary human keratinocytes. We have also profiled the histone modifications on chromatin extracted from native virions isolated from human and bovine warts. We find that, compared to host cells, the viral chromatin is enriched in histone modifications associated with transcriptionally active chromatin (including

histone acetylation), and depleted in those associated with transcriptional repression. To examine the biological role of histone acetylation in the early virus lifecycle, we produced HPV quasivirions with highly acetylated chromatin by assembling the virions in cells treated with histone deacetylase inhibitors. We show that acetylation of viral chromatin results in a reduction of early viral transcription in primary keratinocytes indicating that the histone modifications on virion chromatin do influence the early stages of infection. Collectively, these studies demonstrate that histone modifications on virion chromatin are important for the HPV infectious cycle.

CHROMATIN CONTROL OF PAPILLOMAVIRUS INFECTION

by

Samuel Stephen Porter

Dissertation submitted to the Faculty of the Graduate School of the
University of Maryland, College Park, in partial fulfillment
of the requirements for the degree of
Doctor of Philosophy
2020

Advisory Committee:
 Jeffery DeStefano, PhD, Chair
 Alison McBride, PhD, Co-chair
 Georgiy Belov, PhD
 James Culver, PhD
 Margaret Scull, PhD

Dedication

This dissertation is dedicated to my parents, brother, and sister, who have given me

endless love and support. Without them I would have never had the opportunity to

succeed and I will be eternally grateful for everything they have done for me.

Acknowledgements

I would like to express absolute gratitude to the former and current members of the DNA Tumor Virus Section, NIAID. Foremost, my mentor, Dr. Alison McBride. It is difficult to put into words just how much I have learned from her, not only as a rigorous, thoughtful scientist, but as a compassionate human being who values doing things and treating people the right way. Her laboratory reflects these principles; I can say without a doubt the incredible people here have become my very best friends.

To Dr. Tami Coursey and Alix Warburton, thank you for always answering my questions, entertaining my wild ideas, and being caring friends. To Ashley Della Fera, for going through the gauntlet that is graduate school with me and always being there to talk. To Dr. Simran Khurana and Dan Chen for countless instances of scientific and technical assistance, which have saved me more than once.

Dr. Koenraad Van Doorslaer, I owe a debt of gratitude for your scientific guidance and emotional support over the years. Warda Arman, thanks for being the best person to share a bench and desk with.

Thank you to the members of my dissertation committee: Dr. Jeffery DeStefano, Dr. Georgiy Belov, Dr. James Culver, and Dr. Margaret Scull for thoughtful guidance, new ideas, and helpful feedback.

Lastly, thank you to Catherine Redmond and Margarita Brovkina for being the best friends I could possibly ask for.

Table of Contents

List of Tables

List of Figures

List of Abbreviations

ATP Adenosine triphosphate

ATR Ataxia telangiectasia and Rad3-related serine/threonine kinase

ATRX Alpha thalassemia/mental retardation syndrome X-linked

BPV Bovine Papillomavirus

Brd4 Bromodomain-containing protein 4

CBP CREB binding protein

ChIP Chromatin immunoprecipitation

CREB cAMP response element-binding

Daxx Death-domain associated protein 7

DDR DNA damage response

DMEM Dulbecco's Modified Eagle medium

DNA Deoxyribonucleic acid

DBPS Dulbecco's phosphate-buffered saline

DTT Dithiothreitol

E2BS E2 binding site

EGF Epidermal growth factor

ER Endoplasmic reticulum

EtOH Ethanol

FBS Fetal bovine serum

HAT Histone acetyltransferase

HDAC Histone deacetylase

HFK Human foreskin keratinocyte

HMT Histone methyltransferase

HPI   Hours post infection

HPV   Human Papillomavirus

HSPG   Heparin sulfate proteoglycan

MOI   Multiplicity of infection

MHC   Major histocompatibility complex

NCS   Newborn calf serum

n.s.   Not significant

ORF   Open reading frame

PAGE   Polyacrylamide gel electrophoresis

PBS   Phosphate buffer saline

QsV   Quasivirus

RNA   Ribonucleic acid

SDS   Sodium dodecyl sulfate

SD   Standard deviation

Sp100   Speckled protein of 100 kilodaltons

SV40   Simian vacuolating virus 40

TBP   TATA-binding protein

TCA   Tricholoroacetic acid

URR   Upstream regulatory region

VGE   Viral genome equivalents

VLP   Virus-like particle

WT   Wildtype

Chapter 1: Introduction

Papillomaviruses

Classification

Papillomaviruses are an ancient group of viruses that have evolved alongside their host for at least 300-600 million years [1]. Before *Homo sapiens* emerged as a distinct species, they were likely already infected with papillomaviruses. All papillomaviruses belong to the family *Papillomaviridae* that is further subdivided into *Firstpapillomavirinae* and *Secondpapillomavirinae*. While the latter only has one genus, *Firstpapillomavirinae* can be further organized into genera; generally viruses with 60% or greater similarity of the nucleotide sequence of the L1 gene are considered part of the same genus [2]. Five of these genera contain papillomaviruses that infect humans (Alpha-, Beta-, Gamma-, Mu-, and Nupapillomavirus) and are known as HPVs. Bovine papillomavirus, used as a model for much of the foundational work in the field, belongs to the Deltapapillomavirus genus. Papillomaviruses that share between 71-89% L1 sequence identity are further grouped together into species. Viruses are further separated into types that share 90% or more identity in the L1 gene [3, 4].

In the HPV field, a virus is designated as an official reference type once the complete sequence has been submitted to, and validated by, the HPV Reference Center in Sweden. To date, there are 225 officially recognized HPV types, although

there are many more non-reference types catalogued by the Papillomavirus Episteme database [5, 6].

Medical Relevance and Public Health Impact

Infection by HPV is a significant public health burden in the United States and around the world. It is the most common sexually transmitted infection in the United States, with approximately 14,000,000 new infections each year [7]. Most infections are asymptomatic or cause relatively minor diseases such as genital warts (Table 1.1), and 90% of these infections are cleared within two years [8-10]. However, persistent infections with high-risk HPV types (16, 18, 31, 33, 35, 39, 45, 51, 52, 56, 58, 59 and 66) are associated with the development of several different types of cancer [11]. HPV is the etiological agent of nearly all incidences of cervical cancer. For women, cervical cancer is the second deadliest cancer worldwide; each year 240,000 succumb to the disease. This morbidity is of particular concern in the developing world, where about 80% of new cases occur.

In recent years a rapidly growing body of evidence implicates HPV infections in a number of other cancers. In 2015, HPV was shown to be associated with 91.1% of anal, 75.0% of vaginal, 70.1% of oropharyngeal, 68.8% of vulvar, 63.3% of penile, 32.0% of oral cavity, and 20.9% of laryngeal cancers [12]. In particular, the rise of head and neck cancers in men has reached near epidemic proportions in the last two decades [13].

Table 1.1. Diseases Associated with HPV Infection. [10, 14]

Disease	Commonly Associated HPV Types
Common warts	2, 4, 7
Plantar wart	1, 2, 4
Oral warts	2, 4
Anogenital warts	6, 11, 42, 43, 44, 45, 51, 52, 54, 61, 72, 81, 89
Nonmelanoma skin cancer	8, 15, 20, 23, 36, 38
Oropharyngeal cancer	16, 18
Oral cancer	2, 6, 7, 11, 16, 18, 32, 57
Intraepithelial neoplasias	16, 18, 31, 33, 35, 39, 42, 44, 45, 51, 52, 53, 56, 58, 59

The greatest success in reducing the public health impact of HPV infection has been prophylactic vaccination. In 2006, the first vaccine against HPV infection (marketed as Gardasil) was approved by the FDA, and protected against HPV types 6, 11, 16, and 18. The vaccine is comprised of virus-like-particles (VLPs) consisting of the L1 protein for each of the four HPV types [15]. Since then, two more vaccines have been approved. Cervarix, that provides protection against HPV 16 and 18, was approved in 2009. Gardasil 9, the vaccine currently in use in the United States, was approved in 2014 and protects against five additional HPV types (31, 33, 45, 52, and 58). Overall, HPV vaccines are incredibly safe and effective, with efficacies well over 90% for both males and females [16-18]. Vaccinees are effectively protected against cervical cancer, and in countries where vaccine uptake is high, a drastic reduction in rates of cervical precancer has been reported [19].

Unfortunately, the situation in the United States is not as positive. As of 2018, only half of American adolescents were up to date on their HPV vaccinations [20].

The main factors influencing the low vaccination rate have been reported to be financial burden and negative perceptions of the vaccines by parents of patients [21]. Without a substantial increase in vaccine uptake, HPV infection and its associated diseases will remain a major public health burden in the United States for the foreseeable future. In the developing world, the high cost of the vaccine prevents a global approach to the reduction of new HPV infections [22].

Papillomavirus Biology

Virions

Papillomavirus particles are non-enveloped, icosahedral capsids with T=7d symmetry (Figure 1.1) [23]. Virions are comprised of the two structural proteins encoded in the late region of the genome: the L1 (major) and L2 (minor) capsid proteins. Each capsid consists of 360 individual L1 molecules arranged into 72 pentamers (also known as capsomers). Although not strictly required for assembly, virions have an undefined number of L2 molecules (generally believed to be between 12 and 72 per particle) [24, 25]. The virions are approximately 55 nm in diameter [23]. The capsids are stabilized by intracapsomeric disulfide bonds, which make them resistant to chemical and enzymatic degradation [26-28].

The capsid contains a covalently closed circular DNA genome that is organized into nucleosomes comprised of host cellular histones H2A, H2B, H3, and H4 [29]. This feature is relatively novel amongst DNA viruses that infect humans as *Polyomaviridae* are the only other family of DNA viruses in this category known to package their genome with host histones [30].
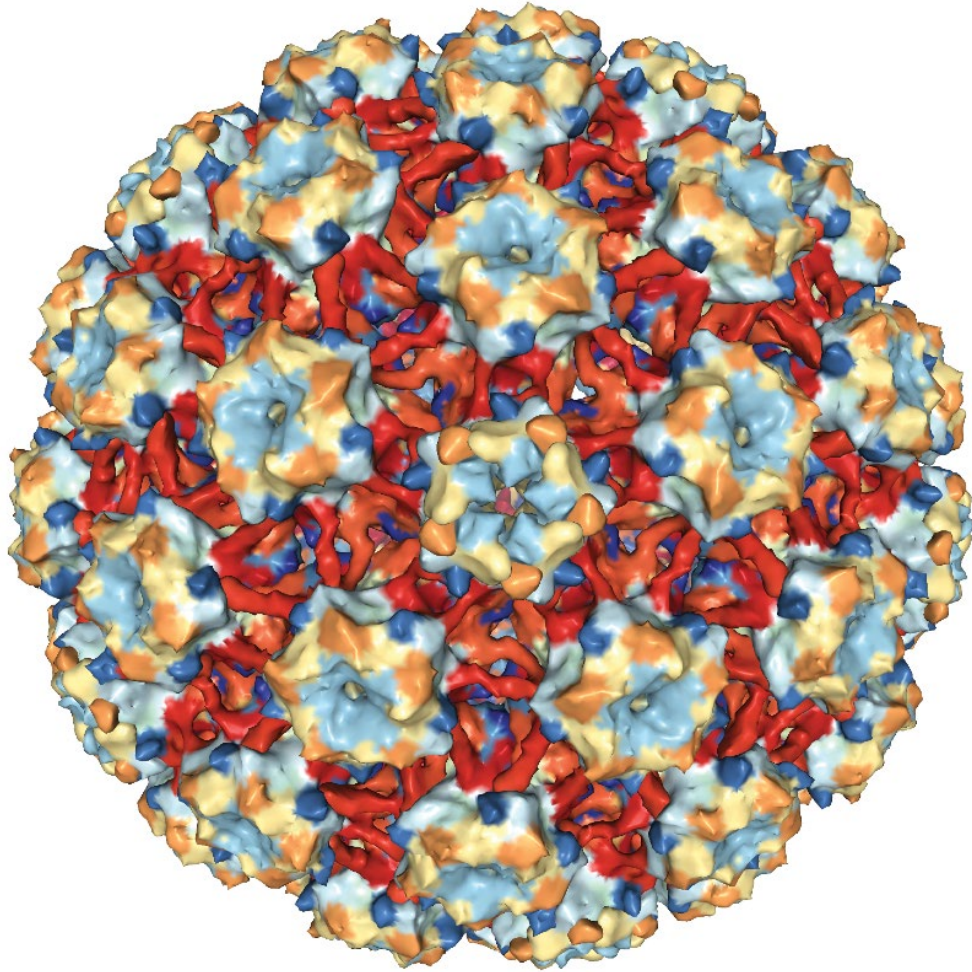
Figure 1.1. Structure of the HPV16 L1 capsid. Cryo-electron microscopy was used to determine the structure of an HPV16 capsid, created from the PDB structure 3J6R [31]. The HPV virion is comprised of 360 molecules of the major structural protein L1 arranged into 72 pentamers known as capsomers. Full virions also contain an undetermined number of molecules of L2, the minor capsid protein (not shown). Adapted from [32].

Genome

Papillomaviridae have small, circular, double stranded DNA genomes

(approximately 8 kb in length) that are generally highly conserved across genera

(Figure 1.2). The viral genome is organized into three main parts. The early region

encodes proteins expressed in early and maintenance phases of the lifecycle. The late

5

region encodes the proteins expressed during the late lifecycle. The E4 protein, despite being encoded in the early region, is also expressed during the late lifecycle. The upstream regulatory region (URR) (sometimes known as the long control region or LCR) contains regulatory elements that modulate viral transcription, replication, and genome partitioning.
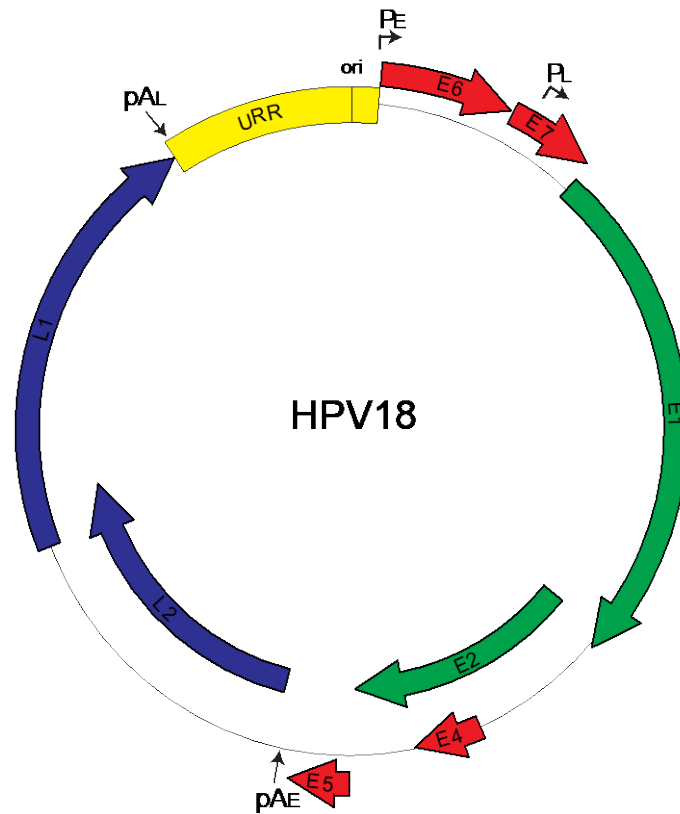
Figure 1.2. HPV18 Genome. Alpha-HPVs have circular, double stranded DNA genomes of approximately 8,000 base pairs. The upstream regulatory region (URR) is shown in yellow, with the origin of replication as a thin black bar. The early (P_E) and late (P_L) promoters are indicated by arrows at right angles. The early (A_E) and late (A_L) polyadenylation sites are indicated by straight black arrows. The early viral replication protein ORFs are colored in green and the late structural proteins in blue. The E4, E5, E6, and E7 genes are shown in red. Adapted from [33].

All papillomavirus genomes have four conserved open reading frames (ORFs), encoding two replication proteins (the replicative helicase E1 and the helicase loader/master regulator E2) and two structural proteins (L1 and L2). HPV genomes also encode two spliced transcripts, for the viral repressor E8^E2 and the intermediate protein E1^E4. Most HPV types also express additional early proteins E6 and E7, which have oncogenic properties in the high-risk HPV types (Reviewed in [34]).

All viral mRNAs are transcribed from the same strand of DNA. Early transcripts are transcribed from the early promoter located in the URR and terminate at the early polyadenylation site. Late viral genes are expressed from the late promoter (located inside the E7 ORF) and terminate at the late polyadenylation site. There is an additional class of transcripts known as intermediate transcripts where transcription initiates from the late promoter and terminates at the early polyadenylation site [35, 36]. Other promoters in the early region have also been reported [37]. Papillomaviruses use these genomic elements to synthesize a diverse range of polycistronic transcripts and can generate additional coding diversity from alternative splicing.

Host and Tissue Tropism

All papillomaviruses are extremely trophic for their host species and the tissues that they infect. HPVs specifically infect human mucosal and cutaneous keratinocytes. Their trophic nature is possibly due to a keratinocyte-specific transcriptional enhancer in the URR [38, 39]. Furthermore, different HPV types replicate in specific regions of the host epithelium.

Lifecycle

The lifecycle of HPV is intricately entwined with the host keratinocyte differentiation program. The epithelium is the largest organ in the body and is continuously self-renewing. A single layer of dividing basal keratinocytes renew the epithelium by replicating by asymmetrical mitosis. After division, one cell remains a basal cell, while the other daughter becomes suprabasal and begins to differentiate, stopping cell cycle progression [40, 41]. As the cell progresses upward through the epithelium, it undergoes drastic global changes to its physiology. Consequently, the HPV lifecycle is divided into multiple stages (Figure 1.3) that are temporally and spatially regulated by the differentiation status of the infected keratinocyte (Figure 1.4).
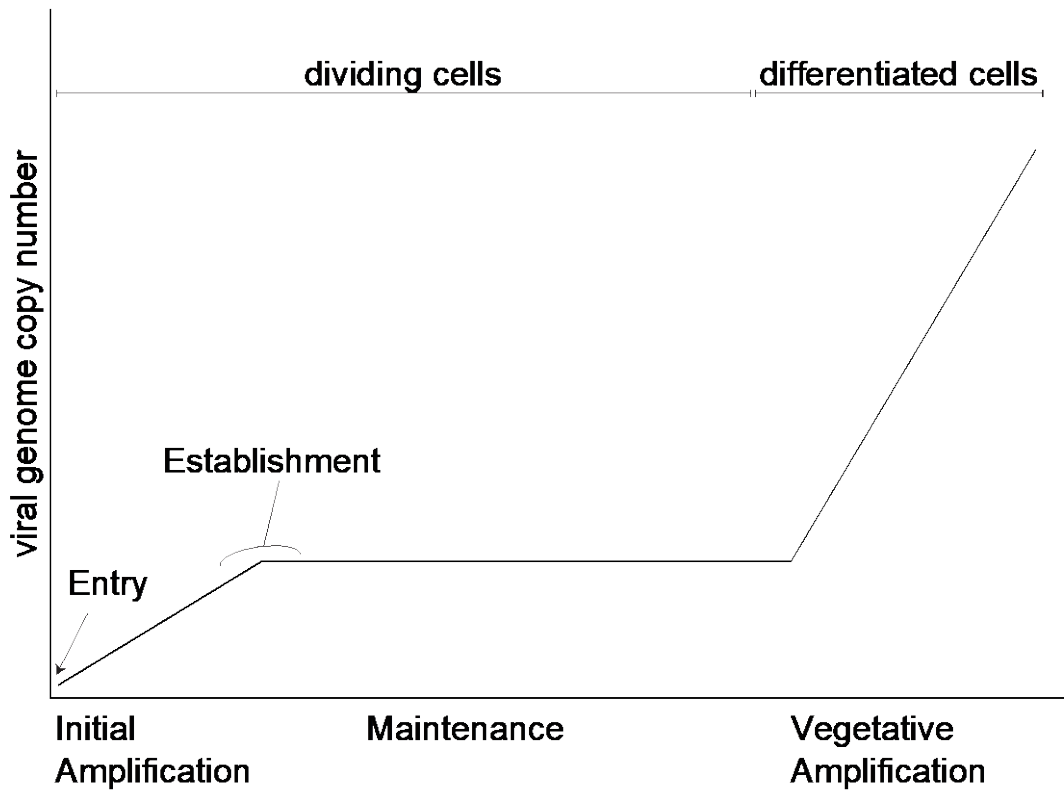
Figure 1.3. Three phases of HPV genome replication. After HPV enters the nucleus, it amplifies its genome to a low copy number and establishes a persistent infection where the genome is maintained as an extrachromosomal element that is faithfully passed to daughter cells in each division. As the infected cell begins to differentiate, the viral genome is replicated to a high level in preparation for the production of progeny virions. Adapted from [42].
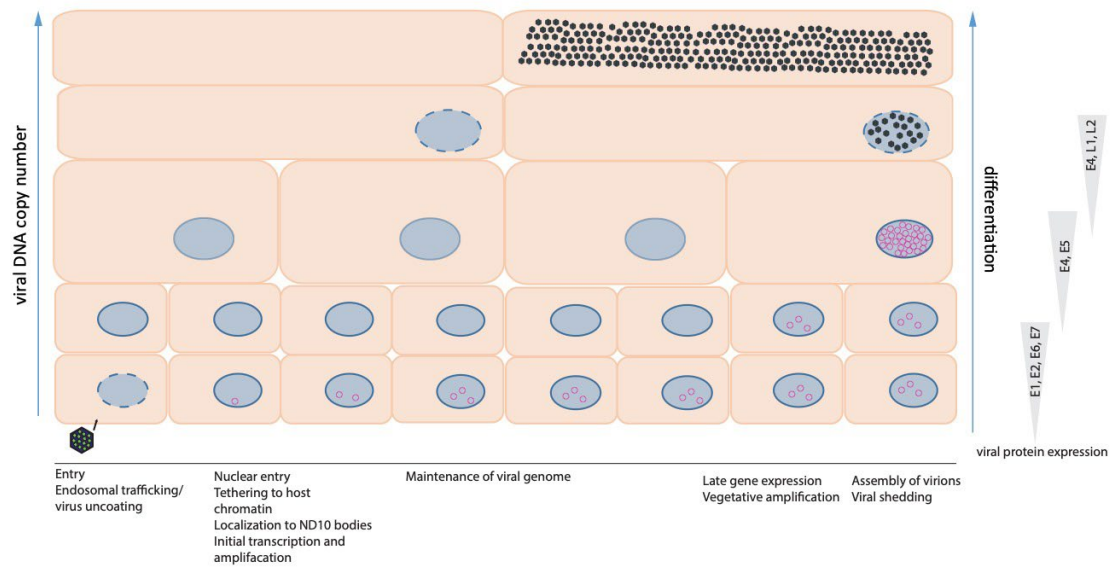
Figure 1.4. Differentiation dependent lifecycle of HPV. Virions gain access to basal keratinocytes through microabrasions in the host epithelium. After entry, the virus partially uncoats and is trafficked to the nucleus in an endosome. The vesicle gains access to the nucleus after breakdown of the nuclear envelope during mitosis. Once the cell cycle is complete, the virus escapes the vesicle and begins transcribing its early genes. The viral genome is replicated to a low copy number and establishes a persistent infection. As the infected cell divides, the viral genome is passed on to the daughter cells by tethering to the host chromatin. Once the keratinocyte begins to differentiate, the viral genome is replicated to high copy number and the viral late, structural genes are transcribed and progeny virions are assembled. Adapted from [43].

Attachment and Entry

The HPV infectious cycle begins when a virion infects a basal keratinocyte through microabrasions in the host epithelium. Virions can come into contact with keratinocytes in the upper layer of the skin, but cannot initiate a productive infection in these cells, as only basal keratinocytes divide in a stratified epithelium. Only dividing cells undergo mitosis, during which nuclear envelope breakdown occurs, a process that is essential for nuclear entry and initiation of the early infectious cycle [44].

The virion first interacts with the extracellular matrix through L1-mediated contact with heparin sulfate proteoglycans (HSPGs) expressed on the basement membrane. Primarily, HPVs use syndecan-1 as the attachment point; its expression is highest in keratinocytes compared to other cells, and it is upregulated as the epithelium recovers from wounds such as microabrasions [45]. HPVs have also been shown to bind to laminin-332 as a transient binding receptor [46]. After attachment to the HSPGs, the virion undergoes a conformational change that exposes L1 to cleavage by the serine protease Kalilkrein-8 (KLK8) [47]. After L1 cleavage, cyclophilin B exposes an epitope of L2 known as RG-1 (consisting of residues 17-36) to cleavage by furin [48-51]. Furin cleavage of L2 facilitates the transfer of the virion from the HSPG molecule to a still-unknown secondary receptor [52, 53]. Various studies have identified several possibilities for this receptor including CD63. While the literature remains inconclusive on the exact identity of the receptor that triggers endocytosis, there is consensus that the signaling cascade involves EGFR signaling [54]. Recent evidence has identified the Src-related kinase Abl2 as a crucial

12

downstream component and that viruses enter the cell in an asynchronous manner through actin-dependent, clathrin and lipid-interdependent endocytosis [55, 56].

In the endosome, a combination of low pH and cyclophilin B removes L1 capsomeres from the L2-DNA viral subparticle [51]. Here, γ-secretase cleaves and promotes the insertion of L2 into the membrane [57]. Transmembrane L2 recruits and binds to the retromer, a cytoplasmic endosomal coat complex normally involved in exporting cellular transmembrane proteins from the endosome to the trans-Golgi network (TGN) or plasma membrane. L2-retromer association redirects the virus-containing endosome to the TGN [58-60]. Transmembranous L2 in the late endosome also binds to the cellular proteins SNX17 and SNX27 to direct vesicle trafficking through the cytoplasm [61, 62]. The virus remains in the lumen of the ER during interphase [63]. After transiting through the TGN, the DNA-L2 complex enters the nucleus only after nuclear membrane breakdown during mitosis and remains encased in a membrane vesicle until the nuclear envelope reforms at the next stage of the cell cycle [44, 64-66].

Early Nuclear Activities

Once the nuclear membrane reforms, the L2-viral genome complex escapes the membrane vesicles and colocalizes with nuclear elements called nuclear domain 10 (ND10) bodies [67]. L2 rearranges the components of the ND10 bodies, including displacing the restriction factor Sp100 [68-70]. At this point, the early viral promoter drives transcription of the early viral genes using the host transcriptional machinery. Among these genes are the viral replication proteins E1 and E2. E1 is the major replication protein and functions as a replicative helicase [71]. E2, a multifunctional

protein, functions in replication as the helicase loader [72]. E1 and E2 cooperatively bind their respective binding sites on the viral genome at the origin of replication. Binding induces a conformational shift that displaces E2, and recruits additional E1 molecules to form a functional double hexamer helicase to unwind the viral DNA bidirectionally [73-76]. E1 then recruits cellular DNA replication machinery to bind and process the template during S-phase [77-79]. The HPV genome is replicated to a low copy number per cell [80].

Maintenance Replication

As the infected basal cell divides, the HPV genome is replicated along with the cellular genome. The virus must ensure its genome is partitioned into each daughter cell to maintain a persistent infection [81]. To accomplish this, the E2 protein binds to E2 binding sites on the viral genome and, through protein-protein interactions (using a cellular protein, such as Bromodomain containing protein 4 (Brd4)), tethers the viral genome to host mitotic chromosomes [82-84]. The specific region of the chromosome to which the E2-genome complex binds varies and is dependent on the HPV type [85]. This binding ensures the virus is partitioned to, and maintained in, approximately equal numbers in daughter cells, perpetuating persistent infection.

Vegetative Viral Genome Amplification

When infected basal cells detach from the basement membrane, they begin to undergo differentiation. HPV E6 and E7 protein activities dysregulate the normal differentiation program and block the exit from the cell cycle. These cells progress

14

through S phase and into a G2-like phase that contains cellular factors conducive for vegetative viral DNA replication [86, 87]. In these upper layers of the epithelium, the virus switches from its maintenance replication program to a productive viral genome amplification phase and the viral late promoter is activated, triggering the expression of the late genes L1 and L2 [88-90]. This replication occurs in distinct nuclear foci containing the viral E1 and E2 replication proteins, high levels of HPV DNA, and several other cellular factors [91, 92]. The process activates the cellular DNA damage response (DDR), whose components are hijacked by the virus to faithfully replicate its DNA outside of the S-phase in a recombination dependent manner [93-95].

Virion Assembly and Viral Shedding

Progeny virions are assembled in the highly differentiated cells [72, 96, 97].. L1 and L2 contain nuclear localization sequences and are translocated to the nucleus after synthesis [98, 99]. The minor capsid protein L2, through an interaction with E2, recruits L1 to promonocytic leukemia protein (PML) bodies (also known as nuclear domain 10 or ND10 bodies) through a direct protein-protein interaction [100, 101], though it is not clear whether this interaction is important at early or late stages of infection Then, L1 and L2 assemble around viral DNA to form infectious particles [100]. VLPs can be assembled from L1 alone (Figure 1.1), but L2 enhances the affinity for viral DNA [102, 103]. The incorporation of the viral genome into the capsid is not well understood, but it is thought that packaging is not sequence specific, as no packaging signals have been found in the viral genome [104-106]. HPV may instead use a size discrimination system to selectively incorporate its own genome over other double stranded DNAs present in the nucleus [104].

After assembly, the redox gradient present in the cornified layers of epithelium promotes intermolecular disulfide bonds between L1 molecules, allowing the capsid to fully mature [107]. As the infected cells rise to the cornified layer of the epithelium, they begin to die. Through a complex process mediated in part by release of a cascade of proteases, the corneocytes are shed into the environment in a process known as desquamation [108]. It is here that the nascently formed infectious virions are released and can encounter a new host to infect and begin the infectious cycle again.

Functions of Viral Proteins

In addition to initiating HPV replication, E1 activates the host cellular DDR pathways [109]. E1 works with E2 to recruit the DNA repair machinery to sites of viral replication [110]. In differentiated cells, viral hijacking of the ATM and ATR DDR pathways is required for vegetative amplification of the genome [111]. High concentrations of nuclear E1 are toxic to cells. To mediate this toxicity, E1 is transported out the nucleus when it is not needed for active genomic replication [112]. The E2 protein contributes to nearly all aspects of the viral lifecycle; it is involved in replication, transcription, and tethering of the viral genome. In viral genome replication, it functions to assist in the loading of the E1 helicase onto its sequence-specific binding site through complex formation, as the binding affinity of E1 alone to its target sequence is significantly weaker [74, 113-115]. Additionally, E2 displaces nucleosomes from the viral genome and recruits the cellular DNA replication machinery to HPV DNA [116].

16

E2 is also known as the master transcriptional regulator of papillomaviruses; it binds to locations on the viral DNA known as E2 binding sites (E2BSs) and has been shown to recruit both active and repressive cellular transcriptional factors to the viral genome [117-122]. E2 can also repress transcription by interfering with the binding of cellular transcription factors to the viral genome [123]. Many factors govern whether E2 regulation of transcription is activating or repressive. E2 expression levels in the cell can govern whether E2 activates or represses transcription; E2 is initially activating at low concentrations, but becomes repressive once additional E2 proteins are synthesized [124]. Lastly, E2 is known to recruit cellular machinery to manipulate the viral chromatin, providing another way to regulate viral transcription [125].

Papillomaviruses express the E4 gene as a spliced transcript, that encodes the first few codons from E1 joined to the E4 ORF to form a protein known as E1^E4 [126]. E1^E4 is a small protein mostly found in the cytoplasm. It is expressed during the intermediate or late phases of the viral life cycle, correlating with the start of productive viral DNA replication, although its exact role in viral genome replication is still not fully understood [127]. In infected cells, E1^E4 is the most abundant protein in the cell during the late lifecycle of HPV [128]. E1^E4 interacts with a range of cellular proteins, including sequestering cyclin and cyclin dependent kinases to induce G2/M cell cycle arrest [129, 130]. Additionally, E1^E4 aids in the release of progeny virions by binding to and destabilizing cornified cell envelopes and keratin filaments [131].

Alpha-HPVs encode E5, a small, hydrophobic membrane protein with oncogenic properties. Their major function is to increase the proliferation of infected

cells by intensifying the signal capacity of the epidermal growth factor receptor (EGFR) pathway [132, 133]. E5 also impedes host cell immune signaling in a multitude of ways. E5 binds to and blocks HLA-I from trafficking to the cell surface for antigen presentation and inhibits the maturation of MHC class II [134-136]. E5 also interacts with the 16K subunit of the V-ATPase, impairing cell to cell communication [137, 138]. An additional role for E5 is to aid in the egress of progeny virions by inducing koilocytic vacuoles in the nucleus of infected cells [139].

The E6 oncoprotein is comprised of two zinc finger domains that bind to a multitude of cellular proteins which have helical, acidic LxxLL motifs [140]. Most notably, E6 interaction with cellular E6 attachment protein (E6AP) induces the degradation of the cell cycle regulatory protein p53 [141, 142]. This degradation is required for long term maintenance of the viral genome [143]. E6 also blocks infected, proliferating cells from senescence by telomere shortening by inducing telomerase expression [144]. The E6 proteins from beta and mu papillomaviruses bind LxxLL motifs on the mastermind-like protein (MAML), inhibiting Notch signaling and suppressing squamous epithelial differentiation [145]. E6 has also been shown to down regulate the expression of interferon responsive genes [146, 147].

The E7 protein is encoded by nearly all HPVs and is considered to be oncogenic in high-risk types. E7 binds dozens of cellular targets, with the main function being to maintain infected cells that have begun to differentiate in a DNA synthesis competent state [148]. E7 accomplishes this in part by binding to and inducing the degradation of the tumor suppressor retinoblastoma protein (pRb), eliminating its ability to inhibit the cell from progressing from G1 into S phase. [149,

150]. E7 also induces global epigenetic changes in the host cell by upregulating the lysine-specific demethylase 6A (KDM6A) [151].

The E8^E2 protein is expressed from a spliced transcript that is encoded by the E8 ORF (overlaps the E1 ORF) fused to the 3' end of the E2 gene. E8^E2 competitively binds to E2BSs and recruits cellular repressive NCoR/SMRT complexes to restrict viral transcription and replication, and is the major reason HPV replicates to only a low copy number in undifferentiated cells [152]. Additionally, E8^E2 interacts with HDAC3 and this mediates its repressive activity [153]. E8^E2 is also required for long-term extrachromosomal maintenance of the viral genome in some HPV types, but not in others [154, 155].

Biology of Histone Modifications

In eukaryotic cells, the genome exists as chromatin, a complex of protein and DNA. Chromatin plays an enormous role in the regulation of replication and repair of DNA as well as transcription. On the most basic level, chromatin exists in two different physical states with divergent implications for transcription. Heterochromatin tightly compacts DNA, leaving it inaccessible to transcriptional machinery, and is thus generally considered transcriptionally repressed. Euchromatin is less condensed, and therefore more accessible, and generally provides a viable template for transcription. Switching between these two chromatin states is governed by epigenetic modulations. These can take the form of modifications to the chemical structure of the DNA itself (such as DNA methylation) or posttranslational modifications (PTMs) of the histones or other proteins bound by DNA (reviewed in [156]).

The fundamental unit of chromatin is the nucleosome, where 147 base pairs of DNA are wrapped around histone octamers comprised of two molecules of each core histone, H2A, H2B, H3, and H4 [157]. The α-helical C-terminal domain of the core histones engages in histone-histone interactions to form the basis of the nucleosome structure [158]. The N-terminal "tails" of histones are relatively unstructured [159]. Nucleosome occupancy (the fraction of a population of cells in which a certain region of DNA is bound by a nucleosome octamer) and positioning (where individual nucleosomes are located on the genome) are one of the primary features by which cells can tightly regulate gene expression [160, 161]. Nucleosomes can impede transcription by physically blocking access to DNA and hindering transcription factor binding by bending the DNA [158, 162]. A further level of regulation is achieved by histone PTMs. A notable feature of histone proteins is the large number and diversity of modifications, especially on the N-terminus tails. To date, there have been nine main types of histone PTMs discovered, (outlined in Table 1.2) [163, 164].

Table 1.2. Common histone modifications.

Residue	Modification	Function(s)

	Acetylation	Transcription, replication, DNA repair, chromatin condensation
Lysine	Methylation (mono, di, and tri)	Transcription, DNA repair
	Ubiquitylation	Transcription, DNA repair
	SUMOylation	Transcription
Arginine	Methylation (mono and di)	Transcription
	Deimination	
Glutamic Acid	ADP ribosylation	Transcription
Serine		Transcription, DNA repair, chromatin condensation
Tyrosine	Phosphorylation	
Threonine		
Proline	Isomerization	Transcription

Chromatin Regulation of Transcription

Acetylation of histone lysine residues (particularly H3 and H4) neutralizes their positive charge and reduces chromatin compaction by weakening histone-DNA interactions and disrupting interactions between nucleosomes [163]. This results in the unfolding or relaxing of chromatin and is often correlated with increased transcription from the genomic region [165, 166]. Acetylated lysines can also serve as binding sites for various transcription factors and a variety of epigenetic modulators (writers, readers, and erasers) that impact histone PTMs and nucleosome occupancy [167]. Acetylation of histones is regulated by two main classes of enzymes. Histone acetyltransferases (HATs) catalyze the transfer of an acetyl group from acetyl-CoA to the amino group of the side chain of a lysine (generally on the N-terminus of a histone protein). Histone deacetylases (HDACs) perform the opposite reaction and remove the acetyl group. Generally, histone acetylation occurs at multiple lysine residues at once and is typically associated with regions of active transcription [168].

Like acetylation, methylation of histone lysine residues regulates transcription but there are significant differences in the biochemical properties and biological

21

implications of histone methylation. Methylation does not alter the charge of the histone protein and there is added complexity in that there are three levels of methylation: each lysine can be mono-, di-, or trimethylated [156]. Histone methylation is catalyzed by histone specific histone methyltransferases (HMTs), that have far more specificity than HATs or HDACs, which normally transfer a methyl group to a specific residue [169]. Methylation of histones can stimulate or repress transcription depending on which residue is methylated and to what degree. Actively transcribing regions of chromatin are enriched in H3K4me3 and H3K36me3 while transcriptionally inactive regions are marked by high levels of H3K9me3 and H3K27me3 [168].

Chromatin and Viral Infection

Given the intricate and essential nature of histone modifications to the life of the eukaryotic cell, it should come as no surprise that the viruses which infect these host cells manipulate these pathways to their own advantage. In recent years, there have been major advances in the field of examining the interplay of chromatin and regulation of viral infection. The genome of most viruses that spend a part of their infectious cycle in the nucleus is packaged into chromatin or a chromatin-like structure at some point in their life cycle (reviewed in [170]). As histone PTMs have numerous, multifaceted biological functions, both viruses and cellular hosts utilize them to their respective advantage during viral infections (Reviewed in [171]).

Chromatin Regulation of HPV Infection

As the HPV genome exists in various chromatin states throughout its entire lifecycle, there has long been interest in epigenetic regulation of HPV infection. A substantial body of work has been done to investigate the role of epigenetics in HPV transformation of cells and HPV associated cancers (reviewed in [172]). In recent years several notable studies have shown that the HPV infectious cycle is subject to extensive and intricate epigenetic regulation, particularly the PTMs of histones on the viral genome [171].

As HPV progresses through the different phases of its differentiation-dependent lifecycle, the structure of the viral chromatin is regulated to control viral gene expression at appropriate timepoints. Studies have shown that, upon differentiation, the viral chromatin is significantly remodeled. In undifferentiated cells a region corresponding to the E6 ORF is mostly free of nucleosomes, but after differentiation this DNase I hypersensitive region shifts to the E7 ORF, corresponding to the initiation of late transcripts [173]. Follow up studies have revealed that histones with active modifications are greatly enriched at both early and late promoter regions upon differentiation [174].

Histone Acetylation

Viral protein regulation of histone acetylation on both the viral and cellular genome is critical for creating a cellular environment conducive for HPV replication [175]. Throughout the lifecycle, both the early and late viral promoters are enriched in acetylated H3 and H4, but this increases significantly after differentiation [174]. HPV regulates gene expression by mediating the activity of several different cellular

23

HATs. Both E6 and E7 interact with and modulate the activity of the HAT

p300/CREB Binding Protein (CBP), which acetylates all four of the canonical

nucleosome histones [176, 177]. After binding, p300/CBP recruit cellular

transcriptional machinery through both its HAT activity and direct protein-protein

interactions [178-180]. E2 requires p300 to activate the early promoter [181]. CBP,

modulated by the viral proteins, upregulates transcriptional activation from the URR

in HPV18 by acetylating K14 on the H3 bound to that region [182, 183].

The HAT Tip60 is involved in multiple viral functions. Tip60 interaction with

E2 assists in the repression of E6 and E7 transcription by acetylating regulatory

regions of the URR, causing increased Brd4 binding [184, 185]. E6 destabilizes

Tip60 when expressed alone [186]. In cells stably infected with HPV, Tip60

expression and activity is upregulated through the action of the innate immune

regulator STAT-5, and helps to activate the DDR, aiding in productive HPV genome

amplification [187].

HPVs also hijack the activity of HDACs for their own advantage. E7-directed

manipulation of HDACs induces the global upregulation of H3 acetylation in infected

cells [188]. The viral repressor E8^E2 interacts with HDACs 1, 2, and 3 to assist with

its repression of transcription from the viral early promoter [189]. E7, in complex

with all three type I HDACs, activates cellular E2F2-mediated transcription to

promote S-phase entry in differentiated keratinocytes [190]. E7-HDAC interaction is

required for both stable maintenance and productive replication of the viral genome

[191]. While the exact mechanism by which E7's HDAC binding affects viral

replication is not yet understood, E7 is thought to sequester HDACs away from the

viral genome and the resultant increase in acetylation of the viral histones promotes the recruitment of factors that promote homologous recombination (HR) to viral replication foci [192, 193].

Histone Methylation

Histone methylation of both the viral and cellular chromatin also plays an important role in the viral lifecycle. During differentiation, the late promoter is enriched in the transcriptionally active modification H3K4me2 [174]. In undifferentiated cells, the viral chromatin is generally in a transcriptionally repressed state, in part due to the deposition of H3K27me3 by the polycomb repressor complex (PRC1/2) [194]. The expression of high risk E6 and E7 upregulates the methyltransferase component of PRC2 known as Enhancer of Zeste homologue 2 (EZH2), although in an enzymatically inactive form [195, 196]. Interestingly, E7 protein also induces expression of the demethylases KDM6A and KDM6B to globally reduce H3K27me3 levels, but how this impacts the epigenetic status of the viral genome is not well understood [197]. E7 upregulates the HMT SETD2, which catalyzes the deposition of transcriptionally active H3K36me3 on the viral chromatin, both of which are essential for viral replication [198]. H3K6me3 deposition is enriched at splice sites, suggesting that this modification is essential for proper splicing of viral transcripts [198]. Lastly, E6 also plays a role in histone methylation by interacting with and down regulating the activities of the HMTs CARM1, PRMT1, and SET7 to suppress the transcription of genes downstream of p53 [199].

Summary

In this body of work, we seek to further understand the role of histone modifications in the early HPV lifecycle. In particular, we are interested in the contents of the virion-packaged viral epigenome and its effects on viral transcription and replication immediately after delivery to the host nucleus. In the following chapters we will describe our work in: 1) improving assembly and delivery of recombinant HPV quasivirus particles; 2) profiling virion packaged histone PTMs in quasivirus and native papillomavirus particles, and 3) determining the effects of histone acetylation on the early HPV lifecycle.

Chapter 2: Materials and Methods

Plasmids

Table 2.1. List of plasmids used in this work.

ID#	Name	Use	Reference
4024	pMC.BESPX-HPV18	Minicircle genome; HPV18 qPCR standard	[200]
4390	pUC18-HPV18	HPV18 viral genome	[201]
4244	pBR322-HPV18	HPV18 viral genome	[202]
4245	pUC18-HPV18E1mut	HPV18 viral genome with E1 mutation	[70]
4220	pUC18-HPV18E2I77A	HPV18 viral genome with E2 mutation	[203]
4117	pBR322-HPV18Neo	HPV18 viral genome with drug selectable marker	[204]
4116	pBR322-HPV18NeoE1mut	HPV18 viral genome with drug selectable marker and E1 mutation	[204]
4280	pBR322 HPV18NeoSV40	HPV18 viral genome with drug selectable marker	
4391	pShell16	Expression vector for HPV16 L1/L2	[205]
4163	pMEP4	Empty vector	[110]
4165	pMEP9	Empty vector	[110]
4162	pMEP4/HPV18 FLAG E2 recoded	HPV18 E2 expression vector	[203]
4164	pMEP9-EE HPV18 E1, recoded	HPV18 E1 expression vector	[203]
4097	pMA-RPPH1	RNase P qPCR standard	
4227	pUC57-HPV18E6*I	HPV18 E6*I RT-qPCR standard	[70]
4226	pUC57-HPV18E1^E4	HPV18 E1^E4 RT-qPCR standard	[70]
4228	pCMVsport6-TBP	TBP qPCR standard	[70]
0699	pMl2d-BPV1	BPV1 DNA qPCR standard	[206]

Production of HPV Minicircle Genomes

50 µl of electrocompetent *E. coli* ZYCY10P3S2T (Systems Biosciences # MN900A-1) were electroporated with pMC.BESPX-HPV18 [200] and allowed to recover in 950 µl SOC medium (Thermo Fisher #15544034) by incubating at 37°C for one hour shaking at 225 rpm. 20 µl culture was spread on an LB plate containing 50 µg/ml kanamycin (KD Medical #BPL-2650) and incubated overnight at 37°C. A single, isolated colony was picked and used to inoculate a 14 ml round bottom test tube containing 5 ml LB (Thermo Fisher #10855021) supplemented with 50 µg/ml kanamycin (Sigma #10106801001). The culture was grown at 37°C for 6 hours shaking at 225 rpm. 50 µl of starter culture was used to inoculate 200 ml Terrific broth (Thermo Fisher #A1374301) in a 2 L beveled flask and grown overnight at 37°C and shaking at 225 rpm. The OD_{600} of the culture was measured with a Biophotometer (Eppendorf #6133000010). When the culture reached an OD_{600} of between 6-8, 200 ml of induction mix (200 ml LB, 0.02% L-Arabinose (System Biosciences #MN850A-1), and 0.04 N NaOH (Sigma # S2770)) was added to the culture and it was grown at 32°C for 7 hours. To confirm successful induction, a 1.5 ml aliquot of culture was processed with the Wizard Plus SV Minipreps DNA Purification System (Promega # A1465) to isolate DNA. 20 µl restriction digests with 10 U BglII (NEB #R0144S) and 1X Cut Smart Buffer (NEB #B7204S) were prepared with 500 ng of miniprep DNA or the parental pMC.BESPX-HPV18 plasmid. The samples were digested for 60 minutes at 37°C, mixed with Gel Loading Dye (NEB #B7024S0 to a final concertation of 1X, and separated by electrophoresis on a gel of 0.8% agarose (Lonza #50074) in TAE buffer (Quality Biological 351-008-131) with

0.5 ng/ml EtBr (Invitrogen #15585011). Gels were imaged on a G:Box (Syngene). If induction was successful, the remainder of the culture was processed with the NucleoBond Xtra Maxi Plus EF Maxi Kit (Machery Nagel #740426.50) per manufacturer's instructions.

Production of Recircularized HPV Genomes

To free the HPV18 genome from the bacterial plasmid backbone, 10 µg pUC-HPV18 or pBR322-HPV18 were digested for 60 minutes at 37°C with 50 U NcoI (NEB #R0193T) or EcoRI (NEB# R0101L), respectively, in a 50 µl reaction with 1X CutSmart Buffer. The enzyme was heat inactivated at 80°C for 20 minutes. A 1 µl aliquot was taken and stored at 4°C. To re-ligate the DNA, a 900 µl ligation reaction was set up with 49 µl digested DNA, 180 µl 10X T4 DNA Ligase Reaction Buffer (NEB #B0202S), and 40 U T4 Ligase (NEB #M0202S) and incubated overnight at 16°C. To precipitate the DNA, 600 µl isopropanol and 180 µl 5M NaCl were added and the samples were incubated overnight at -80°C. The samples were brought to room temperature and centrifuged at 16,000 x g for 30 minutes at 4°C. The supernatant was removed, and the pellet was washed with 100 µl 70% ethanol and centrifuged at 16,000 x g for 30 minutes at 4°C. The supernatant was removed, and the pellet was briefly air dried before being resuspended in 15 µl TE. A 1 µl aliquot of ligated sample and digested sample were used to confirm successful re-ligation by agarose gel electrophoresed as described.

Tissue Culture

Swiss J2/3T3 murine fibroblasts feeder cells (J2s) (ATTC #CCL-92) were cultured in a 37°C, 10% CO_2 incubator with DMEM-10 (DMEM (Invitrogen #11960-069) supplemented with 10% Newborn Calf Serum (NCS) (Gemini #100-504), 2 mM L-Glutamine (Invitrogen #25030081), 100 units/ml Penicillin, 100 μg/ml Streptomycin (Invitrogen #15140-163) in T175 flasks before being harvested by trypsinization and lethally irradiated in suspension with 6000 rads γ-irradiation.

Primary human foreskin keratinocytes (HFKs) and bovine epidermal keratinocytes (BEK6) were cultured at 37°C and 5% CO_2 in Rheinwald-Green F-medium (3:1 Ham's F12 (Life Technologies #21700075)/DMEM-high glucose, 5% FBS (Thermo Fisher Hyclone SH30071.03), 0.4 μg/ml hydrocortisone (Sigma #H4001), 8.4 ng/ml cholera toxin (Calbiochem #227036), 10 ng/ml EGF (Invitrogen #PHG0311), 24 μg/ml adenine (Sigma #A-2786), and 6 μg/ml insulin (Gemini #700-112P), 100 units/ml Penicillin, 100 μg/ml Streptomycin) on a layer of lethally irradiated J2s.

To co-culture HFKs, 1×10^6 lethally irradiated J2s were plated on a 10 cm dish with 10 ml DMEM-10 and incubated overnight in a 37°C, 10% CO_2 incubator. The medium on the dish was changed to 10 ml Rheinwald-Green F-medium and 3×10^5 HFKs were plated onto the feeder monolayer and incubated for three to four days in a 37°C, 10% CO_2 incubator until the HFKs were approximately 70% confluent. Media was changed every 48 hours.

For differentiated (Ca++) keratinocytes, cells were grown to confluence, feeders were removed with Versene, and media was switched to low calcium basal

medium (Lonza #CC-3101) supplemented with SingleQuots for keratinocytes (Lonza #CC-4131) containing bovine pituitary extract, hydrocortisone, and epidermal growth factor for 24 hours. Media was changed to basal medium (Lonza #CC-3104) supplemented with 1.5 mM $CaCl_2$ and cells were differentiated for 5 days.

For organotypic raft cultures, 0.8 ml each of Reconstitution Buffer (2.2% $NaHCO_3$, 0.05 N NaOH, 200 mM Hepes free acid) and 10X Ham's F12 medium were combined in a 15 ml conical tube. To the tube, 7.6 ml Collagen Type I, from rat tail (Sigma #08-115) was added slowly. 2 million 3T3-Swiss albino J2 mouse embryonic fibroblasts were suspended in 0.4 ml FBS and gently mixed with the collagen solution. 0.75 ml mixture was added to 10 wells of a 12 well tissue culture plate (Corning #3513) and incubated at 37°C and 5% CO_2 for 1 hour. Each gel was overlaid with 1 ml Raft Culture Medium (3:1 DMEM/F12, 10% FCS, 0.4 g/ml hydrocortisone, 0.01 nM cholera toxin, 5 µg/ml transferrin (Sigma #T3309)) and returned to incubator for 2 days. Media was removed and $1x10^5$ keratinocytes suspended in 1 ml Raft Culture Medium were added to each well and incubated overnight. Media was replaced with Raft Culture Medium supplemented with 5 ng/ml epidermal growth factor and incubated until keratinocytes were confluent. A sterile needle was run around the edge of the well to separate the collagen gel from the wall and the plate was returned to incubator for several hours. A sterile raft grid was placed in a 10 cm plate. Raft Culture Media with 5 ng/ml EGF was added to the plate until it was just touching the bottom of the grid. With a sterile spatula, rafts were transferred to the grid and cultured for two days. Media was swapped for Raft Culture Media with 5 ng/ml every two days until harvest on day 10.

To harvest, the raft was transferred onto a circular type HA nitrocellulose filter and cut in half with a scalpel. Halves were fixed in 3.7% formaldehyde for 4 hours at room temperature before being stored in 70% ethanol at 4°C. Samples from each type of keratinocyte were sent for embedding, sectioning and hematoxylin and eosin staining (American Histolabs).

HPV Quasivirus Production

HPV quasiviruses were produced as described in [207].

Transfection

293TT cells were cultured in DMEM-10, 10% FBS, 2 mM L-Glutamine, 100 units/ml Penicillin, 100 µg/ml Streptomycin, 1X non-essential amino acids (Thermo Fisher #11140050), 1 mM sodium pyruvate (Life Technologies #11360-070), 0.33 mg/ml Hygromycin B (Roche 10843555001). Seven million cells were seeded in a T-75 flask, in DMEM-10 without antibiotics and incubated overnight at 37°C in 10% CO_2. 19 µg of genomic HPV18 DNA (either recircularized minicircle HPV18 or religated HPV18 genome), 19 µg pShell16 L1/L2 expression vector (Addgene #37320), 6 µg codon-optimized pMEP9-HPV18 E1, and 6 µg codon-optimized pMEP4-HPV18 E2 [203] were added to 2 ml Opti-MEM (Thermo Fisher #31985070). In a separate tube, 100 µl Lipofectamine 2000 (Invitrogen #11668019) was combined with 2 ml Opti-MEM. Tubes were incubated separately at room temperature for 10 minutes, combined, and incubated for another 20 minutes. The DNA/Lipofectamine complexes were added directly to cell monolayers and incubated

overnight. The next morning, transfection medium was aspirated and replaced with fresh 293TT medium without antibiotics, and cells were incubated overnight.

Harvest and Maturation

Transfected cells were removed from flasks by trypsinization, collected by centrifugation at 5,000 x g, resuspended in 1 ml PBS, and transferred to a siliconized microfuge tube. Cells were centrifuged at 5,000 x g and the cell pellet size was estimated and resuspended in 1.4 pellet volumes of DBPS (Invitrogen #14040-141) supplemented with 9.5 mM $MgCl_2$. Triton X-100 (Sigma #T8787) and ammonium sulfate pH 9 were added to final concentrations of 0.5% and 25 mM, respectively. 25 units Benzonase (Millipore #70664-3) and 10 units of Plasmid Safe (Lucigen #E3110K) were added and the cell suspension was incubated overnight at 37°C, inverting to mix at 1, 4, and 20 hours.

Salt Extraction

NaCl was added to the matured lysate to a final concentration of 850 mM and the samples were incubated on ice for 10 minutes and centrifuged at 5,000 x g at 4°C for 5 minutes. The supernatant was transferred to a new tube. The pellet was resuspended in DBPS containing 800 mM NaCl and centrifuged at 5,000 x g at 4°C for 5 minutes. The supernatant was combined with the previous supernatant and centrifuged once more at 5,000 x g at 4°C for 5 minutes. The clarified supernatant was layered onto OptiPrep ultracentrifuge gradient.

"Ripcord" Quasivirus Preparation

Quasivirus preparations made with the "Ripcord" protocol were transfected and harvested by trypsinization as described above. The cell pellet was resuspended in 1.5 pellet volumes of DBPS supplemented with 9.5 mM $MgCl_2$. Triton X-100 (Sigma #T8787) and ammonium sulfate pH 9 were added to final concentrations of 0.5% and 25 mM, respectively. 1 µl RNase-IT (Agilent #400720) (2 ng RNase A and 5 U RNase T1) was added to the lysate. The cell suspension was incubated overnight at 37°C, inverting to mix at 1, 4, and 20 hours. Samples were centrifuged at 5,000 x g at 4°C for 5 minutes and the supernatant transferred to a new tube. The pellet was resuspended in two pellet volumes DBPS and centrifuged at 5,000 x g at 4°C for 5 minutes. The supernatant was transferred to the new tube and the pellet was resuspended in one pellet volume DBPS and flash frozen in a dry ice-ethanol bath. The samples were thawed and the and centrifuged at 5,000 x g at 4°C for 5 minutes. The supernatant was transferred to the new tube. The pellet was resuspended in one pellet volume DBPS supplemented with 650 mM NaCl, centrifuged at 5,000 x g at 4°C for 5 minutes. The supernatant was transferred to the new tube and the combined supernatants were centrifuged at 5,000 x g at 4°C for 5 minutes.

Ultracentrifugation

46% Optiprep solution (Optiprep (#Sigma D1556) in 1X PBS pH 7.4 (Thermo Fisher #70011044), supplemented with 650 mM NaCl, 920 µM $CaCl_2$, 520 µM $MgCl_2$, 2 mM KCl) was further diluted in DBPS+NaCl (1x PBS supplemented with 625 mM NaCl, 900 µM $CaCl_2$, 500 µM $MgCl_2$, 2.1 mM KCl) to create solutions of

27%, 33%, and 39% Optiprep. 1.4 ml 27% Optiprep solution was added to 5.2 ml

polyallomer tubes (Beckman #326819) and underlaid with equivalent volumes of

33% and 39% Optiprep solutions. The gradients were allowed to diffuse for 1 hour.

The double clarified lysate was loaded on top of gradients and centrifuged in a

Sw55Ti rotor for 3.5 hours at 23,7020 x g at 16°C. Gradient tubes were removed

from the rotors and a hole was made in the bottom with a 22 Ga needle (Monoject

#15141-136). Ten 200 µl fractions were collected dropwise into siliconized

microfuge tubes.

Screening for Virus Containing Fractions

To screen for the viral proteins, 9 µl was removed from each fraction and LDS

Sample Buffer (Thermo Fisher #NP0007) and DTT were added to final

concentrations of 1X and 50 mM, respectively. Samples were heated at 72°C for 10

minutes and separated on a 26 well 4-12% Bis-Tris acrylamide gel (Thermo Fisher

#WG1403BOX) in 1X MOPS running buffer (Thermo Fisher #NP0001). Samples

were electrophoresed at 150V until the dye front reached the bottom of the gel at

which point the gel was removed and fixed for 1 hour in Fixation Buffer (50%

methanol, 7% acetic acid). The gel was stained overnight with Sypro Ruby (Thermo

Fisher #S12000) on an orbital shaker at setting 1. The gel was washed with Wash

Buffer (10% methanol, 7% acetic acid) for 1 minute followed by a second wash with

H_2O. The gel was imaged using UV-light (254 nm wavelength) in a G:BOX

(Syngene). Fractions that contained both the viral L1 and L2 proteins were considered

positive for viral capsids.

To screen for viral genomes, a 1 µl aliquot was taken from each fraction and mixed with 99 µl H_2O. qPCR for HPV18 DNA was performed. Fractions that contained HPV18 DNA were considered positive.

Fractions that were positive for HPV18 DNA, L1, and L2 were selected and pooled.

Quantitating Viral Titer

From each quasivirus stock, 5 µl viral stock was digested in a 20 µl reaction with TURBO DNA-free Kit (Invitrogen #1907) for 30 minutes at 37°C and the nuclease was inactivated per manufacturer's instructions. 16 µl was removed from the reaction and mixed with 100 µl Capsid Digest Buffer (20 mM Tris-HCl pH 8, 20m M DTT, 20 mM EDTA, 0.5% (w/v) SDS, 0.2% Proteinase K (Qiagen #19133)) and incubated at 60°C for 20 minutes. Viral DNA was extracted with QIAquick PCR Purification Kit (Qiagen #28104) and eluted into 50 µl of elution buffer. qPCR for HPV18 DNA was performed as described and Viral Genome Equivalents (VGE) for the quasivirus stock were calculated.

Quantitating Virions

From each quasivirus stock, 5 µl was combined with LDS Sample Buffer (Thermo Fisher #NP0007) and DTT to final concentrations of 1X and 50 mM, respectively. Using Pierce BCA Protein Assay Kit (Thermo Fisher #23225), a standard curve of BSA from 2000 ng/µl to 0 ng/µl was prepared per manufacturer's instructions. 1 µl each standard was combined with 4X LDS, and DTT to final concentrations in of 1X, and 50 mM, respectively. Samples were separated by SDS-

PAGE, stained with Sypro Ruby, and imaged as described. Using the BSA standard curve, the mass of L1 molecules in each virus sample was calculated and from there, the number of virions was determined.

Infection Assay of Primary HFKs with HPV Quasiviruses

Seeding

Primary HFKs were co-cultured with J2s as previously described. $1x10^6$ lethally irradiated J2s were plated in a 12 well plate with 12 ml J2 media ($8.3x10^4$ cells, 1 ml media per well) and incubated overnight in a 37°C, 10% CO_2 incubator. J2 media was removed and HFKs were seeded at a density of $5x10^5$ cells per well in 1 ml F media per well. Plates were incubated in a 37°C, 5% CO_2 incubator for 16-48 hours until 6-12 cell colonies formed.

Infection

"Infection media" was prepared for each well to be infected by combining 400 μl of F media with the calculated volume of quasivirus stock needed for an MOI of between 10 and 100 VGE/cell. Media on the plate was aspirated and 400 μl infection media was added to each well. The plate was rocked at 4°C for 60 minutes. 600 μl F media was added to each well. Small molecule chemical modulators were added to the culture media at this time. The plate was returned to the incubator until the desired collection time, generally 24 to 96 hours post infection.

Transcription Assay

Media was aspirated from the wells. Feeders were removed using a 1000 μl pipette to apply 1 ml Versene to the surface of each well. Versene was aspirated and cells were lysed with 350 μl Qiagen Buffer RLT + 1% β-mercaptoethanol (Sigma #M625). Lysates were transferred to a QiaShredder (Qiagen #79656) and centrifuged at 16,000 x g for 2 minutes at room temperature. RNA was extracted with the RNeasy Mini Kit (Qiagen #74106) according to manufacturer's instructions. During extraction, the optional on-column DNA digestion was performed with RNase-free DNase (Qiagen #79254). The RNA was quantitated using the Qubit RNA BR Assay Kit (Life Technologies #Q19219) on a Qubit 3.0 Fluorometer (Life Technologies #Q33216) and normalized to 100 ng/μl. RNA integrity was verified using the RNA 6000 Nano Kit (Agilent #5067-1511) on a 2100 Bioanalyzer Instrument (Agilent #G2939BA) per manufacturer's instructions. cDNA was synthesized from 1 μg RNA using the Transcriptor First Strand cDNA Synthesis Kit (Roche #04897030001) per manufacturer's instructions, using oligo(dT)18 primer and random hexamer primers in a 20 μl reaction. After synthesis, cDNA was diluted to 50 μl in H_2O. qPCR was performed as described for the viral transcripts E1^E4 and E6*I and the cellular normalizing gene TATA-Binding Protein (TBP). The amount of mRNA for each transcript was quantified using the corresponding standard curve and viral transcripts were normalized to TBP.

Replication Assay

Media was aspirated from wells. Feeders were removed using a 1000 μl pipette to spray the surface of each well with 1 ml of Versene. Versene was aspirated and cells

were harvested by trypsinization. Cells were resuspended in PBS and centrifuged at 300 x g for 5 minutes. The supernatant was removed, and DNA was extracted using the DNeasy Blood & Tissue Kit (Qiagen # 69506). DNA was eluted into 200 μl elution buffer and the elution step was repeated. The eluates were combined. To precipitate DNA, 40 μl 3M Sodium acetate, pH 5.2 and 1320 μl 90% ethanol were added and the samples were incubated on ice for 30 minutes. Samples were centrifuged for 5 minutes at 16,000 x g at room temperature. The supernatant was discarded, and the pellet was washed with 100 μl 70% EtOH, and the sample was centrifuged at 16,000 x g for 5 minutes. The supernatant was discarded, and the pellet was air dried before being resuspended in 50 μl TE Buffer. DNA samples were quantified with a Nanodrop 1000 (Thermo Fisher). 100 ng of extracted DNA was digested in three 20 μl reactions with either DpnI (NEB # R0176S), MboI, or no enzyme (a mock digest with H_2O). Digests were diluted to 50 μl total volume with H_2O. qPCR was performed as described for HPV18 DNA on all digests and for normalizing gene RNase P on the mock digests. The amount of HPV18 DNA and RNase P were quantified using the corresponding standard curves and viral DNA levels were normalized to RNase P.

qPCR

In a 384 well plate (Life Technologies #4309849), 10 μl reactions consisting of 1X FastStart Universal SYBR Green Master (Roche #4913914001), 750 nM primer mix, and 2.5 μl sample or standard curve were performed in triplicate. The reaction was performed on a QuantStudio 7 Flex Real-Time PCR System (Life Technologies #4485701) with the temperature cycle described in Table 2.2. 40 cycles

in total were run using standard settings for SYBR Green reagents. The data were

analyzed with Quant Studio Software (Life Technologies).

Table 2.2. **Temperatures for each stage of the qPCR reaction.**

Stage	Temperature (°C)	Time (min:sec)	Cycles
1	50	2:00	1
2	95	10:00	1
3	95	0:15	40
4	60	1:00	
5	95	0:15	1
6	60	1:00	1
7	95	0:15	1

Fluorescent signal was measured during Stage 4 and continuously between Stages 6

and 7. All temperature changes were 1.6°C/sec, except between Stages 6 and 7 where

it was 0.05°C/sec.

Standard Curves

Standard curves for qPCR experiments were prepared by performing 10-fold

serial dilutions of the indicated plasmid from $1x10^{-1}$ ng/µl to $1x10^{-8}$ ng/µl in 0.1

mg/ml yeast tRNA (Invitrogen #AM7119). Table 2.3 contains the standard curves

used in qPCR experiments.

Table 2.3. Standard curves used in qPCR reactions.

Standard	Plasmid Name	Reference
HPV18 DNA	Minicircle HPV18	[200]
RNase P	pMA-RPPH1	
E6*I	pUC57-HPV18E6*I	[70]
E1^E4	pUC57-HPV18E1^E4	[70]
TATA Binding Protein	pCMVsport6-TBP	Open Biosystems #MHS6278-202802567
BPV1	pMl2d-BPV1	[206]

Primers

Primer mixes were prepared by combining the forward and reverse primer

(Table 2.4) from 100 µM primer stocks to 3 µM in TE.

Table 2.4. Oligos used in qPCR experiments

ID#	Target	Direction	Sequence
3220	HPV18 DNA	Forward	CACAATACTATGGCGCGCTTT
3221		Reverse	CCGTGCACAGATCAGGTAGCT
3427	RNase P	Forward	CGGAGGGAAGCTCATCAGTG
3428		Reverse	TGGCCCTAGTCTCAGACCTT
3210	E6*I Viral Transcript	Forward	CAAGACAGTATTGGAACTTACAGAGGTG
3211		Reverse	CTGGCCTCTATAGTGCCCAGC
3212	E1^E4 Viral Transcript	Forward	CAACAATGGCTGATCCAGAAGTAC
3213		Reverse	TAGGTCTTTGCGGTGCCC
3226	TATA Binding Protein	Forward	TAAACTTGACCTAAAGACCATTGCA
3227		Reverse	CAGCAAACCGCTTGGGATTA
726	BPV1 DNA	Forward	TTGGTGAGGACAAGCTACAAGTTG
727		Reverse	TGGCTCCCGCCTTTTTG

Primers against viral DNA are across DpnI restriction sites for use in the replication

assay. Primers against viral transcripts are across splice sites.

Production of Bovine Papillomavirus Virions

Bovine wart tissue (3-5 g) (harvested from BPV1 infected cows by Carl

Olson, University of Wisconsin School of Veterinary Medicine in 1986) was minced

into 1 mm^3 chunks with sterile razor blades. 15 ml Mincing Buffer (10 mM Tris-HCl

pH 7.5, 1 mM MgCl$_2$, 1% (w/v) Brij58 (Sigma #P5884), in PBS) was added and the

chunks were further processed using the stopper of a 60 ml syringe (Covidien

#8881560125) to squish into smaller pieces. Processed wart tissue was transferred

into a 50 ml conical tube and vigorously vortexed 5 times for 2 seconds on high

setting. 75 U Benzonase and 50 U Plasmid Safe were added and samples were

incubated at 37°C for 1 hour. 2 mg collagenase H (Sigma #C8051) were added and

the pH was adjusted to 7-7.5. Samples were incubated at 37°C for 15 minutes

followed by 4°C overnight on a rotator. The next day, samples were brought to room

temperature, checked to ensure pH was still neutral, and 0.17 volumes (2.55 ml) 5M

NaCl was added. After shaking for 15 minutes, samples were centrifuged at 1,000 x g

for 5 minutes at room temperature. Supernatant was transferred into a fresh tube and

the pellet was resuspended with Salt Extraction Buffer (10 mM Tris-HCl pH 7.5, 800

mM NaCl, 1% Brij58, 1% PBS). Resuspended pellets were sonicated in a Vibra-Cell

VC505 (Sonics & Materials, Inc) for 30 seconds on setting 4 and chilled on ice for 2

minutes. This step was repeated until the solution no longer changed in viscosity

(generally three to four times) and the samples were centrifuged at 1,000 x g for 5

minutes at room temperature. The supernatant was combined with the previous

supernatant and together they were centrifuged at 1,000 x g for 5 minutes at room

temperature. The supernatant was transferred to a 40 ml polyallomer tube (Beckman

#326823) and underlaid with 1.5 ml 39% Optiprep using a syringe and needle. The

samples were centrifuged in a Sw32Ti rotor at 30,000 rpm for 2 hours at 16°C. The

top of gradient was discarded and the bottom 3 ml was transferred to a 15 ml tube and

vortexed for 5 minutes followed by centrifugation at 1,000 x g for 10 minutes at 4°C.

The supernatant was transferred to a new tube and 900 µL DBPS+0.8M NaCl was

added to dilute the Optiprep concentration below 15%. Gradients were prepared by

adding 0.5 ml 15% Optiprep/0.8M NaCl and successively underlaying 0.9 ml each of

27%, 33%, and 39% solutions and allowing to diffuse for 1 hour. Clarified lysate was

loaded on top of the gradient. Gradients were loaded into a Sw55Ti rotor and

centrifuged at 50,000 rpm at 16°C for 3.5 hours.

A 22 Ga needle was used to puncture a hole at the bottom of the tube and 10 200 µL fractions were collected dropwise into 2.0 ml siliconized tubes. From each fraction a 16 µL aliquot was taken. 1 µL was diluted 1:100 in H_2O and screened for the presence of BPV1 DNA by qPCR. The remaining 15 µL was combined with LDS and DTT to concentrations of 1X and 50 mM, respectively in a final volume of 30 µL and heated to 70°C for 10minutes. 10 µL each sample was loaded onto three separate 26 well 4-12% Bis-Tris acrylamide gel (Thermo Fisher #WG1403BOX) in 1X MOPS running buffer (Thermo Fisher #NP0001) and run at 150V until dye front reached the bottom. Two of the gels were transferred to 0.45 µm PVDF membrane and immunoblots for H3 and L1 were performed. The remaining gel was fixed and stained with Sypro Ruby. Fractions positive for H3, BPV1 L1, and BPV1 DNA were combined, aliquoted, and stored at -80°C.

Production of Wart Derived Human Papillomavirus Virions

Extraction of virions was conducted by the Tumor Virus Molecular Biology Section of the Laboratory of Cellular Oncology, National Cancer Institute. A 0.65 cm diameter biopsy of a wart from the right palm of a 16-year-old female patient was minced in a petri dish with a scalpel in 0.5 ml DBPS supplemented with 10 mM $MgCl_2$ and 1% Brij58 (described in [208]). The minced wart was transferred to a microfuge tube and the plate was washed with 0.5 ml mincing buffer, which was transferred to the same tube. 50 U Benzonase and 20 U Plasmid Safe was added and incubated for 20 minutes at 37°C. 5 mg collagenase H was added and incubated for 30 minutes at 37°C before an overnight incubation at 4°C. 180 µl 5 M NaCl was

43

added and the sample was rocked at 4°C for 2 hours. The sample was sonicated twice

for 1 minute at max power and then centrifuged at 5,000 x g for 5 minutes. The

supernatant was transferred to a new tube and the pellet was washed with 0.5 ml

DBPS+0.8 M NaCl, before centrifuging again. The supernatants were combined and

then virions were purified by Optiprep ultracentrifugation (as described in quasivirus

section above).

Mass Spectrometry Analysis of Histone PTMs

Sample Preparation

Quasiviruses: 1.41×10^9 VGE HPV18WT quasiviruses (prepared as described

in Chapter 3) were precipitated overnight at 4°C with 33% TCA. The precipitate was

centrifuged at 20,000 x g at 4°C for 10 minutes and the supernatant was removed.

Pellet and tube walls were washed with 1 ml cold acetone + 0.1% HCl and

centrifuged at 20,000 x g at 4°C for 10 minutes and the supernatant was removed.

Pellet and tube walls were washed with 1 ml cold acetone and centrifuged at 20,000 x

g at 4°C for 10 minutes and the supernatant was removed. The pellet was dried

overnight in a SpeedVac on low vacuum, no heat setting. The pellet was dissolved in

60 µl buffer (54.16 mM Tris-HCl pH 8, 1X LDS Sample Buffer, 50 mM DTT) and

heated at 70°C for 10 minutes. Samples were centrifugated 16,000 x g for 1 minute.

The supernatant was transferred to new tube. 20 µl sample was loaded into three

adjacent wells of a 12 well, 1.0 mm NuPAGE 4-12% SDS-PAGE gel (Thermo Fisher

#NP0322BOX) and ran at 100V until the dye front reached the bottom of the gel. The

gel was stained with 50 ml Coomassie staining solution (1% Coomassie G-250

(Thermo Fisher #20279), 2.55% ortho-phosphoric acid (Sigma #5438280250), 10% (w/v) ammonium sulfate (Sigma #20450), 20% ethanol) for 2 hours and washed with H_2O overnight. Using sterile razor blades, bands corresponding to the molecular weight of histones (10-20 kDa) were excised from the gel and stored at -80°C. As controls, 293TT cells were cultured as previously described, collected by trypsinization, washed with PBS, and flash frozen before storage at -80°C. Samples were sent to our collaborators at the University of Pennsylvania (Weitzman and Garcia Laboratory) for further processing.

Bovine viruses: Two 20 μl aliquots of BPV1 virion isolation stocks were precipitated with the addition of TCA to a final concertation 33% and incubated overnight at 4°C. Samples were centrifuged at 16,000 x g for 30 minutes. The supernatant was removed, and the pellet was washed with 1 ml cold acetone with 0.1% HCl and centrifuged at 16,000 x g at 4°C for 10 minutes and the supernatant was removed. The pellet was washed with 200 μl cold acetone and centrifuged again. The supernatant was removed, and the pellet was allowed to air dry. The pellet was dissolved in 20 μl 1X LDS Sample Buffer, 50 mM DTT, heated at 70°C for 10 minutes, and centrifuged at 16,000 x g for 1 minute. The supernatant was transferred to a new tube. 10 μl sample was loaded into two adjacent wells of a 12 well, 1.0 mm NuPAGE 4-12% SDS-PAGE gel (Thermo Fisher #NP0322BOX) and ran at 100V until the dye front reached the bottom of the gel. The gel was stained with 50 ml Coomassie staining solution for 2 hours and then de-stained with H_2O for 2 hours. Using sterile razor blades, bands corresponding to the molecular weight of histones

(10-20 kDa) were excised from the gel and stored at -80°C. Samples were sent to our collaborators at the University of Pennsylvania for further processing.

Sample Processing, Data Collection, and Analysis

Our collaborators at the University of Pennsylvania and Children's Hospital of Philadelphia performed the following steps. Briefly, histones were extracted from cell pellets or histone gel slices, propionylated, digested with trypsin, and propionylated again. The samples were then separated by a C18 LC column and analyzed by mass spectrometry. The data were searched using EpiProfile v2.3 to calculate the relative abundance of individual PTMs on each peptide [209].

Acid-Urea Polyacrylamide Gel Electrophoresis (AU-PAGE)

For both normal acid urea (AU) and Triton acid urea (TAU) experiments, sample preparation was the same.

Acid Extraction of Cellular Histones

Cellular samples were cultured as described above. Proliferating (growing) samples were collected at 80% confluence. Feeders were removed with Versene (Thermo Fisher #15040066) before cells were collected by trypsinization and centrifuged at 234 x g for 5 minutes at room temperature. The supernatant was removed, and the pellet was resuspended in PBS before centrifuging again for 5 minutes at room temperature. The wash was repeated, and the pellets were flash frozen in ethanol and dry ice and stored at -80°C. The differentiated samples were collected in the same way, except without the Versene wash to remove feeders. Raft samples were produced as described and then frozen at -80°C.

For each cellular control, frozen cell pellets and rafts were thawed on ice and

histones were extracted by resuspending the pellet (or raft section) in 750 μL 0.4N

H_2SO_4 and incubating for 4 hours at 4°C on a rotator. Lysates were centrifuged to

pellet debris at 16,000 x g at 4°C for 10 minutes. The supernatants were transferred to

new tubes and 100% TCA was added dropwise to a final concentration of 33% and

lysates were incubated on ice overnight. Samples were centrifuged at 16,000 x g at

4°C for 10 minutes. The supernatant was removed and discarded, and the pellet was

washed with 100 μL ice-cold acetone and centrifuged for 5 minutes at 16,000 x g at

4°C. The supernatant was removed, and the acetone wash was repeated. The pellets

were air dried and dissolved in 100 μL H_2O, aliquoted into 10 μL aliquots and stored

at -80°C until use.

Virion Preparation

Virions were TCA precipitated as described above. The pellets were air dried

and stored on ice until use.

Gel Preparation

For AU gels, 18 x 16 cm glass gel casting plates (Amersham #80-6178-99)

were assembled according to the manufacturer's instructions. The components of the

separating gel were mixed (15% acrylamide, 0.1% bis-acrylamide, 6M urea, 5%

acetic acid) and degassed before polymerization by the addition of

tetramethylethylenediamine and ammonium persulfate to final concentrations of

0.06% and 0.14%, respectively. The separating gels were poured to 3 cm below the

top of the plate, overlaid with a 1 cm layer of ddH_2O and allowed to polymerize for

2.5 hours. The stacking gel components (6% acrylamide, 0.04% bis-acrylamide, 6M urea) were mixed before adding tetramethylethylenediamine and ammonium persulfate to final concentrations of 0.06% and 0.14%, respectively. The water layer was removed, and the stacking gel was poured to 1.5 cm below the top of the plate, overlaid with H_2O and allowed to polymerize for 2.5 hours. After polymerization, gels were placed in a running chamber filled with 4 L 5% acetic acid (AU Running Buffer). 500 μL AU Sample Buffer (6M urea, 5% acetic acid, 0.02% Pyronin Y, 12.5 mg/ml protamine sulfate) was loaded directly on top of the stacking gel and the gel was electrophoresed at 300V overnight.

For TAU gels, the components of the gel were mixed (15% acrylamide, 0.1% bis-acrylamide, 6 M urea, 5% acetic acid, 0.37% Triton X-100) before adding tetramethylethylenediamine and ammonium persulfate to final concentrations of 0.06% and 0.14%, respectively. The acrylamide mixture was poured into plastic cassettes (13.3 x 8.7 cm) with a 12+2 well comb (BioRad #3459901) and allowed to polymerize for one hour.

Electrophoresis

Cell extracts were thawed, and normalized amounts were distributed to new tubes. As controls, 0.5 μg recombinant histone H3.1 (NEB #M2503S) and H3.3 (NEB #M2507S) were used. 10 μg cytochrome C was used as a visual marker of protein migration during electrophoresis. Cellular and control samples were dried by centrifugation in a Savant DNA 120 SpeedVac (Thermo Fisher) on low vacuum setting (no heat). All samples (including the TCA-precipitated virion-derived extracts) were dissolved in 20 μL in AU Sample Buffer (6 M urea, 5% acetic acid,

0.02% Pyronin Y, 12.5 mg/ml protamine sulfate) with DTT added to a final

concentration of 50 mM and incubated at room temperature for 15 minutes. A 10-well

comb was inserted between the glass plates and pushed against the stacking gel to

form a seal (Figure 2.1). Samples were loaded into the space between the teeth of the

comb and proteins were separated by electrophoresis at 200V (TAU) or 400V (AU)

until the cytochrome C marker had just run off the bottom of the gel.
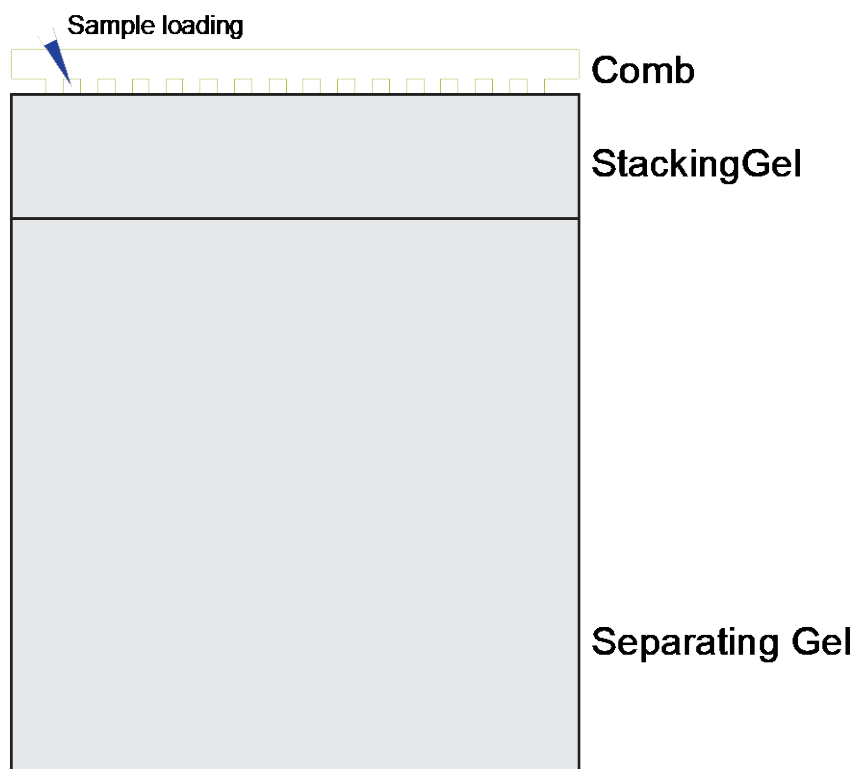
Figure 2.1. Loading of AU-PAGE gels. The comb was inserted roughly 1 mm into the stacking gel. The space between the teeth of the comb served as "wells" into which the samples were loaded.

Transfer

Gels were removed from the molds and soaked in AU Transfer Buffer (0.7% acetic acid) for 15 minutes. 0.45 μm PVDF membrane sheets were activated in methanol for 30 seconds and washed with ddH$_2$O for 1 minute before soaking in AU Transfer Buffer for 15 minutes. A transfer sandwich consisting of a transfer sponge, 2 sheets of Whatman paper (GE #3030-917), the AU/TAU gel, a 0.45 μm PVDF membrane (Millipore # IPVH304F0), 2 sheets of Whatman paper, and a transfer sponge was assembled in a tray of AU Transfer Buffer and placed into a transfer chamber filled with AU Transfer Buffer. Transfer was conducted at 500 mA for 20 minutes with the proteins moving out of the gel towards the membrane positioned on the negative anode side. Immediately after transfer, immunoblots were performed as described below.

Sodium Dodecyl Sulfate Polyacrylamide Gel Electrophoresis (SDS-PAGE)

Extraction

Growing and differentiated cellular samples were cultured as described. Media was removed and J2 fibroblast feeder cells were removed with Versene (Thermo Fisher # 15040066). Keratinocyte monolayers were rinsed with ice-cold PBS. Growing and differentiated cells were lysed on the plate with 1 ml SDS Lysis Buffer (1% w/v SDS, 10 mM Tris-HCl pH 8, 1 mM EDTA pH 8) heated to 95°C. After scraping the plate, samples were transferred to low protein binding microfuge tubes and sonicated using a Bioruptor (30 seconds on, 30 seconds off, for 6 cycles, at high power). After sonication, samples were heated at 95°C for 10 minutes in a heat

block before being cooled to room temperature. To remove any debris, samples were centrifuged at 16,100 x g for 5 minutes. The supernatant was transferred to low protein binding microfuge tubes and stored at -80°C.

For the raft samples, the samples were thawed on ice, suspended in 200 μl SDS Lysis Buffer and heated to 95°C for 10 minutes. Samples were sonicated using a Bioruptor (30 seconds on, 30 seconds off, for 6 cycles, at high power). The samples were ground with ReadyPrep Protein Mini Grinders (BioRad #1632146). The samples were centrifuged at 20,000 x g at 4°C, transferred to a new tube, and stored at -80°C. A Pierce BCA Protein Assay Kit (Thermo Fischer #23225) was used to determine protein concentrations.

Electrophoresis

Normalized samples were added to low protein binding tubes. To denature the samples, LDS Sample Buffer (Thermo Fisher #NP0007) was added to a final concentration of 1X, along with DTT to a final concentration of 50 mM with a total volume of 15 μl before heating at 70°C for 10 minutes. Before loading, samples were centrifuged at 16,000 x g for one minute to remove any debris. The supernatant was transferred to a new tube and samples were loaded onto a 12 well, 1.0 mm NuPAGE 12% Bis-Tris Protein Gel (Thermo Fischer #NP0342BOX) with 1 L MES running buffer (Thermo Fischer #NP0002). To mark protein sizes, 7.5 μL Page Ruler Plus (Thermo Fischer #26620) was loaded into a well adjacent to samples. The gel was run at 150V until the dye front reached the bottom of the gel.

Transfer

To transfer, the gel was removed from the cassette and a "transfer sandwich" was constructed. From bottom to top the sandwich consisted of: the black side of transfer cassette, followed by 1 sponge (Biorad #1703914), 1 sheet Whatman Filter Paper (GE #3030-917), the protein gel, a 0.45 μm PVDF membrane (Millipore # IPVH304F0) (activated in methanol and washed with H_2O), another sheet of Whatman Filter Paper, sponge, and clear side of plastic transfer cassette. The transfer cassette was placed in transfer apparatus (BioRad #1703946) with 2.5 L transfer buffer consisting of 1X NuPAGE Transfer Buffer (Thermo Fisher NP0006) and 10% methanol. Transfers were conducted at 60V for 3 hours or 20V overnight.

Immunoblots

After transfer, the membranes were immediately placed in a Perfect Western Container (Gene Hunter #B144S) and stained with Ponceau S (Sigma #P7170) for 5 minutes and washed 3 x with H_2O to check for uniform loading and transfer. The membrane was blocked in 5% skim milk in TBST (50 mM Tris-HCl pH 7.5, 150 mM NaCl, 0.1% Tween) for 1 hour. Primary antibodies were diluted as indicated (Table 2.5) in 5% milk/TBST. Blots were rocked overnight in primary antibody at 4°C and washed 5 x 5 minutes in TBST on an orbital shaker. Horseradish peroxidase conjugated secondary antibodies (anti-rabbit Invitrogen #31460, anti-mouse Invitrogen #31430) were used at a dilution of 1:10,000 for 1 hour rocking at room temperature. Blots were washed 5 x for 10 minutes in TBST. To image, blots were immersed in 3 ml SuperSignal West Dura Extended Duration Substrate (Thermo Fisher #34075) for 30 seconds before placing in a transparent sheet protector. A

G:Box (Syngene) was used to capture immunoblot signals. Each blot was quantitated

using Syngene GeneTools software.

For histone modification immunoblots, after imaging, the blots were stripped

with One Minute Plus Stripping Buffer (GM Biosciences #GM6015) per

manufacturer's instructions and re-probed with the pan-H3 antibody to check for even

loading.

Antibodies

Table 2.5. Antibodies used in immunoblot experiments.

Antigen	Manufacturer	Catalog #	Dilution
H3	Millipore	07-690	1:5000
H3K9me3	Abcam	Ab8898	1:500
H3K27me3	Abcam	Ab6147	1:200
H3K9ac	Santa Cruz	sc-56616	1:200
H3K14ac	Millipore	07-353	1:1000
H3K18ac	Active Motif	39755	1:1000
H3K4me	Abcam	ab8895	1:1000
H3K4me3	Millipore	05-745	1:500
H3K27ac	Millipore	07-355	1:1000
H3.3	Abcam	ab176840	1:500
Papillomavirus L1	Millipore	MAB837	1:10000

Chapter 3: Optimization of the HPV Quasivirus Production System

My contribution to this work was producing recombinant marker neomycin resistant quasiviruses and performing the quantitative colony forming assay (Figure 4A and 4B).

The efficient production of infectious papillomaviruses is difficult due to their strict species and tissue tropism. Furthermore, papillomaviruses will only complete their infectious cycle in the stratified epithelium of their specific host species. Despite these difficulties, several methods have been developed for the generation of virions. Currently, there are five commonly used methods for producing papillomavirus particles (reviewed in [210]).

First, wart derived virions can be isolated from human patients that have natural infections or animals that have been inoculated in an experimental setting. This can be achieved by removing a portion of infected tissue (for example, a wart), disrupting the tissue by physical, chemical, and enzymatic methods, and purifying virions on a density gradient [211, 212]. These samples have the greatest degree of physiological relevance but can be difficult to obtain and do not always contain the desired PV type.

Second, virus like particles (VLPs) consist of the papillomavirus capsid proteins (L1, or both L1 and L2) and can spontaneously self-assemble without any encapsidated DNA. They were first produced in insect cells using recombinant baculoviruses, but other production organisms, such as *Saccharomyces cerevisiae,* have also been developed. [213-215]. VLPs are mostly used in immunological studies of HPV, such as testing antibody binding. VLPs are also the basis for the HPV vaccine; these particles are sufficient to elicit a protective antibody response [216, 217].

Third, viruses can be produced by keratinocytes transfected with the viral genome and grown in a 3D organotypic raft system that supports epithelial differentiation [218, 219]. Virions produced by this method contain the HPV type of interest and are capable of initiating a productive infectious cycle. However, this process is technically challenging, can be laborious and expensive, and only wild type genomes that can complete the entire viral life cycle can be used, limiting the breath of the technique for studying viral mutants.

A major advancement in the area of studying papillomavirus infections was the development of the pseudovirus system [105]. In this system, 293TT cells are used to package reporter plasmids into papillomavirus capsids. 293TT cells were derived from the existing 293T cell line, which are human embryonic kidney (HEK) cells with an integrated copy of the SV40 genome, expressing small amounts of the SV40 T antigen. Researchers transfected the pTIH plasmid into 293T cells to stably express higher levels of T antigen. Reporter plasmids containing the SV40 origin of replication are therefore replicated to a very high copy number in these cells. The expression levels of the viral capsid proteins were massively enhanced by using plasmids that encode L1 and L2 with silent mutations to remove rare codons. To prevent the plasmid from being packaged, "stuffer DNA" was inserted to increase the size above 8 kb (HPV virions cannot efficiently package DNA greater than this size). To generate pseudoviruses, the plasmids expressing L1 and L2 and the reporter plasmids are transfected into the 293TT cells. L1 and L2 proteins spontaneously self-assemble around the replicating reporter plasmid. These particles can be extracted from the cells, allowed to mature in vitro, and isolated by an iodixanol

ultracentrifugation gradient [220, 221]. The resulting particles are useful for studying viral entry, early events in infection, such as the trafficking of the viral capsid, as well as neutralization assays. However, they do not contain any HPV genes and thus cannot complete the viral life cycle or be used to study any HPV-specific functions.

The pseudovirus system was taken a step further by the demonstration that full-length papillomavirus genomes (rather than reporter viruses) could be packaged into papillomavirus particles, dubbed "quasiviruses" [222]. The resulting virus preparations can be generated at high yield, contain the desired HPV type, and have low cost. Quasiviruses are infectious *in vivo*, and are capable of infecting keratinocyte cell lines and primary keratinocytes isolated from humans [70, 223]. The quasivirus-based production system has several additional advantages over other methods of producing infectious HPV particles. Importantly, the process allows the packaging of mutant or recombinant viral genomes that do not need to complete the viral life cycle, resulting in powerful new tools to study infection.

Our laboratory has considerable experience using HPV18 quasiviruses for infection of primary human foreskin keratinocytes (HFKs) to study immediate early viral processes and host cell factor involvement [70, 121]. We use HPV18 genomes because they have more efficient replication and immortalization potential in cell culture compared to other common high-risk HPV types [202, 224, 225]. Using this genome allows for increased signal-to-noise ratios in the readouts of infection. In this chapter, we describe optimization of the existing quasivirus production system to improve the physiological relevance by increasing the genome to particle ratio,

streamline the workflow, and expand the capabilities of quasivirus-based infection assays of primary HFKs.

Results

HPV18 Quasiviruses Produced with HPV16 L1/L2 Capsids Exhibit Higher Infectivity than Those with HPV18 L1/L2

Several laboratories in the HPV field (including ours) find that, for unknown reasons, HPV18 pseudovirions do not infect cells as efficiently as other HPV types (personal communications). To confirm this difference in infectivity of HPV18 genome quasivirus preparations that had the L1 and L2 structural proteins from HPV18 (18L1/L2) or HPV16 (16L1/L2) were prepared as described in Methods, both containing the HPV18 genome. The resulting quasiviruses were used to infect primary HFKs at an MOI of 100. To determine whether furin treatment prior to infection would enhance infectivity of either the 18L1/L2 or 16L1/L2 viruses, 8 U/ml of recombinant furin or vehicle control was added to the media at the time of infection. At 72 hours post infection (hpi), RNA was collected and early viral transcripts were quantified by RT-qPCR. Cells infected with 16L1/L2-HPV18 chimeric quasiviruses expressed significantly higher levels of HPV18 E1^E4 and E6*I than those infected with 18L1/L2 quasiviruses (Figure 3.1A and B). Furthermore, furin treatment did not significantly enhance the transcription from either virus, except in the E6*I from the 16L1/L2 virus, which was slightly enhanced (p=0.045 in an unpaired t-test). These results confirm the findings of others that the use of an HPV16 capsid results in higher infectivity than the use of an HPV18 capsid.

59

Furthermore, furin pretreatment is of limited benefit in the quasivirus infection of primary HFKs. Therefore, all further experiments used chimeric 16L1/L2-HPV18 quasiviruses in the absence of furin.

A

B
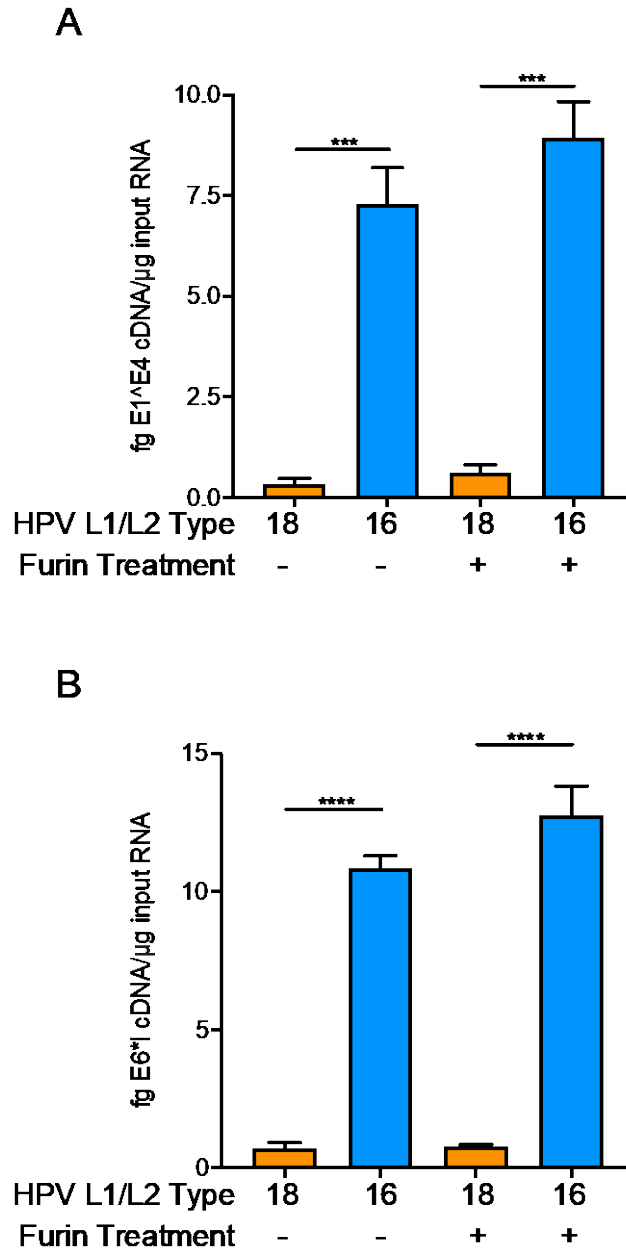
Figure 3.1. HPV18 Quasiviruses Produced with HPV16 L1/L2 Capsids Exhibit Higher Infectivity than Those with HPV18 L1/L2. HPV18 quasiviruses were produced using the L1 and L2 capsid proteins from either HPV18 or HPV16. Primary HFKs were infected at an MOI of 100 in media with or without 8 U/ml recombinant furin. At 72 hpi, RNA was extracted and early viral transcripts were quantified by RT-qPCR and normalized to cellular TBP. A) E1^E4 transcription. B) E6*I Transcription. N=3 technical replicates of infection. Error=SD. Significance determined by an unpaired t-test. ***=p<0.001 ****=p<0.0001.

Using Minicircle DNA Technology to Improve Quasivirus Production,

Physiological Relevance, and Infectivity

The traditional method of producing HPV genomes involves using restriction enzymes to cut the genome from the bacterial plasmid backbone (Figure 3.2A) and performing a dilute ligation reaction to promote intra-molecular recombination. This process does produce recircularized 8 kb viral genomes, but it also produces multiple additional ligation products (Figure 3.2B). Using Minicircle DNA technology, HPV genomes cloned into minicircle backbones (Figure 3.2C) were transformed into E. coli strain ZYCY10P3S2T that expresses the PhiC31 integrase, and I-SceI homing endonuclease [200, 226]. These enzymes are induced by L-arabinose and digest the plasmid backbone and recircularize the viral genome to form an 8 kb monomer (Figure 3.2D). As genomes can be extracted using standard, commercially available plasmid maxiprep kits, this process can be easily scaled for mass production of recircularized genomes for HPV quasivirus production. Additionally, the super coiled covalently closed circular (CCC) genomes produced in this manner are more physiologically relevant as there is no risk of packaging alternative ligation products present in the traditional genome preparations.
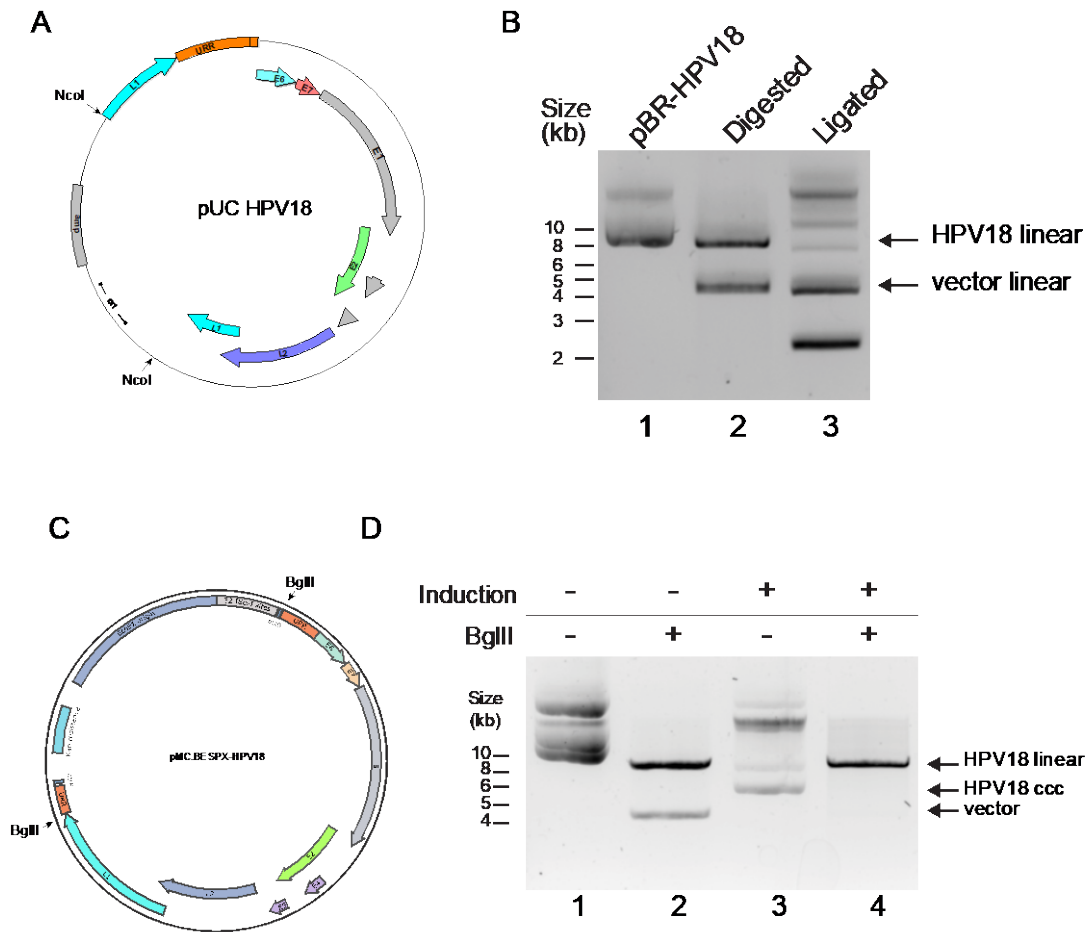
Figure 3.2. Comparison of different HPV genome production methods. A) Map of pUC-HPV18. B) pBR322-HPV18 (lane 1) was digested with EcoRI to remove HPV18 genome from plasmid backbone (lane 2) and then ligated. DNA was precipitated (lane 3), separated on a 0.8% TAE agarose gel, and imaged on a UV lightbox. C) Map of pMC.BESPX-HPV18 D) E. coli ZYCY10P3S2T transformed with the plasmid described in C were induced to generate minicircle HPV18 genomes. Plasmid DNA isolated before and after induction was digested with BglII, separated on a 0.8% TAE agarose gel, and imaged on a UV lightbox. Lane 1: Pre-induction pMC.BESPX-HPV18 undigested; lane 2: pre-induction pMC.BESPX-HPV18 digested; lane 3: post-induction pMC.BESPX-HPV18 undigested; lane 4: post-induction pMC.BESPX-HPV18 digested. CCC-covalently closed circular DNA. A representative genome preparation is shown. Adapted from [207]

To assess whether minicircle HPV18 genomes could be efficiently packaged into HPV quasivirions, we transfected minicircle HPV18WT genomes and a plasmid expressing HPV16 L1 and L2 into 293TT producer cells. Virions were extracted from cells, matured, and isolated by ultracentrifugation through an Optiprep density gradient. To measure viral titer, viral genomes were extracted and quantitated by qPCR. Quasiviruses produced using minicircle genomes had similar titers to those produced with the traditional genomic recircularization process (Figure 3.3A). To measure the amount of the viral capsids, virions were denatured, and virion proteins were separated on an SDS-PAGE gel alongside known quantities of BSA. Quasivirus preparations with minicircle genomes had a similar concentration of virions compared to preparations produced in the traditional manner (Figure 3.3B). To calculate the efficiency of packaging, the number of viral genomes was divided by the number of virions. Quasiviruses with minicircle genomes package HPV18 DNA to similar degrees to those that are made with recircularized genomes (Figure 3.3C). Taken together, these data show that using minicircle genomes to make the quasivirus production workflow more efficient do not compromise yield or packaging of the resulting viruses.
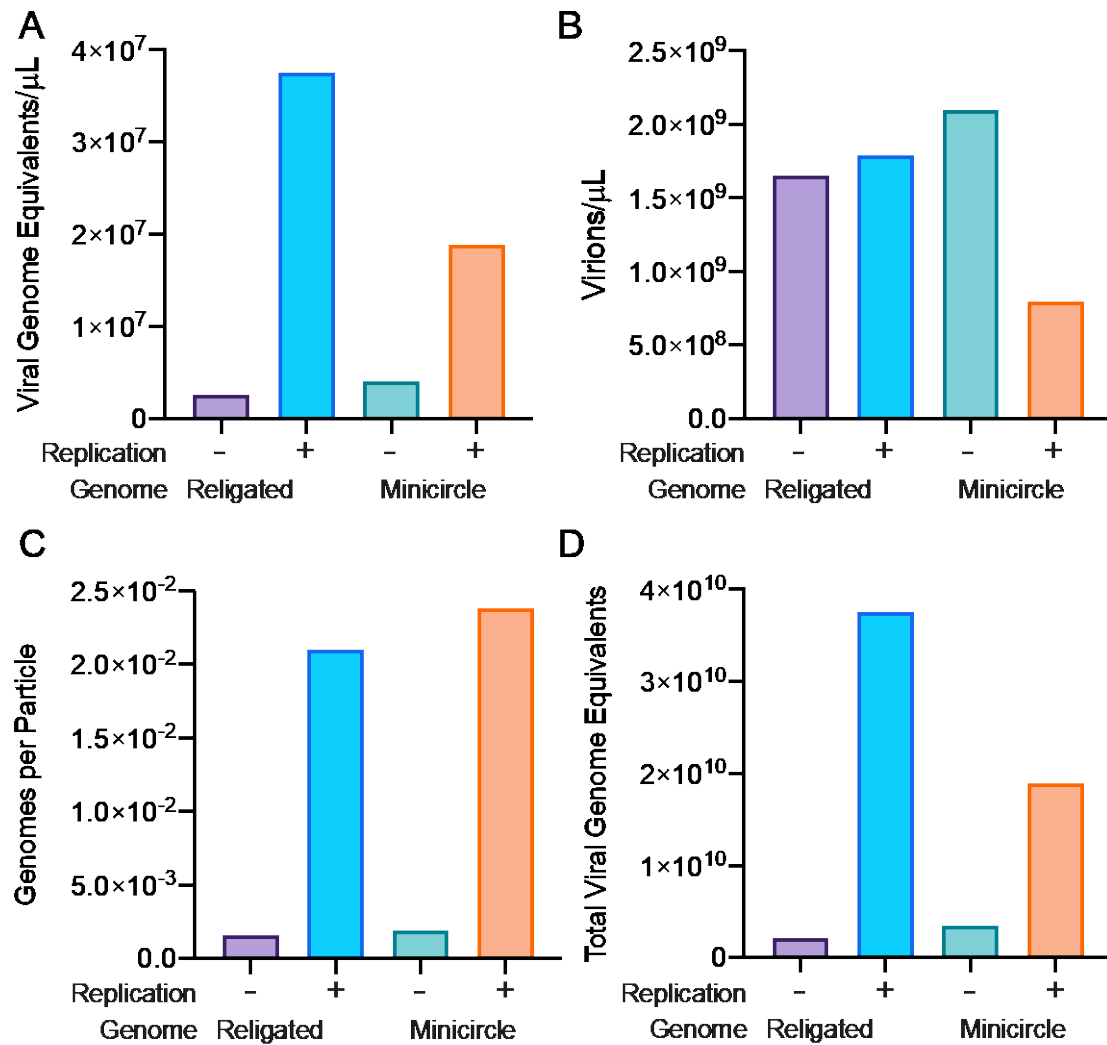
Figure 3.3. Viral titer and virion yield of HPV18 quasiviruses. HPV18 quasiviruses were produced with either minicircle or traditionally religated genomes. For both genome types, viral replication in 293TT cells was optionally induced by the expression of E1 and E2 replication proteins by co-transfection. A) Viral genomes were extracted from virions and quantitated by qPCR. B) Quasivirus preparations were separated by SDS-PAGE alongside a standard curve of BSA. Gel was stained with Sypro Ruby and imaged. Standard curve used to calculate quantity of virions. C) Packaging efficiency of quasivirus preparations. D) Yield of quasivirus preparations measured by total viral genome equivalents. N=1.

Next, we determined if there was any difference in infectivity of these viruses in the infection assays. HPV18 quasiviruses produced using normal and minicircle genomes were used to infect primary HFKs at an MOI of 100. At 72 hpi, RNA was harvested from infected cells. RT-qPCR was performed and the early viral transcripts E1^E4 and E6*I were normalized to cellular gene TATA Binding Protein (TBP). Cells infected with minicircle quasiviruses had significantly higher levels of early viral transcripts than those infected with quasiviruses made with recircularized genomes (Figure 3.4). Overall, these results show that the minicircle genome improves the ability of the quasivirus to perform the early viral functions immediately after infection of the host cell.
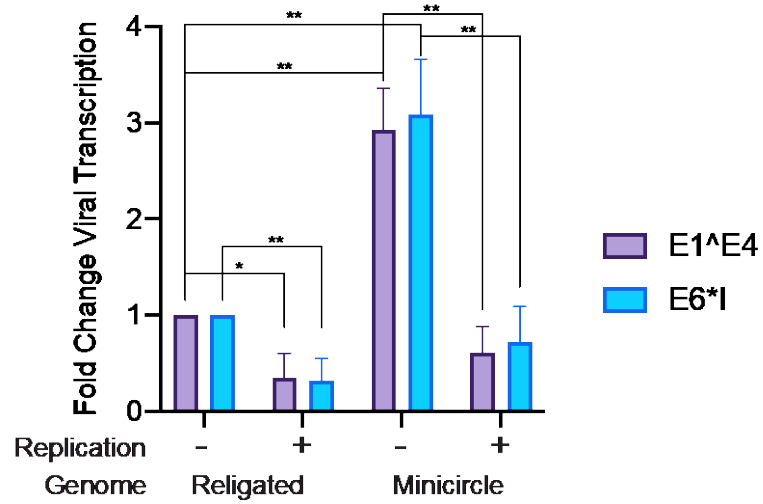
Figure 3.4. Infections of HFKs with different HPV18 quasivirus preparations. Primary HFKs were infected at an MOI of 100 with the indicated preparations of HPV18 quasivirus. RNA was collected at 72 hpi and viral transcripts were quantified by RT-qPCR and normalized to cellular TBP. Data are presented as fold change over religated, unreplicated quasivirus. N=3 biological replicates of infection. Error=SD. Significance determined by an unpaired t-test. *=$p<0.05$ **=$p<0.01$

Inducing Replication of the Viral Genomes in 293TT Packaging Cells

293TT cells are not the natural host of papillomaviruses and the genome is unable to transcribe the viral proteins E1 and E2 necessary for replication of the viral genome. It would be advantageous to induce viral DNA replication inside these packaging cells for three reasons. Firstly, it might increase the maximum yield from each quasivirus preparation as there is a limit on how much HPV DNA can be transfected into the cells. Thus, one way to increase the number of viral genomes being packaged is to induce replication inside the 293TT cells. Secondly, we theorized that this would improve the packaging efficiency (genomes per particle) by increasing the ratio of genomes to L1 and L2 proteins inside the packaging cell. Lastly, nucleosomes preferentially associate with newly replicated DNA [227-229]. Given our interest in the virally packaged chromatin, it was especially important to optimize the physiological relevance of the packaged quasivirus chromatin. To induce replication of the viral genome inside the packaging cells, we transfected 293TT cells with either a recircularized or minicircle HPV18 genome, the L1/L2 expression plasmid, and plasmids expressing codon-optimized version of the viral replication proteins E1 and E2 [203].

To determine whether replicating viral genomes inside 293TT cells would result in higher titers and improved packaging, we prepared quasivirus stocks by co-transfection of either the codon optimized E1/E2 expression plasmids or empty vector controls with both traditionally recircularized and minicircle HPV18 genomes. After virion extraction, the preparations were digested with DNase I to remove any residual

68

DNA outside the capsid and the viral genomes were extracted from the capsid and quantitated by qPCR for HPV18 DNA. As shown in Figure 3.3A, quasivirus preparations produced with the E1/E2 co-transfection had significantly higher titers of HPV18 for both religated and minicircle genomes. To determine if the replicated quasivirus preparations simply had more particles or had a higher genome to particle ratio (better packaging), we quantitated the amount of virion particles by calculating the amount of the viral L1 protein by separating virion preparations on a SDS-PAGE gel stained with total protein stain alongside known quantities of BSA. Quasivirus preparations produced with replicated genomes had comparable concentrations of virions to those made with unreplicated genomes (Figure 3.3B). As shown in Figure 3.3C, the E1/E2 replicated quasiviruses had far higher numbers of packaged HPV genomes per particle for both genome types. The overall yield of quasiviruses improved as well with E1/E2 replication in the packaging cells (Figure 3.3D). The combined data suggest that viral genome replication inside 293TT packaging cells during routine quasivirus production not only increases the yield of quasivirus preparations, but also the physiological relevance by decreasing the relative percentage of "cold" capsids (without viral genomes) that could interfere with infection of "hot" capsids containing viral genomes.

To see if genome replication inside the packaging cells during quasivirus production would impact the infectivity of these preparations, we infected primary HFKs at an MOI of 100. At 72 hpi RNA was harvested. To quantitatively evaluate the infections, RT-qPCR was performed to detect the spliced viral transcripts E1^E4 and E6*I. The levels of viral transcripts were normalized to that of the cellular control

69

gene TBP. Cells infected with quasiviruses with genomes that were replicated in 293TT cells showed a decrease in early viral transcription at 72 hours compared to genomes that had not been replicated (Figure 3.4). Additionally, we observed that the differences in transcriptional activity from religated and minicircle genomes disappeared after genome replication in 293TT cells (Figure 3.4). Therefore, replication of the viral genomes during packaging of HPV quasiviruses reduces early transcription shortly after infection.

"Ripcord" Production of HPV Quasiviruses

One of the major drawbacks of the existing quasivirus production method is that the preparations contain virions that package linearized cellular DNA. This is due to the addition of the nucleases Benzonase and Plasmid Safe during the maturation step. They serve to increase yield by freeing virions stuck to cellular DNA but, consequently, the host genome is cleaved into lengths of DNA the same size, or smaller, than the HPV genome. As the structural capsid proteins L1 and L2 promiscuously package essentially any DNA ~8 kb or smaller without sequence specificity, the spontaneously self-assembling virions can result in particles containing cellular DNA.

To increase the particle to infectivity ratio, we produced quasiviruses using the "Ripcord" method developed for HPV pseudoviruses by the Buck Laboratory [31]. In this protocol, during the maturation step, the DNases are omitted and RNases A and T1 are added instead. Additionally, the concentration of NaCl is lowered to reduce the solubility of capsids that are not fully matured. To determine if this would also enrich for HPV18 genome containing particles in quasivirus preparations, we

measured the viral titer of virions in ripcord and traditionally prepared quasivirus preparations. As expected, ripcord quasivirus preparations had a significantly reduced viral genome equivalents per µl (Figure 3.5A). Ripcord preparations also had a significantly reduced concentration of virions (Figure 3.5B). However, the percent of capsids containing genomes was higher in the ripcord preparations than the controls (Figure 3.5C). To assess whether this would result in increased infectivity, primary HFKs were infected at an MOI of 100 with either ripcord or normal quasivirus preparations. At 72 hpi, RNA was collected and RT-qPCR was performed for spliced early viral transcripts and viral genome replication. In agreement with our hypothesis, cells infected with ripcord quasiviruses had substantially higher levels of early viral transcripts than those infected with traditionally prepared quasiviruses (Figure 3.6A and B). The results suggest that the "ripcord" maturation technique substantially improves quasivirus infection of keratinocytes.
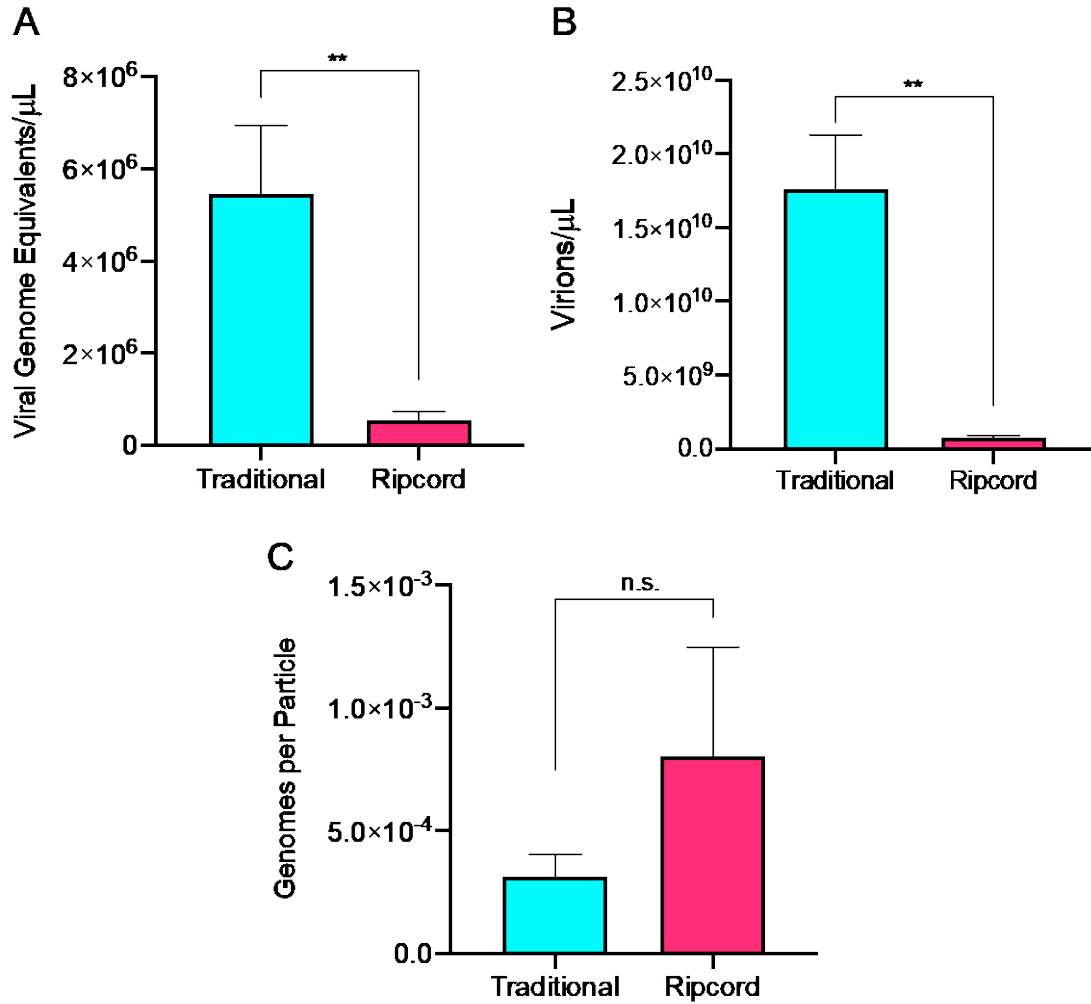
Figure 3.5. Yield and packaging of HPV18 quasivirus preparations produced with the "ripcord" maturation method. HPV18 quasiviruses were produced either by the "ripcord" method or traditional maturation and quantified. A) Viral genomes were extracted from virions and quantitated by qPCR. B) Quasivirus preparations were separated by SDS-PAGE alongside a standard curve of known protein amounts. Gel was stained with Sypro Ruby and imaged. Standard curve was used to calculate quantity of virions. C) Packaging efficiency of quasivirus preparations. N=3 independent preparations. Error=SD. Significance determined by unpaired t-test. n.s.=not significant. **=$p<0.01$
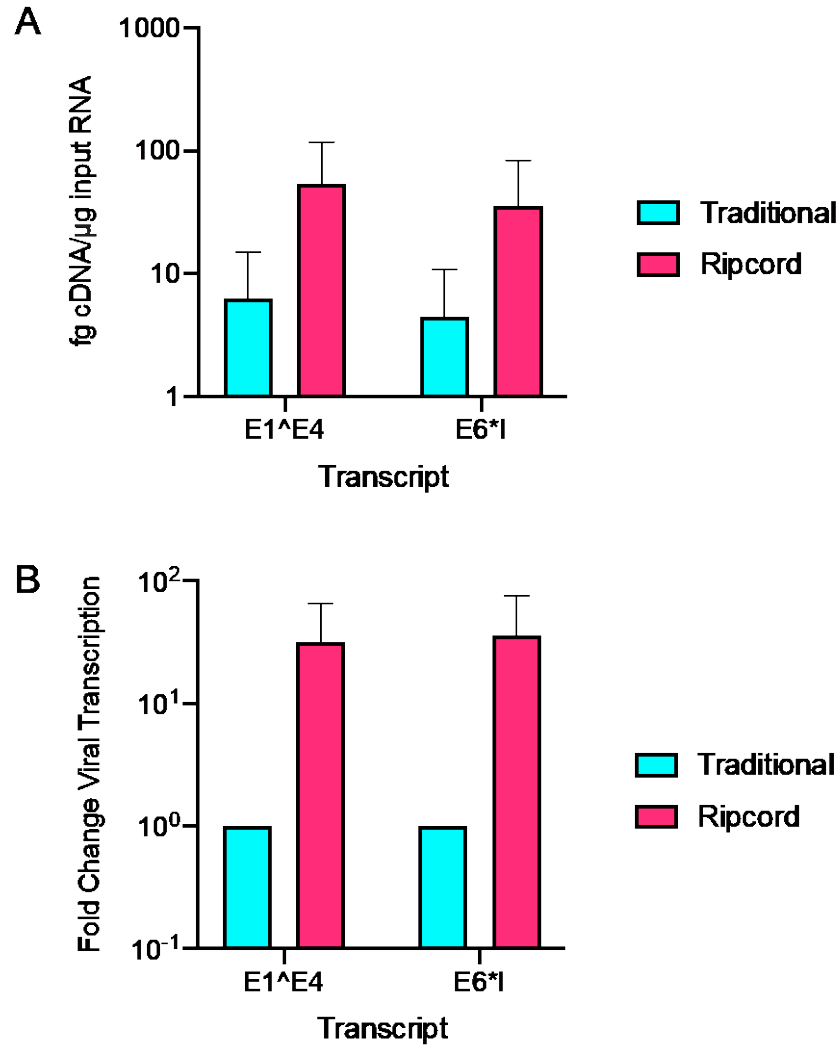
Figure 3.6. Infections of HFKs with ripcord HPV18 quasiviruses. Primary HFKs were infected at an MOI of 100 with ripcord or traditionally prepared HPV18 quasivirus. At 72 hpi, RNA was collected and viral transcripts were quantified by RT-qPCR. A) Viral transcripts E1^E4 and E6*I normalized to cellular gene TBP. B) Data presented as fold change over traditional quasivirus preparations. N=2 biological replicates of infection. Error=SD.

Infection-Based Keratinocyte Colony Formation Assay to Study Viral Establishment

The quasivirus infection system is useful for studying early events in the viral life cycle, but we wanted to extend this to analyze and measure the establishment of the viral genome in infected cells. Recombinant HPV genomes with selectable genes inserted into the late region have been previously developed in our laboratory (Figure 3.7). A cassette containing a gene conferring resistance to the antibiotic neomycin was inserted into wildtype and E1 mutant (replication incompetent) HPV18 genomes. Cells that established the wildtype HPV18neo genome as an extrachromosomal replicon exhibited resistance to neomycin and formed colonies under selection [204]. To determine whether these genomes could be delivered by infection, we packaged the HPV18neo genome in HPV16 capsid proteins in 293TT packaging cells.
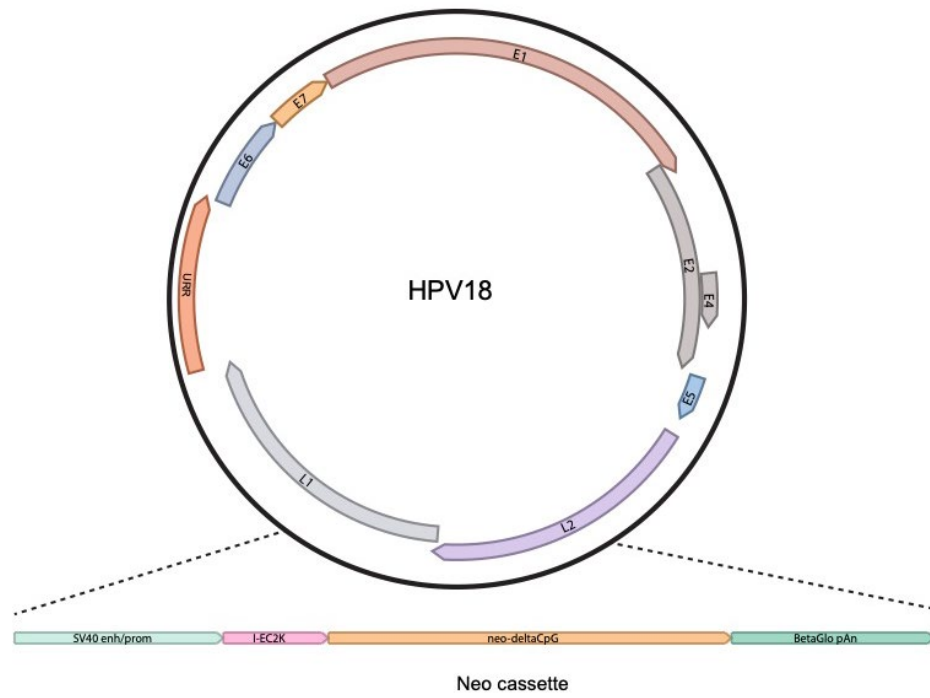
Figure 3.7. HPV18neo genome. The cassette conveying resistance to neomycin is inserted into the late region at Asp718 sites (indicated by dashed lines). Adapted from [204].

To determine whether the genomes delivered by infection could be established as replicating extrachromosomal elements that immortalized primary keratinocytes, we infected primary HFKs with neomycin marker quasiviruses at an MOI of 100. At 48 hpi, we began selection with 50 µg/ml neomycin for either seven days (short selection scheme) or continuously (long scheme). The two separate selection schemes allow us to distinguish between colonies that formed due to transient expression of the neomycin resistance gene and those that formed due to an established, persistently replicating viral genome. Cells were cultured for an additional 14 days until colonies were visible before being fixed in formalin and stained with methylene blue. Plates that underwent the "short" selection scheme showed large colonies in cells infected with the wildtype marker quasivirus, and smaller colonies in those infected with the replication incompetent E1 mutant genome (Figure 3.8A). The colonies of cells that underwent continuous G418 selection were smaller overall and markedly reduced in number (Figure 3.8B). In all cases, no colonies appeared on the mock infected plates. There were far fewer colonies in plates infected with the E1 mutant genome. Therefore, viral DNA replication is required for the establishment of persistent infection.
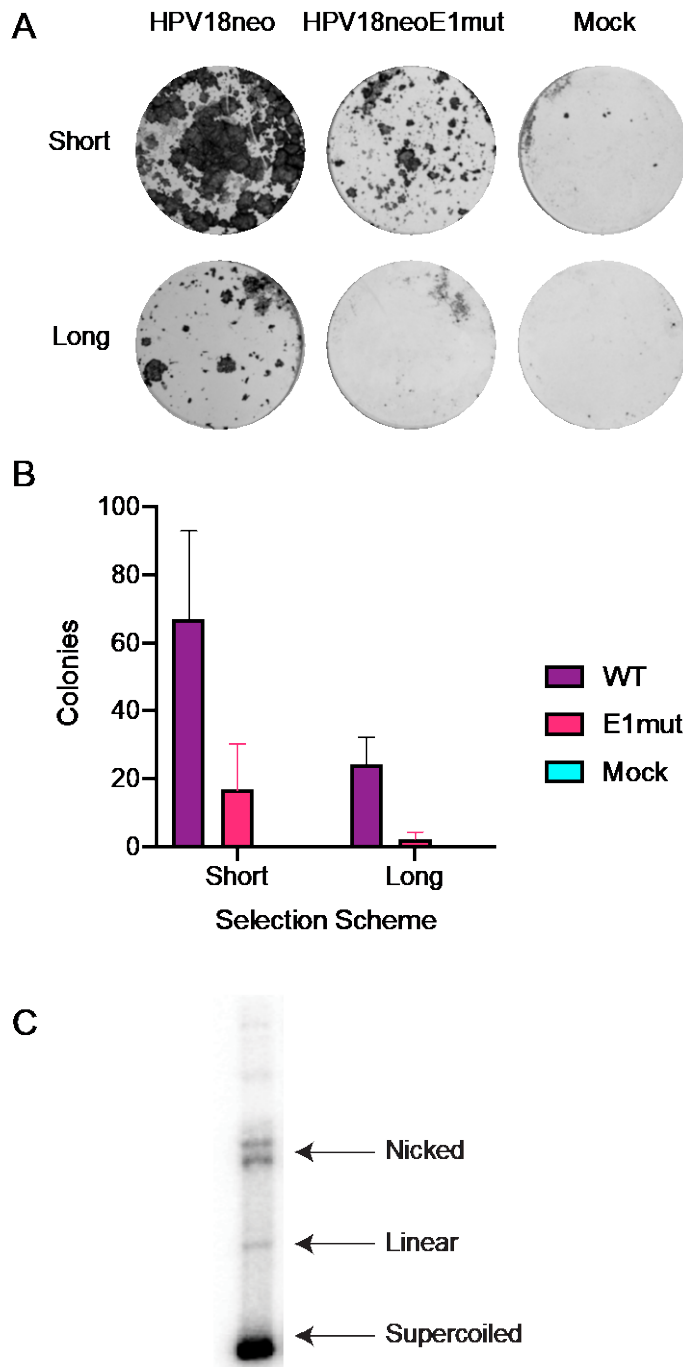
Figure 3.8. Recombinant HPV18 neo quasiviruses establish long-term infections in primary HFKs. A) HPV18neo and HPV18E1mutneo marker quasiviruses were used to infect primary HFKs at an MOI of 100 and selected with 50 μg/ml G418 selection for either seven days (short) or continuously until staining. After 16 days feeders were removed, and keratinocyte colonies were stained with methylene blue. B) Quantification of colonies in A. N=3 biological replicates. Error=SD. C) HPV18neo and HPV18E1mutneo marker quasiviruses were used to infect primary HFKs at an MOI of 100 and selected with 50 μg/ml G418 selection for continuously until colonies formed. At 16 dpi, two colonies were transferred to individual plates and cultured for three passages under continual selection. DNA was extracted and a southern blot was performed to detect extrachromosomal HPV18 DNA. A and B adapted from [204].

To ensure colony formation was the result of the marker genome establishing as a persistently maintained episome and not as a result of viral integration into the host chromosomes, we repeated the colony formation assay with the wildtype and E1 mutant neomycin HPV quasiviruses. The colonies that formed were separately transferred to individual plates. The cells were able to proliferate in the presence of continual selection for at least three passages. DNA was collected and a southern blot was performed to detect extrachromosomal HPV DNA. As shown in Figure 3.8C, cells infected with wild type neomycin marker genomes contained extrachromosomal plasmids. Therefore, the infection-based colony formation assay is a powerful tool to study the establishment of persistent infection.

Large T Directed Replication of HPV Genomes in 293TT Cells During Quasivirus Production

In the HPV18neo genome, the neomycin resistance cassette is driven by an SV40 promoter/ori element. In SV40, the enhancer/promoter and replication origin overlap, and this could have the advantage of allowing the HPV18neo genome to replicate in the 293TT packaging cells, which stably express the SV40 Large T antigen. However, the neomycin resistance cassette was derived from a plasmid that was devoid of CpG dinucleotides to avoid deleterious effects on expression and persistence of the transgene [230, 231]. This could potentially render the SV40 origin of replication nonfunctional. Therefore, we reinstated the CpG dinucleotides in the SV40 origin of replication by gene synthesis. The CpG free and SV40WT HPV18neo genomes were transfected into 293TT cells with the plasmid expressing the HPV16 structural proteins L1 and L2. Quasiviruses were isolated and the genomes were

extracted. The extracted viral genomes were digested with either DpnI or MboI to differentiate between genomes that had been replicated in the 293TTs and those that had not. Quasivirus genomes with the native SV40 origin had significantly higher levels of unreplicated (Figure 3.9A), replicated (Figure 3.9B), and total HPV18 DNA (Figure 3.9C). The CpG free genome did not replicate at all. As the concentration of viral particles in the two preparation was equivalent (Figure 3.9D), the packaging efficiency was significantly higher in quasiviruses with the native SV40 origin (Figure 3.9E). Taken together, the data show that Large T directed replication of the recombinant viral marker genome improves the production of marker genome quasiviruses.
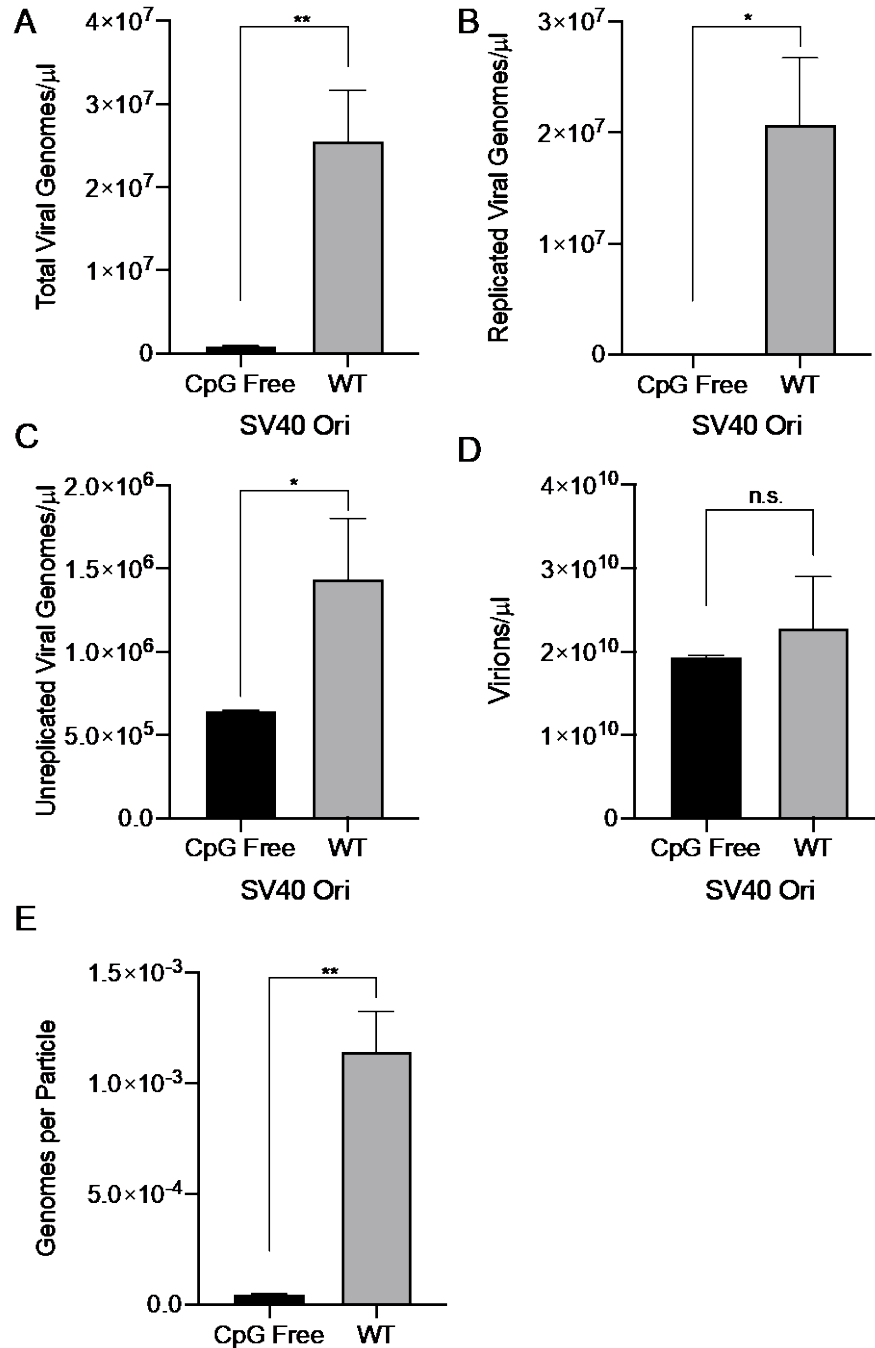
Figure 3.9. Viral titer and virion yield of HPV18neoSV40 quasiviruses. HPV18 marker genomes containing a neomycin resistance cassette with a wild type or CpG free SV40 origin of replication were produced. Viral genomes were extracted from the virions and digested with MboI or DpnI to differentiate between unreplicated and replicated viral DNA. HPV18DNA was quantitated by qPCR. A) Unreplicated packaged viral genome equivalents. B) replicated packaged viral genome equvialents. C) total packaged viral genome equivalents. D) Quasivirus preparations were separated by SDS-PAGE alongside a standard curve of BSA. Gel was stained with Sypro Ruby and imaged. Standard curve used to calculate quantity of virions. E) Packaging efficiency of quasivirus preparations. N=2 to 4 technical replicates (viral preparations). Error=SD. Significance determined by unpaired t-test. *=p<0.05 **=p<0.01

To determine if the increase in titer and packaging would affect the infectivity of these quasivirus preparations, we used the quasiviruses in an infection assay of primary HFKs. The level of early viral transcripts from the marker genomes with the native SV40 origin of replication was significantly lower than the transcripts from marker genomes with the mutated, CpG free SV40 origin (Figure 3.10A and B). However, the level of transcription from the neomycin resistance cassette was equivalent from both genomes (Figure 3.10C). Therefore, replication of the viral genome in packaging cells in a Large T-dependent manner has a deleterious effect on early viral transcription.
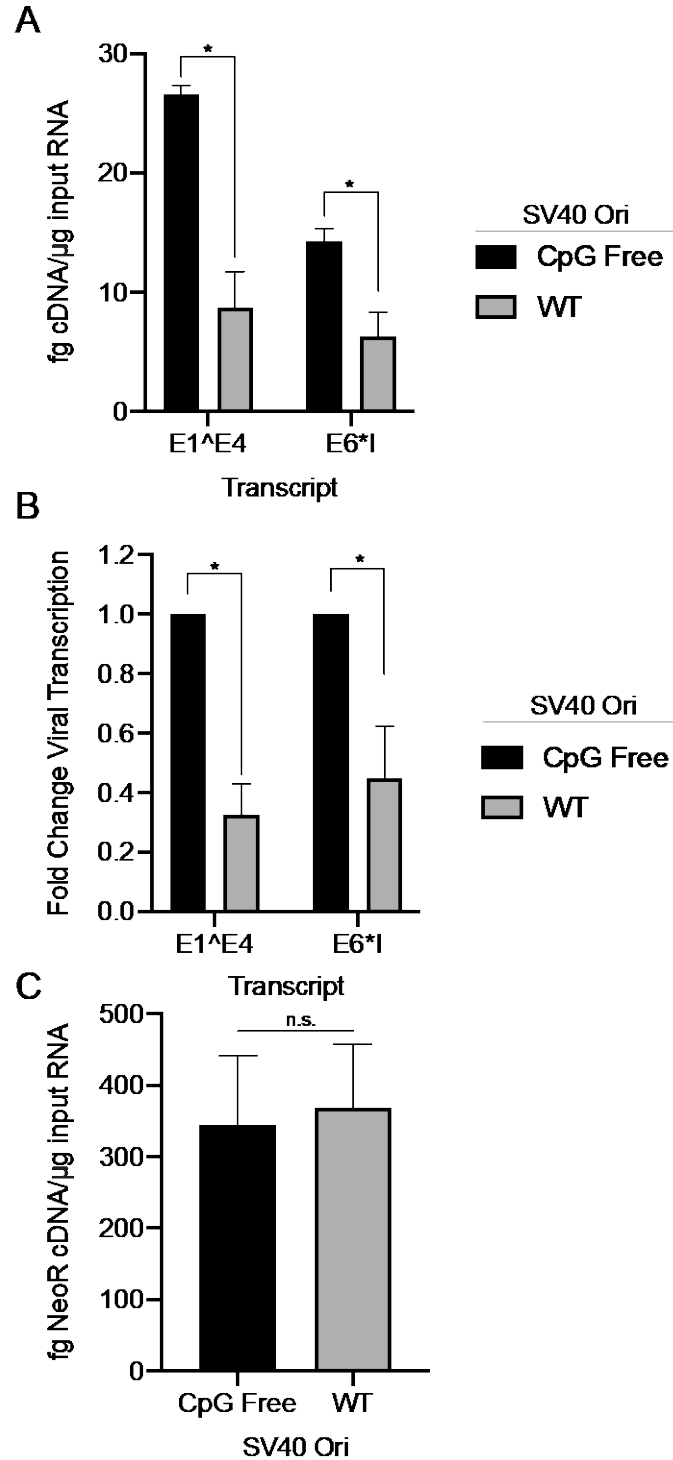
Figure 3.10. Infections of HFKs with HPV18neoSV40 quasiviruses. Primary HFKs were infected at an MOI of 100 with neomycin resistance marker HPV18 quasiviruses with or without a wildtype SV40 origin of replication. At 72 hpi, RNA was collected, and viral transcripts were quantified by RT-qPCR. A) Viral transcripts E1^E4 and E6*I were normalized to cellular gene TBP. B) Data presented as fold change from traditional marker genome. C) Transcription of the neomycin resistance gene. N=2 biological replicates of infection. Error=SD. Significance determined by an unpaired t-test. n.s.=not significant. *=p<0.05

Discussion

The use of minicircle HPV genomes for quasivirus preparations dramatically streamlines the production process and has biological advantages. The original method, which involved restriction digestion to free the genome from the backbone followed by a dilute ligation, precipitation, and resuspension generated multiple undesired ligation products. We found that there was no difference in the titer, yield, or packaging of quasivirus preparations made with minicircle genomes. The finding that viral transcription from these genomes was increased after infection shows that there are enhancements to the early viral lifecycle by using minicircle genomes in addition to the technical benefits. This is likely explained by the minicircle genomes having a more uniform and consistent template; they are essentially 100% genomic monomers while traditional quasiviruses package an assortment of ligation products that may be too large to be packaged or not be able to perform all viral functions. For genomes cloned into the plasmid backbone using EcoRI, the cleavage site disrupts the E1 ORF. An incorrectly religated genome would be unable to synthesize the replication proteins after infection, preventing the initiation of the early viral lifecycle. This idea is supported by the finding that the transcriptional benefit from minicircle genomes was decreased when the viral genomes were induced to replicate inside the 293TT packaging cells. Only properly religated viral genomes will replicate to form additional copies of the correct size, thereby reducing the relative advantage of minicircles.

The ability to induce replication of the viral genome in 293TT cells has both technical advantages to aid the production process and increased physiological

relevance. Increasing the yield from each quasivirus preparation means that more infections can be done with a single preparation, decreasing the variability over multiple experiments. Furthermore, the increase in the infectivity to particle ratio improves the physiological relevance of our virus preparations. In natural infections, the percent of virions containing genomes is higher than in traditional quasivirus preparations. Despite our initial predictions that this improved packaging would improve infectivity, we saw a decrease in early transcription. Previous studies have shown that the genomes of native papillomavirus virions are tightly organized into nucleosomes [29]. Previous studies have shown that the ordering of nucleosomes differs on transfected DNA dependent on its replication state [232]. The positioning of nucleosomes can be transcriptionally repressive, possibly explaining the decreased transcription we observed from quasiviruses with replicated genomes [233]. While this reduces viral transcription, it is likely to increase the physiological relevance.

Using the alternative "Ripcord" maturation protocol, we could greatly improve the infectivity of the infection assays of primary HFKs. We attribute this to two factors. Firstly, it is possible that the improved particle to infectivity ratio decreases the number of capsids without a viral genome competing for entry at the receptor, resulting in a higher percentage of infection events that result in productive viral processes. Secondly, as the maturation step of the "ripcord" process does not involve the addition of nucleases, and thus should drastically reduce the amount of cellular DNA of sufficiently small size to be packaged, there should be a sharp reduction in the proportion of "infections" delivering 293TT DNA to the host keratinocyte. We speculate that the delivery of large amounts of random linearized

segments of cellular genomic DNA would trigger an innate immune response in the host cell, possibly shutting down real viral transcription. We can reduce the MOI and still get useful levels of transcription and replication, again allowing for more physiologically relevant infections, and extending the number of replicates of infection that can be conducted per quasivirus preparation.

Our initial results from the colony formation assay provided some insight into HPV establishment. We observed that not all cells that were successfully infected established as a persistent infection. Some of the cells would be initially resistant to the selection for several days, but then the colony would collapse (preliminary data, not shown). This suggests that there is an additional event or events that govern the transition from the immediate early lifecycle to the establishment of the genome as a persistently maintained plasmid and should be studied further. Transient colonies that formed under short selection in cells infected with the HPV18 E1 mutant neo genome do not represent true establishment. These cells transiently express the neomycin resistance gene and this allows them to survive for a few divisions. In addition, cells might be infected with multiple replication incompetent marker genomes that are partitioned to daughter cells, allowing survival until the selection was removed. Future work using these methods could involve using genomes with mutated viral genes, siRNA depletion or CRISPR-Cas9 deletion of host cell genes, or treatment with epigenetic modulators to gain more insight on the factors that govern HPV establishment.

The ability to induce replication of the marker HPV genomes by utilizing the large T expressed in the 293TT packaging cells has several advantages. Firstly, it

eliminates the need to co-transfect the pMEP4-E2 and pMEP9-E1 plasmids. This had

the benefit of reducing the amount of Lipofectamine needed for the transfection,

reducing toxicity to the packaging cells, which may improve the overall yield of the

preparation. Secondly, E2 (and E1) can be toxic to cells when expressed in high

amounts, so the elimination of this protein could improve the health of the 293TT

packaging cells. The relative levels of replicated HPV18 DNA packaged by the virion

(~90%) are comparable to the previously reported levels of quasivirus preparations

made with E1/E2 co-transfection [121]. We speculate that the decreased transcription

from the Large T-replicated genomes is due to the same causative factor as for the

E1/E2-replicated genomes.

Overall, throughout this chapter we describe significant advancements to the

quasivirus production method. We improved the workflow, allowing for easier and

more high-throughput production. We also took a number of steps to improve the

physiological relevance of the resulting virions, potentially making the infection

assays more representative of natural infections, while still maintaining the

advantages of the quasivirus system. In addition, the ability to package recombinant

genomes with transgene expression cassettes expands the breadth of applications that

the quasivirus system can be used for. Together, the work described in this chapter

materially advanced and aided the work in the subsequent sections.

Chapter 4: Profiling of Chromatin Modifications Packaged in Papillomavirus Particles

Introduction

Post-translational modification (PTM) of the histones in cellular chromatin modulates many cellular processes, such as transcription, DNA replication, DNA repair, and differentiation. In particular, PTMs of the core histone proteins H2A, H2B, H3, and H4 are key to this regulation. The genomes of several DNA viruses are bound by cellular histones to form chromatin at various stages of the lifecycle and this adds an additional layer of regulation to viral transcription and replication [171]. In turn, host cell epigenetic processes can also modify viral chromatin as part of the intrinsic immune response [234].

In papillomaviruses, chromatin modifications regulate many aspects of the viral lifecycle. Transcription of viral genes is regulated by methylation of viral DNA, nucleosome position, histone PTMs, and associated chromatin binding factors (reviewed in [235]). During persistent infection, the viral mini-chromosomes are also attached to specific regions of the host chromosomes to partition viral genomes to daughter cells [91, 236]. HPV proteins also manipulate the cellular chromatin modifying machinery in a manner beneficial to various viral functions. For example, the E6 protein from oncogenic HPVs manipulates the host histone acetyl transferase (HAT) Tip60 to modify cellular transcriptional pathways [186]. The other viral oncoprotein, E7, causes global epigenetic changes in host cells by interacting with the histone acetyltransferase (HAT) CBP/p300 and the lysine demethylase KDM6 [197].

A relatively novel feature of the *Papillomaviridae* is that the viral genomes are packaged in chromatin inside the viral capsid. The viral DNA is wrapped around host histones into about 30-32 nucleosomes inside the capsid [237]. The

Polyomaviridae also share this trait; however, most other DNA viruses package their genome either as naked DNA or utilize other non-histone DNA binding proteins. For example, adenovirus protein VII binds and condenses the viral genome prior to packaging [238]. On the other hand, the genomes of the *Herpesviridae* are not packaged in nucleosomes, but shortly after infection they become associated with histones for most of the lifecycle [239, 240]. Chromatinization of incoming naked viral DNA gives the cell an opportunity to deposit repressive chromatin in an anti-viral manner, but viruses often manipulate and take advantage of these responses to promote the viral lifecycle (Reviewed in [170]). At the late stages of a herpesvirus infection, histones must be stripped off the genome during packaging, and the genome is encapsidated as naked DNA [241-243].

It has been recognized for decades that papillomavirus DNA is packaged in nucleosomes within the virion [237], but little is known about the epigenetic modifications on the packaged chromatin. Chromatin modifications have the potential to regulate immediate early transcription, and thus represent an opportunity to gain insight into a critical phase of the viral lifecycle that has not been extensively studied. In this chapter, we profile the post translational modifications (PTMs) of histones packaged in HPV18 quasiviruses, as well as BPV1 and HPV1 virions isolated from warts. We show that wart derived virions contain histones enriched in modifications usually associated with "active" chromatin.

Chromatin Modifications Packaged in HPV18 Quasivirions

Our initial experiments used HPV quasiviruses as they are the most easily produced papillomavirus virions that contain a full viral genome. Quasivirions were produced as described in Materials and Methods using an HPV18 minicircle genome (supercoiled, recircularized DNA generated in bacteria) that had been replicated in the 293TT packaging cells by co-transfection with E1 and E2 expression vectors (too large to be packaged). Replication was induced in the 293TT packaging cells because nucleosomes are more uniformly ordered on newly replicated DNA, and previous studies of the nucleosomes packaged in native papillomavirus virions indicated that their organization is relatively uniform [229, 237]. After purification of the quasivirus particles on an Optiprep gradient, virion proteins from ~2.4 x 10^{12} virion particles (1.4 x 10^9 VGE) were denatured, separated by SDS-PAGE and stained with methylene blue. The canonical histone bands (H2A, H2B, H3 and H4) were extracted from the gel and processed for mass spectrometry analysis of PTMs (Figure 4.1). Histones from the 293TT packaging cells were acid extracted and used as "input" controls.
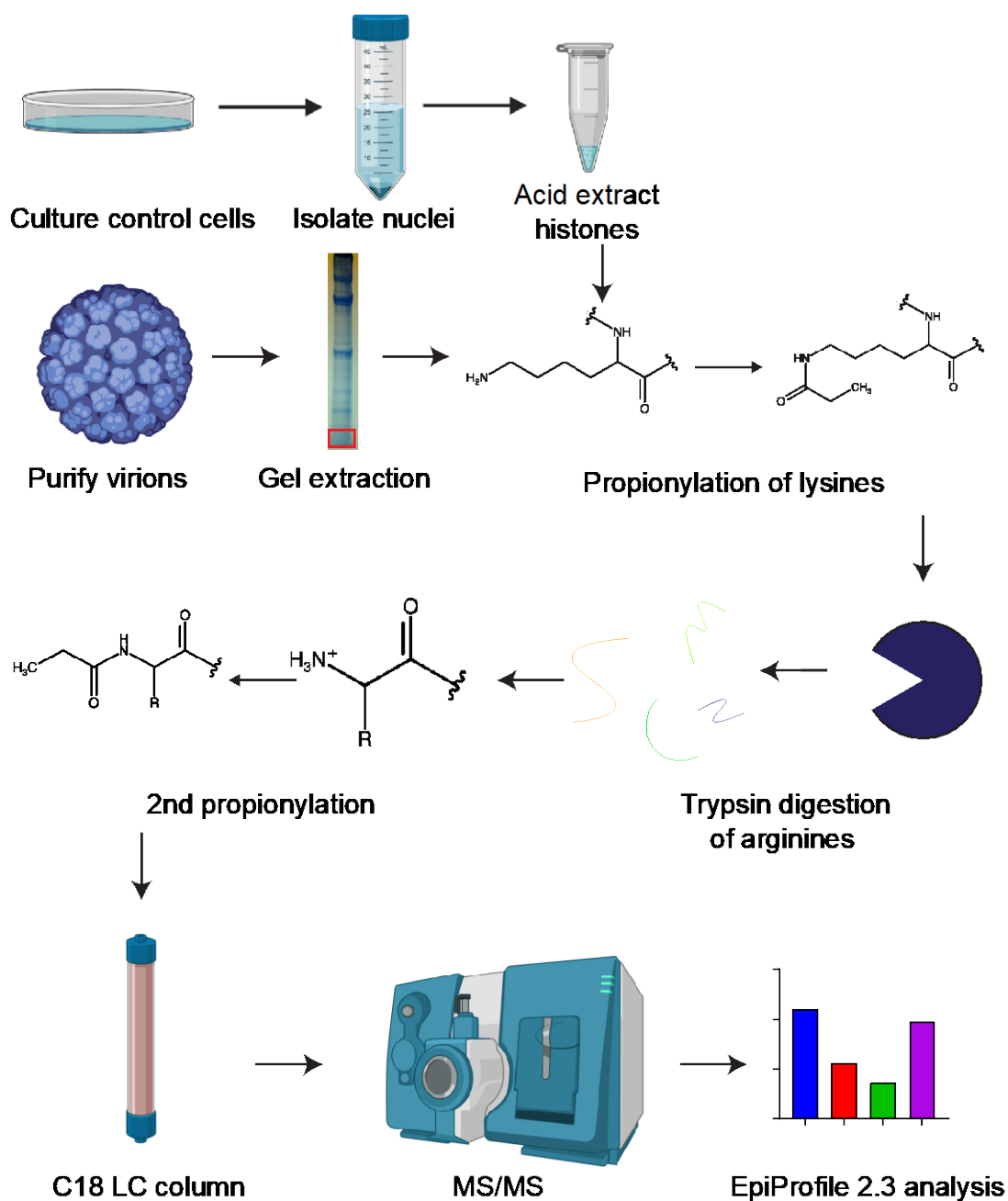
Figure 4.1. Overview of the histone isolation and mass spectrometry experimental workflows. Histones are extracted from virions or cellular controls and chemically derivatized by propionic anhydride. This restricts proteolytic digestion with trypsin to arginine residues, after which another round of propionylation of the N-termini of the resulting peptides is conducted. Samples are desalted and run through a C18 column before DIA MS/MS mass spectrometry analysis.

The highly modified N-terminal histone "tails" contain many basic residues that would be cleaved by the trypsin digestion used for standard mass spectrometry (Figure 4.2). To limit digestion, the histone samples were propionylated prior to trypsin digestion to block proteolytic cleavage of lysine residues (Figure 4.1). As a result, trypsin digestion creates longer, usable peptides (5-20 amino acids in length) by limiting cleavage to arginine residues (Figure 4.2). After trypsin digestion, another round of propionylation was conducted to reduce the charge of the peptides and to improve subsequent chromatographic retention. The peptides were separated by hydrophobicity on a C18 column and loaded into the mass spectrometer where data-independent acquisition (DIA) analysis was performed. The data were analyzed using EpiProfile 2.3 software [209] that enables calculation of the relative abundance of the modification on each histone peptide. This process also allows for the determination of the relative amounts of different histone H3 variants (changes in the amino acid sequence of this histone protein) H3.1 and H3.3 (Figure 4.3).

Figure 4.2. Histone peptides generated from trypsin digest after propionylation. Common modifications on lysines residues are indicated. Arginine and lysine residues are highlighted.
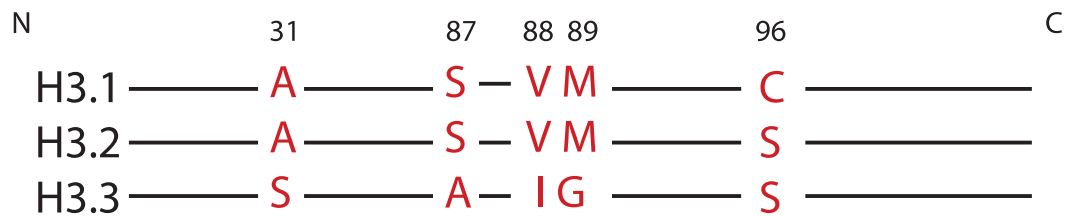
Figure 4.3. H3 variants. Diagram of H3 variants H3.1, H3.2, and H3.3. Differences in amino acid sequence are indicated in red.

As shown in Figures 4.4 and 4.5, and in Supplementary Table 1, the HPV18 quasiviruses contained histones with a wide variety of PTMs. The most common modifications detected on the N-terminus of Histone H3 (Figure 4.4) and H4 (Figure 4.5) were methylation and acetylation of lysine residues. For the most part, the overall distribution of histone PTMs in the HPV18 virions was very similar to those of the host 293TT cells. However, some modifications were present at different abundances between the virus and host cell histone samples. On histone H3, the biggest changes were depletions of acetylation of H3K14 (H3K14ac), dimethylation of H3K27 (H3K27me2), and the combinatorial modification H3K27me2K36me2 (Figure 4.4B, D, and E). We also detected a slight increase in H3K18ac in the quasivirus (Figure 4.4C). For histone H4, the quasivirions had a small increase in acetylation of lysine 5 by itself, and in combination with lysines 8, 12, and 16 (H4K5ac K8ac K12ac K16ac) (Figure 4.5A, Supplementary Table 1). There was also a decrease in acetylation of K16 (Figure 4.5A). Overall, these differences were quite small; even those that were statistically different (by an unpaired T-test) were rarely greater than two-fold.
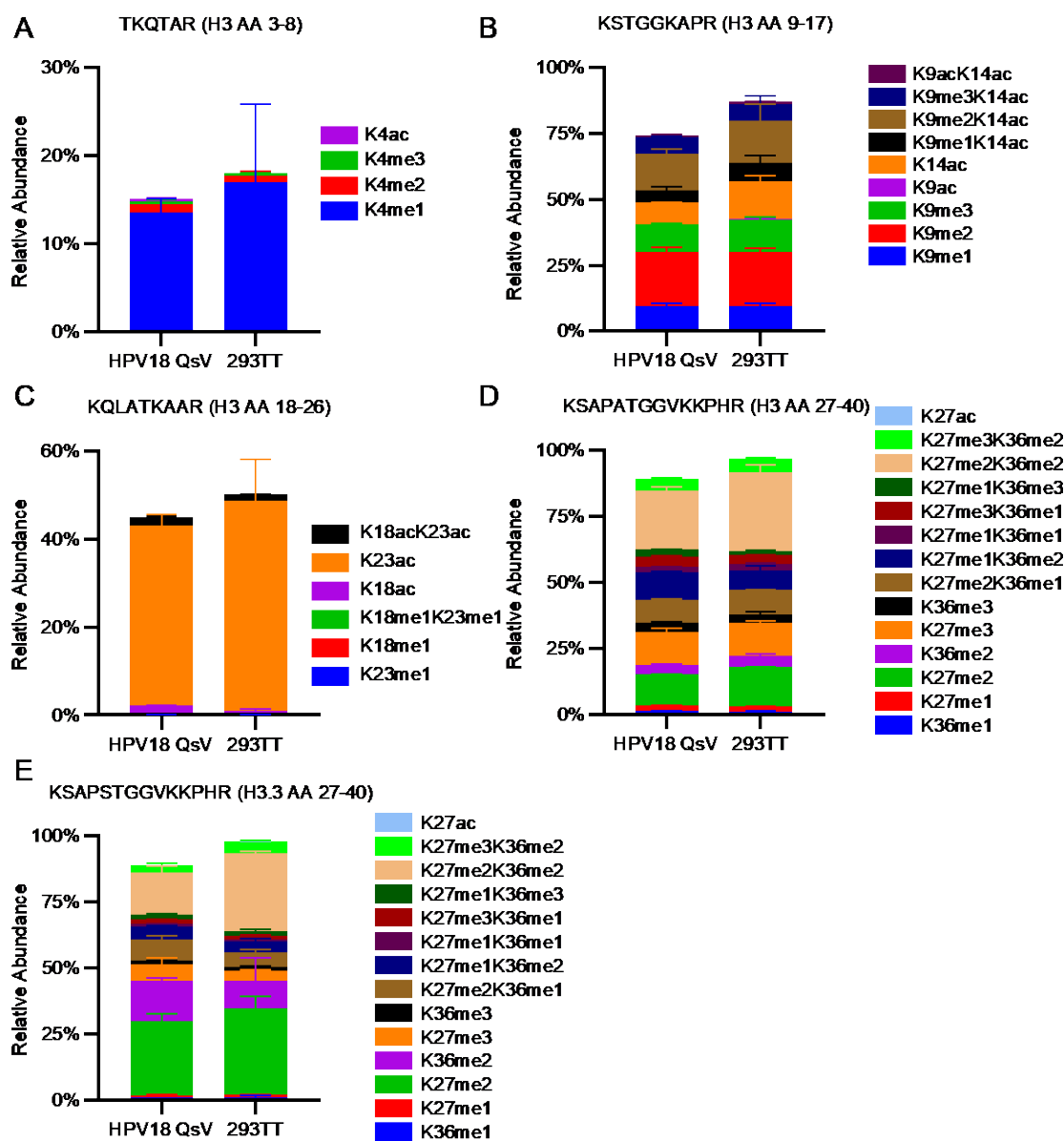
Figure 4.4. Mass spectrometry analysis of PTMs on histone H3 from HPV18 quasiviruses and 293TT control cells. Data are presented as the relative abundance of the given modification as a percentage of total modified and unmodified peptides. A) TKQTAR, histone H3 amino acids 3-8. B) KSTGGKAPR, histone H3 amino acids 9-17. C) KQLATKAAR, histone H3 amino acids 18-40. D) KSAPATGGVKKPHR, histone H3 amino acids 27-40. E) KSAPSTGGVKKPHR, histone H3.3 amino acids 27-40. N=3 technical replicates. Error=SD.
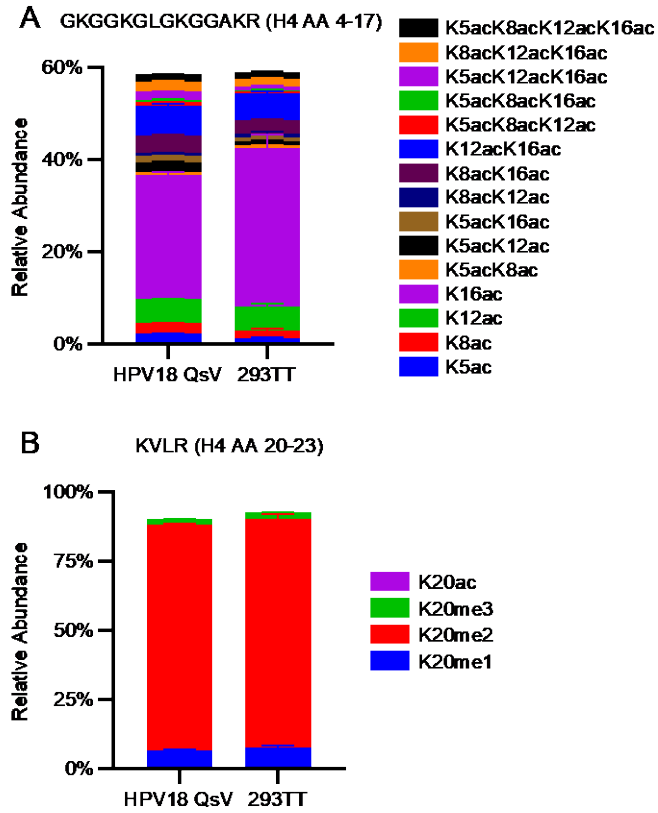
Figure 4.5. Mass spectrometry analysis of PTMs on histone H4 from HPV18 quasiviruses and 293TT control cells. Data are presented as relative abundance of the given modification as a percentage of total modified and unmodified peptides. A) GKGGKGLGKGGAKR, histone H4 amino acids 4-17. B) KVLR, histone H4, amino acids 20-23) N=3 technical replicates. Error=SD.

Overall, these data show that the HPV capsid is biochemically able to package canonical histones containing all of the most common PTMs; no modifications were detected in the cellular histones that were not also present on the viral samples. The relative abundance of the histone modifications in the virion was very similar to those found in the control host cells (Supplementary Table 1 and Figures 4.4-4.5). Taken together, the data suggest that the epigenomes of HPV quasiviruses and their 293TT producer cells are quite similar and there is no overall preference, biochemically or structurally, in packaging histone with specific PTMs. These data also demonstrate that our methods can detect and quantify individual PTMs on histone peptides and compare relative levels between virion and cellular samples. Therefore, our pipeline can be used for other virion and cellular sample types.

Chromatin Post-Translational Modifications in BPV1 Virions extracted from Bovine Warts

Next, we analyzed the chromatin content of native papillomavirus virions. For the most physiological relevance, we used virions produced by natural infections of papillomaviruses. One source of this type of papillomavirus virion is the wart tissue from cows experimentally infected with bovine papillomavirus 1 (BPV1) [119].

BPV1 virions were extracted from three separate batches of wart tissue isolated from BPV1 infected cows. Briefly, the wart tissue was minced, lysed with detergent, and digested with nucleases and collagenase. Next, the samples were salt extracted and "cushioned" before isolating by ultracentrifugation (overview in Figure 4.6). Fractions were collected dropwise from the bottom of the gradient (Figure 4.7D). Each fraction was tested for the presence of BPV L1 and histone H3 by

immunoblot (Figure 4.7A and B) and BPV1 DNA by qPCR (Figure 4.7C).

Additionally, fractions were stained for total protein with Sypro Ruby (Figure 4.7A).

Fractions positive for all three components were selected and pooled. To confirm the

virions were intact, selected fractions were imaged by transmission electron

microscopy (TEM). As shown in Figure 4.7E, the virion samples contained mostly

intact capsids of the correct size and morphology.
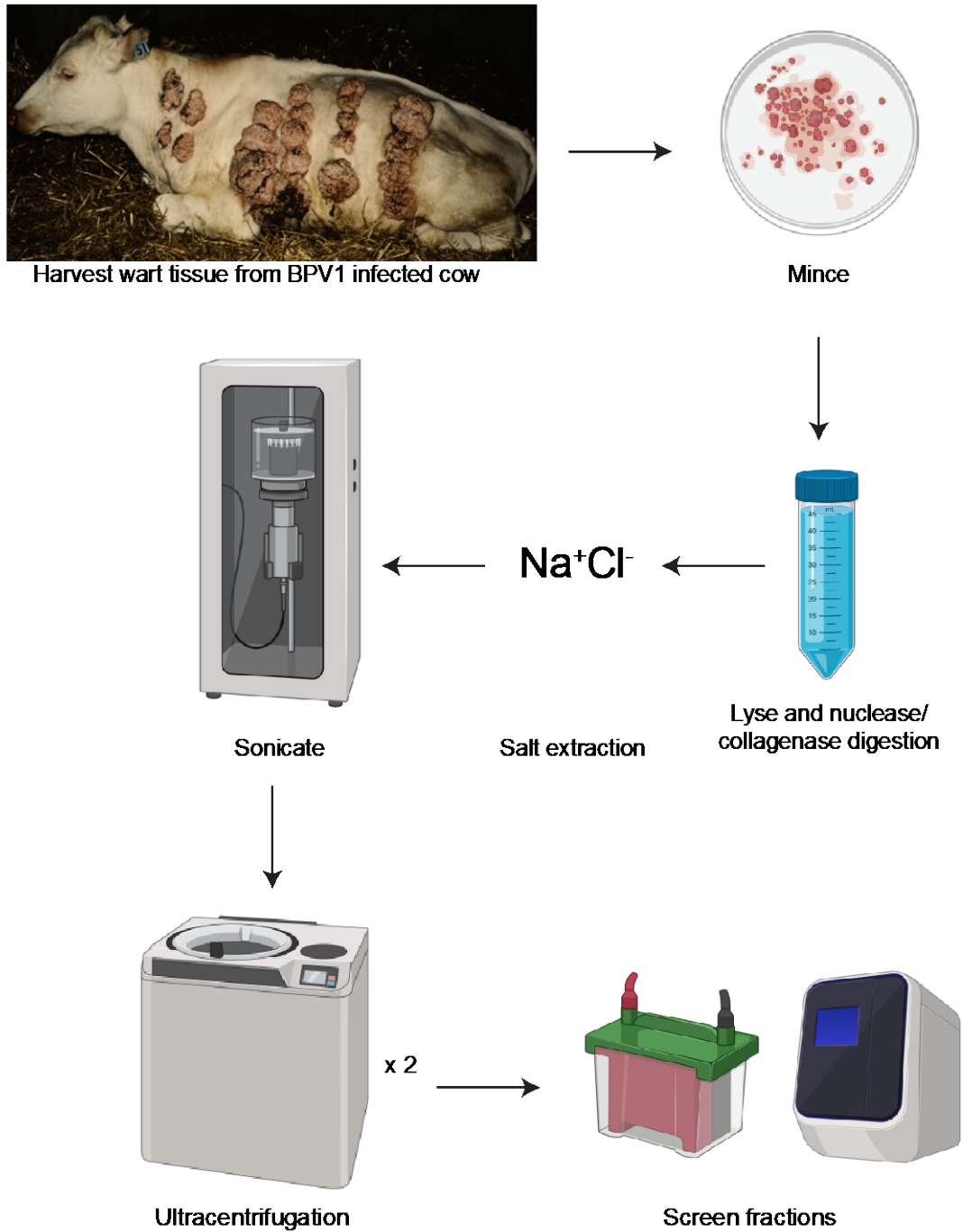
Figure 4.6. Isolation of BPV virions from bovine wart tissue.
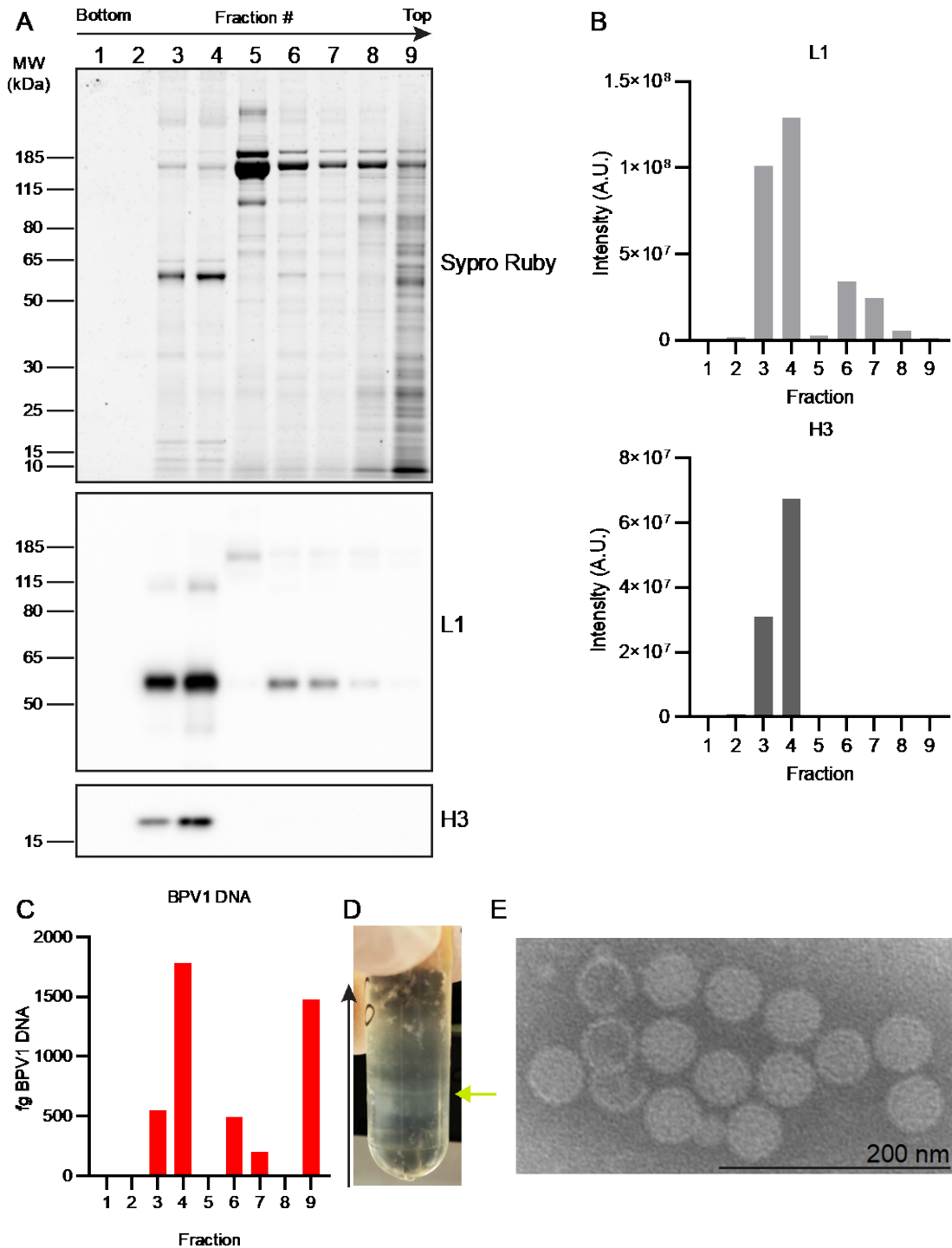
Figure 4.7. Selection of BPV1 positive fractions. 200 µL fractions were collected dropwise from the bottom of the BPV isolation gradient. A) Each fraction was separated by SDS-PAGE and stained for total protein with Sypro Ruby (top), immunoblotted for BPV L1 (middle), and histone H3 (bottom). B) Quantification of immunoblots in A. C) Fractions were measured for BPV1 DNA by RT-qPCR. D) Photograph of gradient, black arrow indicates direction of fraction collection, green arrow indicates approximate location of migration of BPV virions. E) Transmission electron micrograph of isolated BPV virions. Data are representative of 15 independent experiments.

101

Papillomaviruses are assembled in the superficial, differentiated layers of the host epithelium. Therefore, primary bovine keratinocytes (BEK6) were cultured under three conditions to serve as cellular controls for the experiments. Keratinocytes were grown under normal proliferative conditions; they were also induced to differentiate by growing to confluence and adding high levels of calcium; and finally, bovine keratinocyte 3D-oranotypic rafts were prepared (Figure 4.8A). Histones were extracted from the wart and cellular control samples using the same protocol described above for the quasivirus and 293TT cellular samples. Histone PTMs were identified by quantitative mass spectrometry and the relative abundance of each modification was calculated. Similar to the preliminary data with quasiviruses, the natural viral capsids contained histones with each modification detected in the cellular controls. However, in contrast to the quasiviruses, the bovine wart derived virus had a considerably different distribution of post translational modifications as compared to the cellular controls (Figures 4.9-4.15A, Supplementary Table 2).
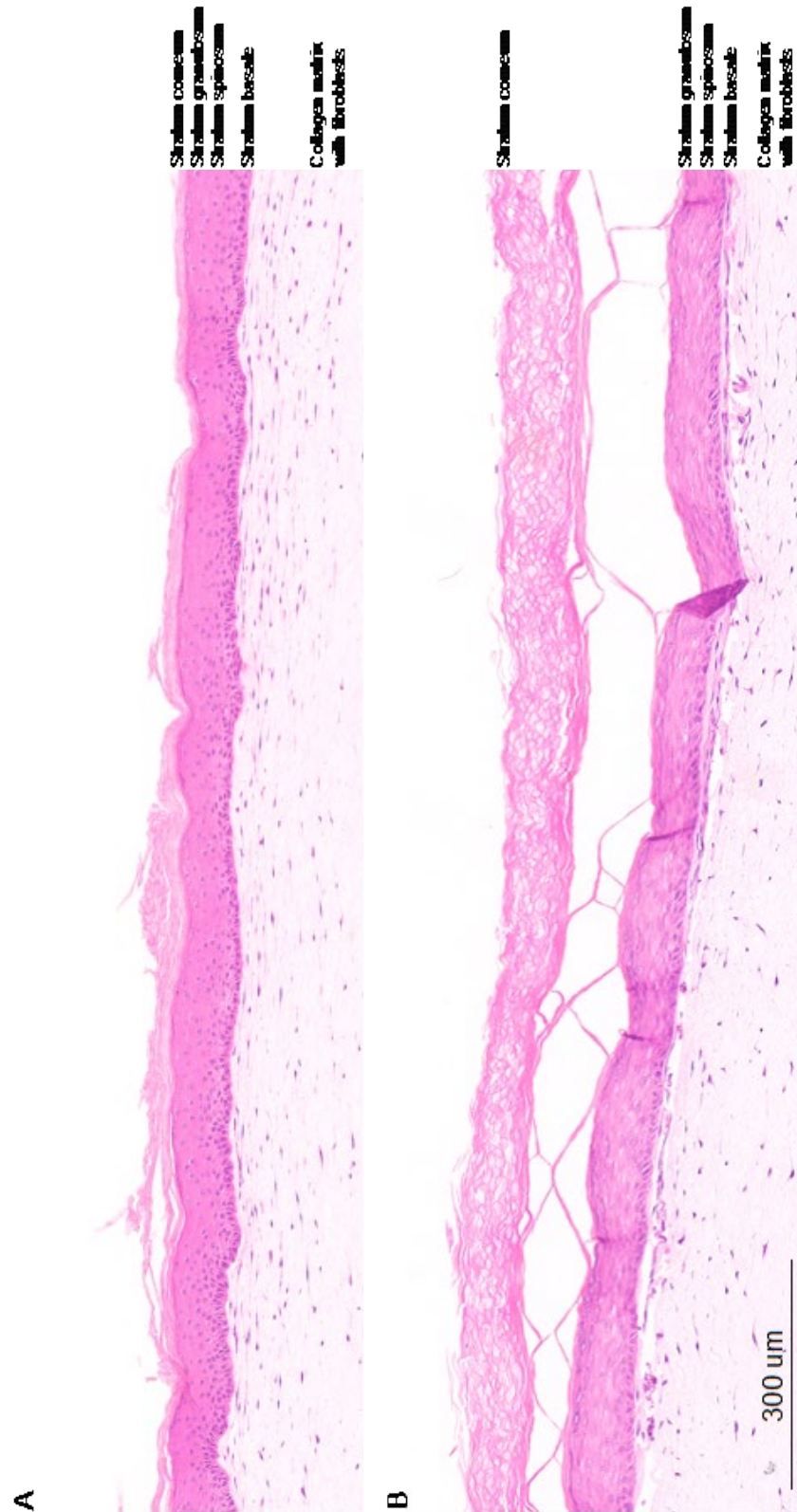
Figure 4.8. Hematoxylin and Eosin stain of primary keratinocyte 3D organotypic raft culture. Primary bovine (A) or human (B) keratinocytes were grown in organotypic raft culture, sectioned, and stained.

103
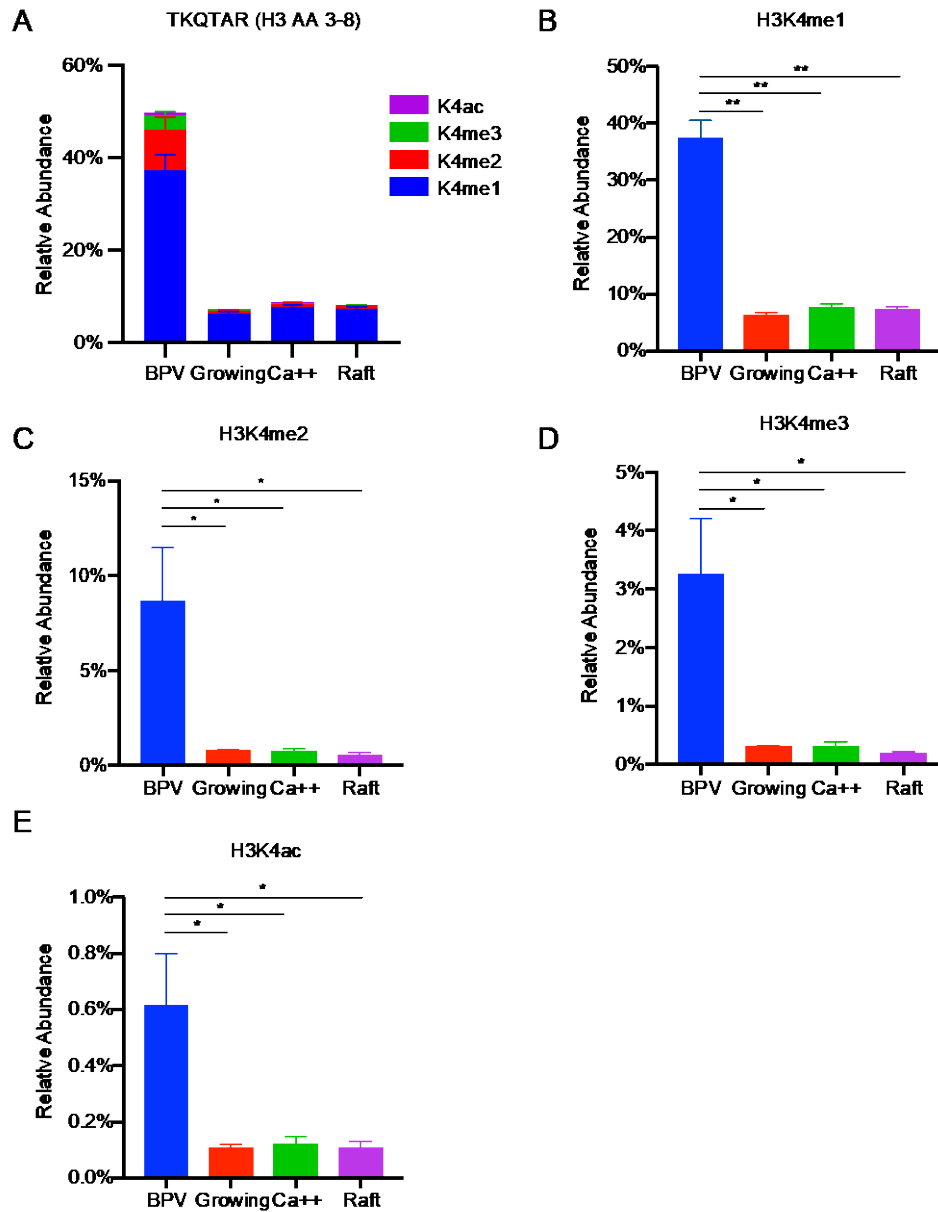
Figure 4.9. Mass spectrometry analysis of PTMs on amino acids 3 to 8 from histone H3 of BPV1 virions and bovine keratinocytes. Data are presented as relative abundance of the given modification as a percentage of total modified and unmodified peptides. (A) Total modifications detected on peptide TKQTAR, histone H3 amino acids 3-8. B-F) Relative abundance of individual modifications. Significance was determined by an unpaired t-test. *=p<0.05 **=p<0.01 N=3 biological replicates. Error=SD.
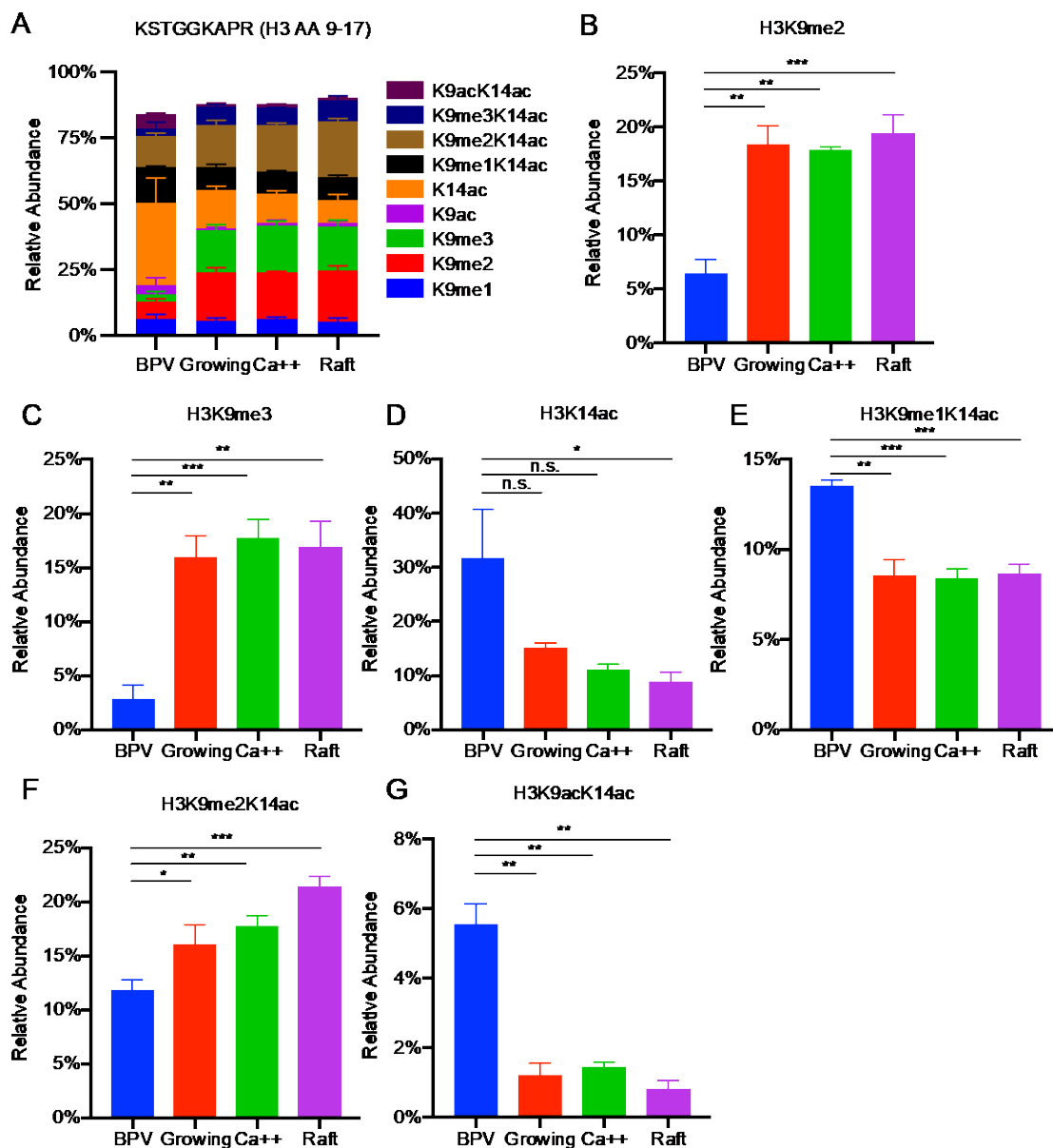
Figure 4.10. Mass spectrometry analysis of PTMs on amino acids 9 to 17 from histone H3 from BPV1 virions and bovine keratinocytes. Data are presented as relative abundance of the given modification as a percentage of total modified and unmodified peptides. (A) Total modifications detected on peptide KSTGGKAPR, histone H3 amino acids 9-17. B-G) Relative abundance of individual modifications. Significance was determined by an unpaired t-test. n.s.=not significant *=p<0.05 **=p<0.01 ***=p<0.001 N=3 biological replicates. Error=SD.
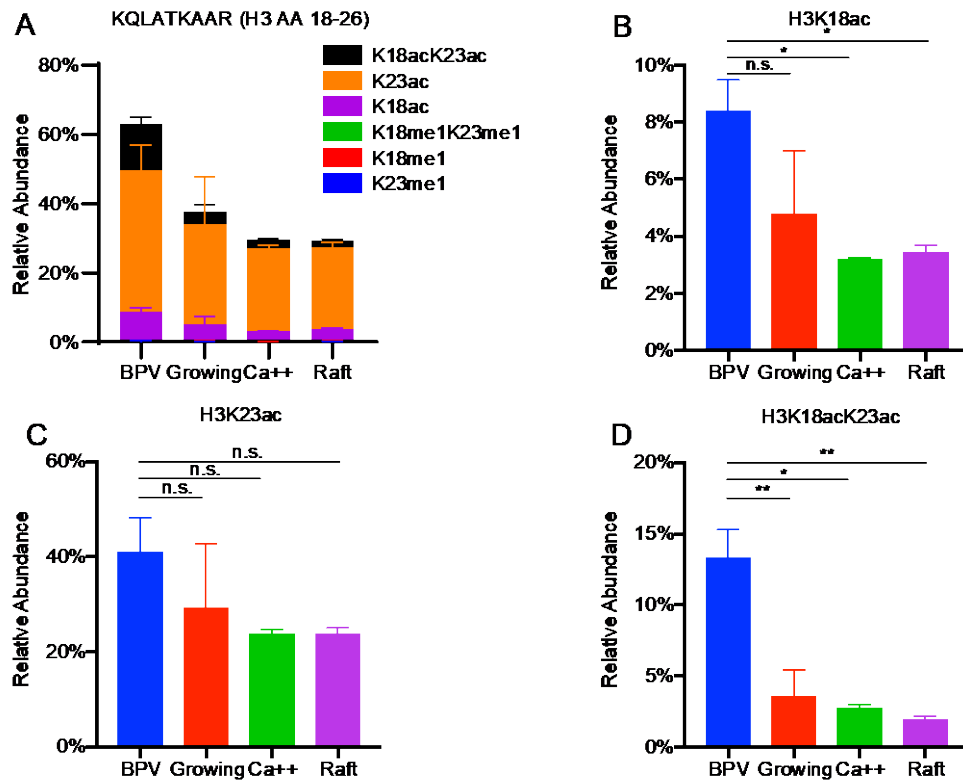
Figure 4.11. Mass spectrometry analysis of PTMs on amino acids 18 to 26 from histone H3 of BPV1 virions and bovine keratinocytes. Data are presented as relative abundance of the given modification as a percentage of total modified and unmodified peptides. (A) Total modifications detected on peptide KQLATKAAR histone H3 amino acids 18-26. B-D) Relative abundance of individual modifications. Significance was determined by an unpaired t-test. n.s.=not significant *=p<0.05 **=p<0.01 N=3 biological replicates. Error=SD.
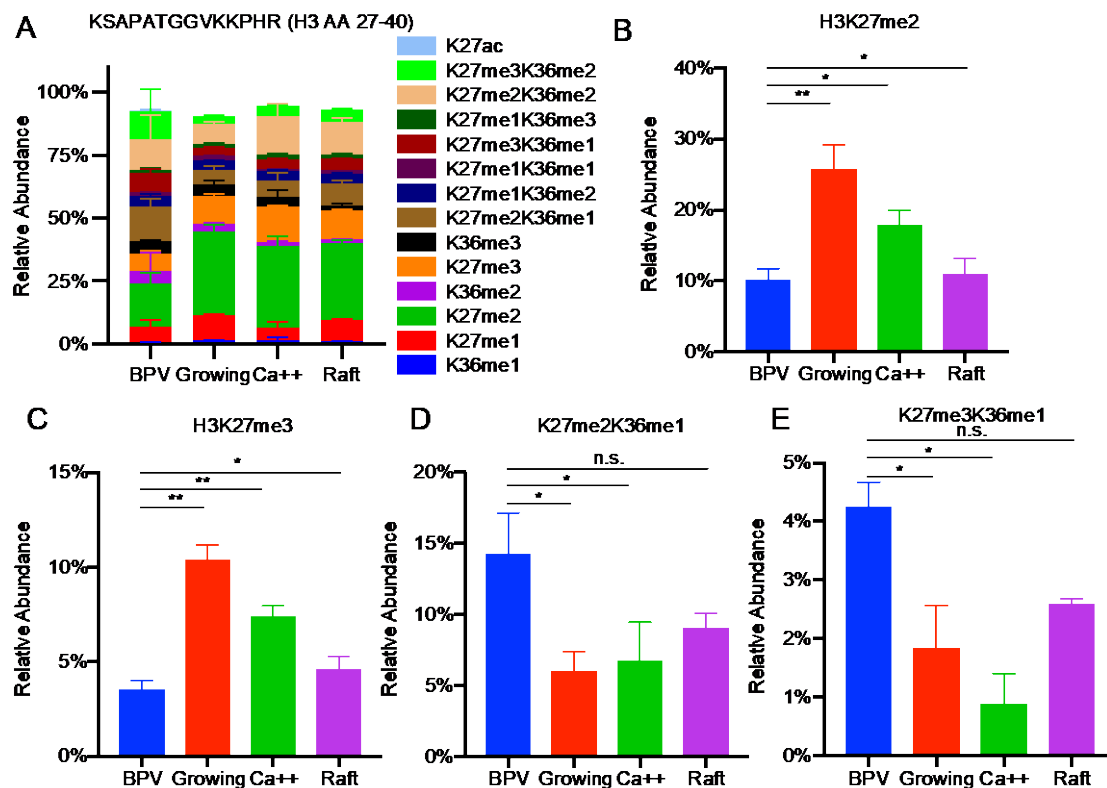
Figure 4.12. Mass spectrometry analysis of PTMs on amino acids 27 to 40 from histone H3 of BPV1 virions and bovine keratinocytes. Data are presented as relative abundance of the given modification as a percentage of total modified and unmodified peptides. (A) Total modifications detected on peptide KSAPATGGVKKPHR, histone H3 amino acids 27-40. B-E) Relative abundance of individual modifications. Significance was determined by an unpaired t-test. n.s.=not significant *=p<0.05 **=p<0.01 N=3 biological replicates. Error=SD.
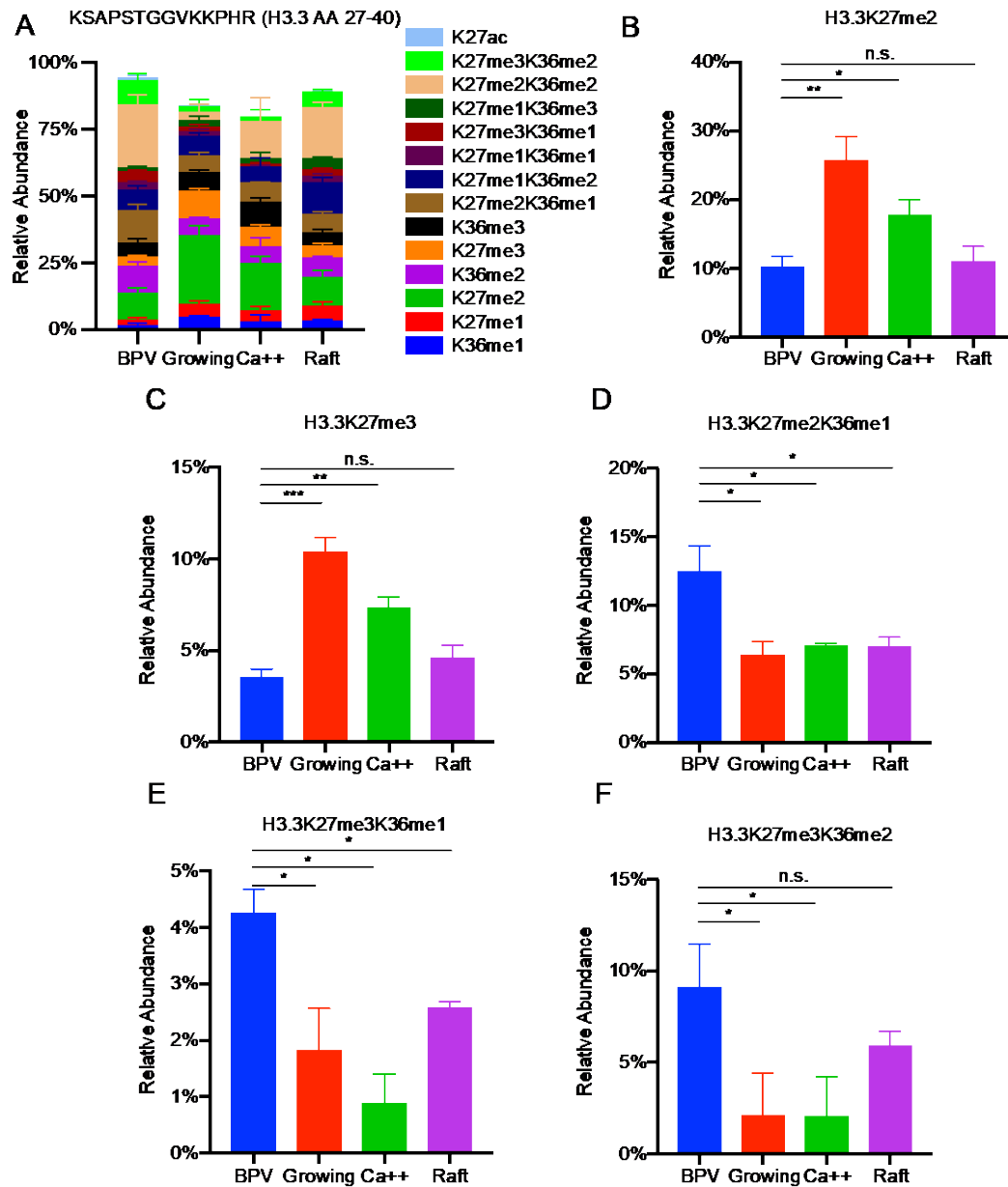
Figure 4.13. Mass spectrometry analysis of PTMs on amino acids 27 to 40 from histone H3.3 of BPV1 virions and bovine keratinocytes. Data are presented as relative abundance of the given modification as a percentage of total modified and unmodified peptides. (A) Total modifications detected on peptide KSAPSTGGVKKPHR histone H3.3 amino acids 27-40. B-F) Relative abundance of individual modifications. Significance was determined by an unpaired t-test. n.s.=not significant *=p<0.05 **=p<0.01 ***=p<0.001 N=3 biological replicates. Error=SD.
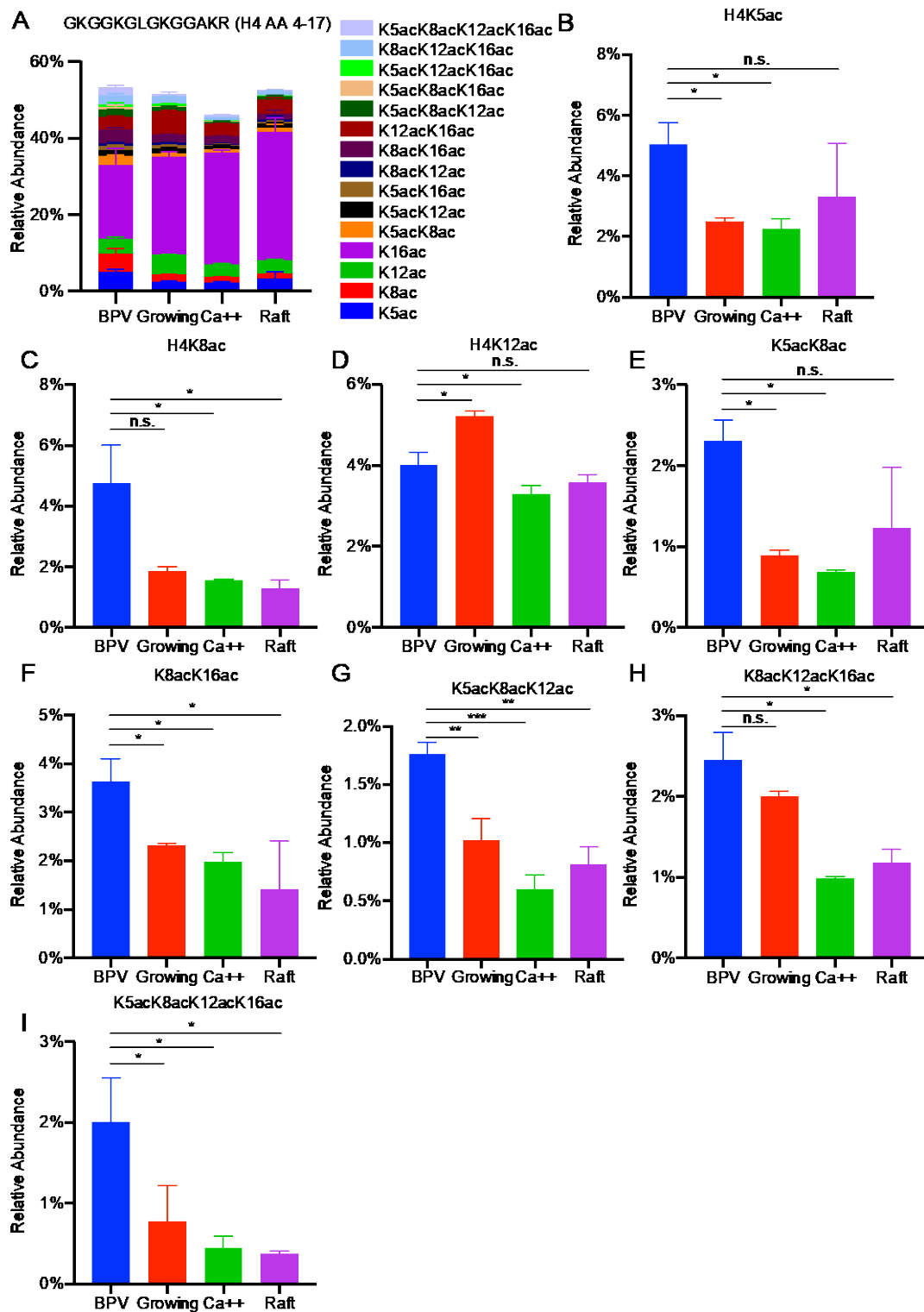
Figure 4.14. Mass spectrometry analysis of PTMs on amino acids 4 to 17 of histone H4 of BPV1 virions and bovine keratinocytes. Data are presented as relative abundance of the given modification as a percentage of total modified and unmodified peptides. (A) Total modifications detected on peptide KVLR, histone H4, amino acids 20-23. B-I) Relative abundance of individual modifications. Significance determined by unpaired t-test. *=p<0.05 **=p<0.01 ***=p<0.001 N=3. Error=SD.
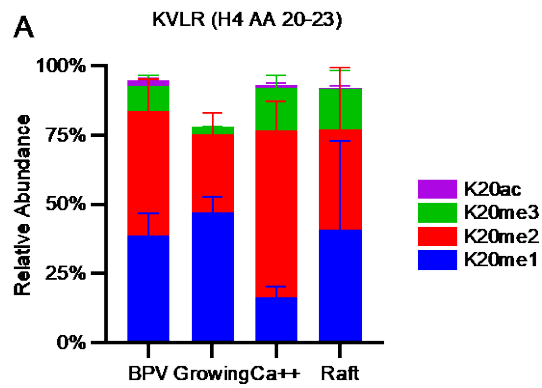
Figure 4.15. Mass spectrometry analysis of PTMs on amino acids 20 to 23 from histone H4 of BPV1 virions and bovine keratinocytes. Data are presented as relative abundance of the given modification as a percentage of total modified and unmodified peptides. (A) Total modifications detected on peptide KVLR, Histone H4, amino acids 20-23. B-I) Relative abundance of individual modifications. Significance was determined by an unpaired t-test. N=3 biological replicates. Error=SD.

Overall, the BPV virions were enriched in acetylated histone H3. We detected significant enrichment of acetylation on multiple lysines: H3K4 (Figure 4.9E), H3K14 (Figure 4.10D), and H3K18 (Figure 4.11B). There was also a large, but not statistically significant, increase in H3K23ac levels detected (Figure 4.11C). Furthermore, several combinations of these acetylated lysines were enriched in the virions, most significantly for K9acK14ac (Figure 4.10G) and K18acK23ac (Figure 4.11D).

There were also significant differences in the methylation patterns of virion-derived histone H3. The virions had much higher levels of the modifications mono-, di-, and tri- methylated K4 lysine, which are associated with active chromatin (Figure 4.9B-D). Conversely, the virions were strongly depleted for di- and tri-methylation of both the K9 (Figure 4.10B, C) and K27 (Figure 4.12B, C and Figure 4.13B, C) residues that are usually associated with repressed chromatin. An exception was that methylation of the K27 residue was not significantly depleted on variant H3.3 when compared to the organotypic raft cultured keratinocyte (Figure 4.13B, C). While there were only small differences in the methylation of K36 by itself, there was an enrichment for combinational marks such as K27me2K36me1 and K27me3K6me1 (Figure 4.12D, E and Figure 4.13D, E). K27me3K36me2 was higher in the virion only on H3.3 (Figure 4.13F).

We also detected changes in the relative abundance of combinatorial modifications with acetylation of one lysine and methylation of another. Acetylation of K14 paired with monomethylation of K9 was increased in the virions compared to

control cells, while the pairing with dimethylation of H3K9 was decreased (Figure 4.10 E and F).

To confirm the initial observations of the mass spectrometry screen, we performed immunoblots using antibodies specific to each of the H3 PTMs that showed the greatest enrichment in the virions compared to control cells. As shown in Figure 4.16A and C, the signal of H3K4me1, H3K4me3, H3K9ac, H3K14ac, H3K18ac, and H3K23ac were much higher in the virion samples compared to cellular controls, when the samples were normalized to the level of total histone H3 (Figure 4.16B). This is in agreement with the initial observations in the mass spectrometry experiments (Figure 4.9-4.11).
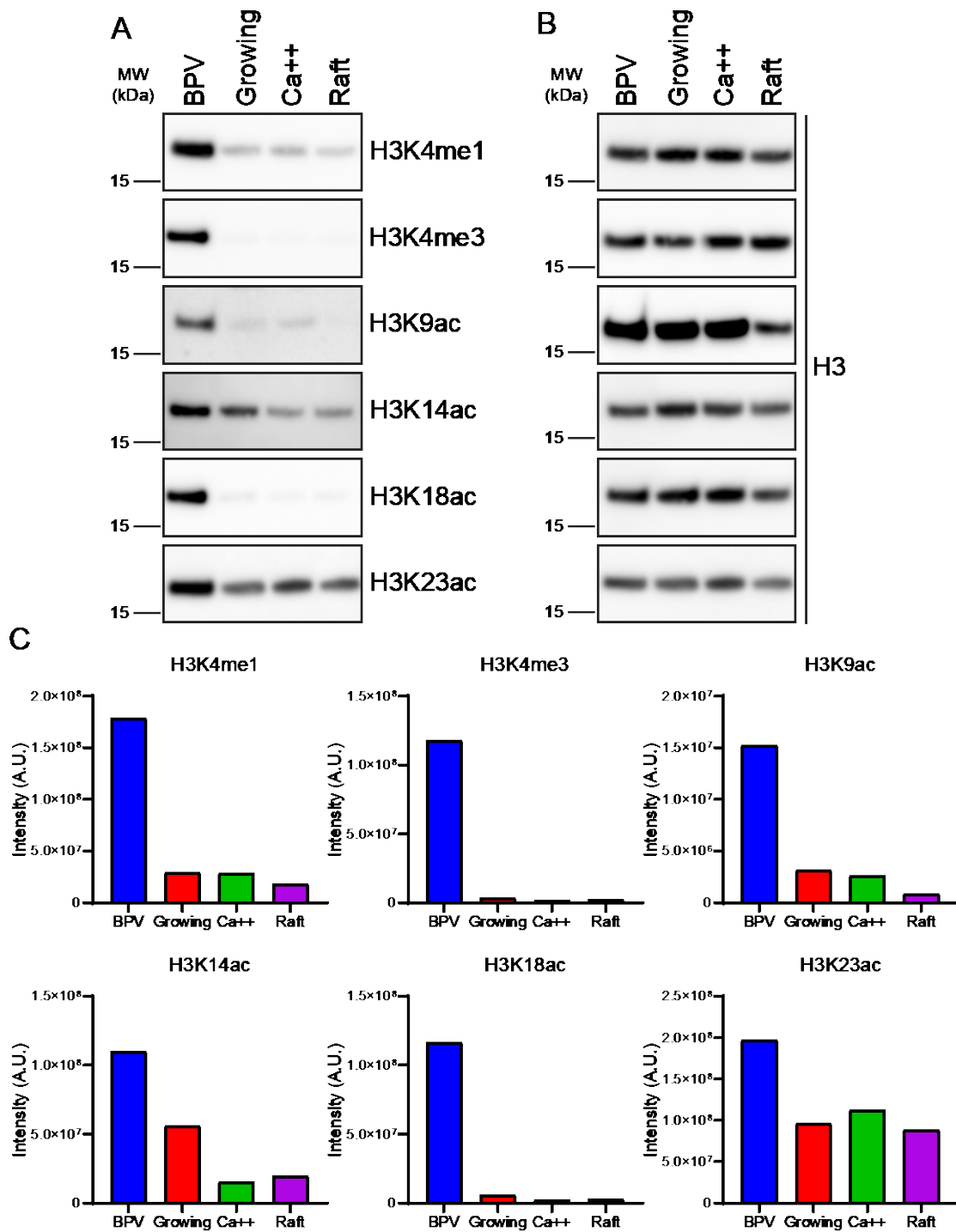
Figure 4.16. BPV Virions were enriched in Histone H3 PTMs associated with transcriptional activation. A) Representative immunoblots of BPV virions and bovine keratinocyte control cells using antibodies against indicated PTMs of histone H3. B) Immunoblots from A were stripped and re-probed with antibody against all forms of histone H3 as a loading control. C) Quantification of the representative immunoblots shown in A. A.U.=arbitrary units. N=2 biological replicates.

113

To further confirm the increased acetylation of histone H3 in the BPV virions, we performed acid-urea (AU) PAGE. In AU PAGE, proteins are separated on the basis of size and charge. Acetylation of lysines reduces their positive charge, and so histones with a higher degree of acetylation will migrate more slowly through the gel. This technique allows us to examine overall protein acetylation levels without the need for specific antibodies against every possible lysine modification. As shown in Figure 4.17, more of the signal from the histones extracted from BPV virions was in the slower migrating, upper bands, when compared to the cellular lanes. This supports the mass spectrometry data that indicated that H3 proteins packaged in the virions are acetylated to a higher degree than those of the cellular controls (Figure 4.9-4.11).
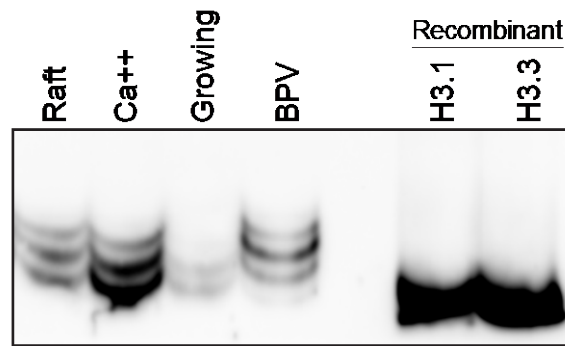
Figure 4.17. Immunoblot of Histone H3 modified species separated by AU-PAGE. Histones were acid extracted from BPV1 virions and bovine cellular controls, separated by acid-urea PAGE, and transferred to a membrane. Immunoblot was performed using an antibody against all forms of H3. Slower migrating, upper bands correspond to an increase in acetylation of H3 lysines. N=1.

We also used immunoblots to confirm that the bovine virions were depleted for repressive methylation of H3 lysines 9 and 27. As shown in Figure 4.18A and C, the virion samples had dramatically lower signal for H3K9me3 compared to the cellular controls, in agreement with the mass spectrometry data (Figure 4.10C). However, in the immunoblots for H3K27me3 the signal from the virion samples was only lower than the calcium differentiated samples, and slightly from that of the raft (Figure 4.18 B and C), in contrast to the mass spectrometry data (Figure 4.12C).
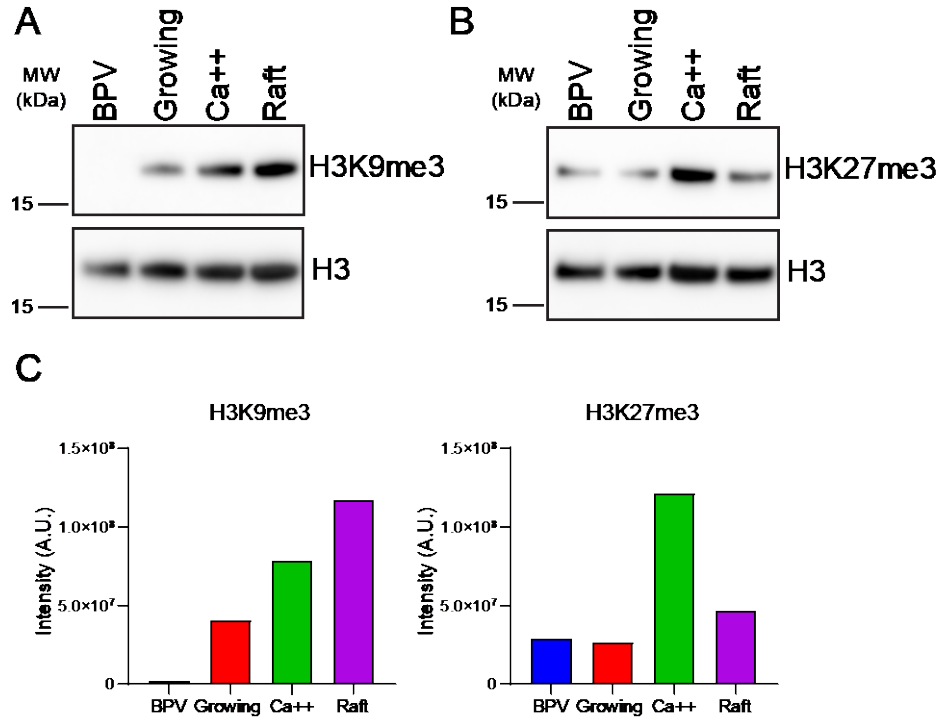
Figure 4.18. BPV Virions are depleted for PTMs on histone H3 associated with transcriptional repression. A) Top, representative immunoblot of BPV virions and bovine keratinocyte control cells using antibodies against H3K9me3. Bottom, immunoblot was stripped and re-probed with antibody against all forms of histone H3 as a loading control. B) Top, representative immunoblot of BPV virions and bovine keratinocyte control cells using antibodies against H3K27me3. Bottom, immunoblot was stripped and re-probed with antibody against all forms of histone H3 as a loading control. C) Quantification of modification from the representative immunoblots shown in A and B. A.U.=arbitrary units. N=2 biological replicates.

Acetylated lysines were also enriched in histone H4, with K5, K8, and K12 being more heavily acetylated in the virion than the growing and differentiated cellular controls (Figure 4.14B, C, D). Furthermore, the level of combinatorial acetylation of several lysines was higher in the virions; K5acK8ac, K8acK16ac, K5acK8acK12ac, K18acK12acK16ac, and K5acK8acK12acK16ac were enriched in the virions (Figure 4.14, E, F, G, H, and I). Contrariwise, levels of H4K16ac were higher in the control keratinocytes, although only with statistical significance in the raft samples. No consistent trend was found for the methylation of lysines on H4 (Figure 4.15).

To confirm the enrichment in lysine acetylation of H4 packed in BPV virions, we performed immunoblots using antibodies specific to H4 acetylated on several different lysines. The native BPV virions showed considerably higher levels of H4K5ac, H4K8ac, and H4K12ac when compared to the control keratinocytes (Figure 4.19A, B, and C). Additionally, the virion samples had significantly higher signal of the combinatorial modification of tetra-acetylated H4K5ac/K8ac/K12ac/K16ac (Figure 4.19A, B, and C). Together these data show that bovine papillomavirus virions contain histone H4 with higher levels of acetylated lysines than host keratinocytes, which is in agreement with our initial observations from mass spectrometry.
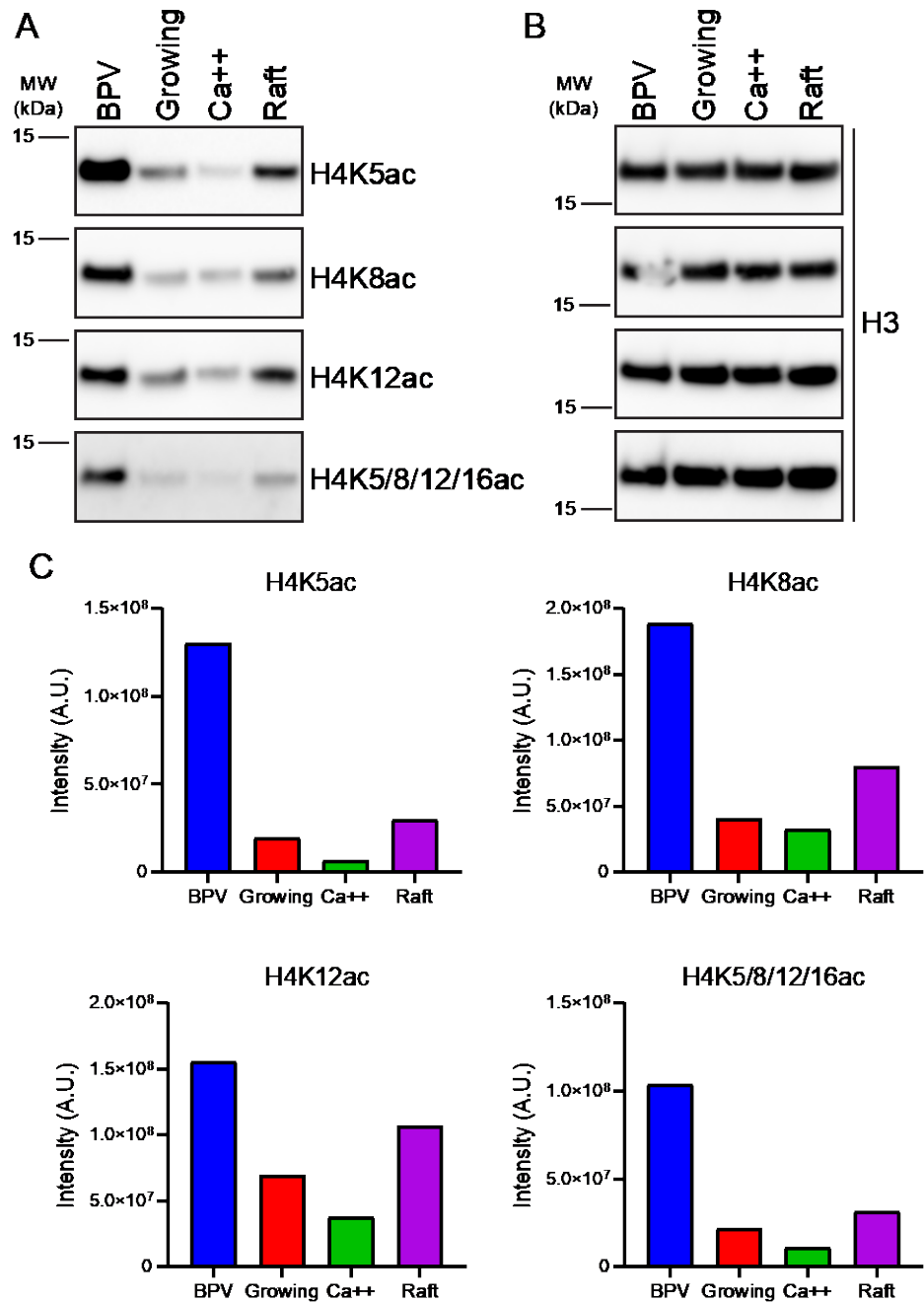
Figure 4.19. BPV Virions are enriched in acetylated Histone H4. A) Immunoblots of BPV virions and bovine keratinocyte control cells using antibodies against indicated PTMs of Histone H4. B) Immunoblots were stripped and reprobed with antibody against histone H3 to ensure even loading. C) Quantification of immunoblots in A. A.U.=arbitrary units. N=1 biological replicate.

Histone Modifications in Wart Derived HPV1 Virions

It was important to confirm these findings in HPV, but isolation of large amounts of HPV virions from warts arising from natural infections is difficult. Nonetheless, our collaborators were able to isolate sufficient quantities of HPV1 virions from an HPV-positive wart from the wrist of a patient to perform quantitative histone PTM mass spectrometry.

We used primary human keratinocytes as control cells. Primary human foreskin keratinocytes (HFKs) were cultured in three conditions: normally proliferating cells; cells differentiated with high calcium; and 3D organotypic rafts (Figure 4.8B). Using the same methods as the bovine experiments, histones were extracted from the human virions and the cellular controls and were analyzed for histone PTMs and variants by quantitative mass spectrometry. Just as we saw in the native bovine samples, the wart derived human virions had a noticeable difference in the overall distribution of PTMs on Histone H3 (Figure 4.20A-E, Figure 4.21A-B, Supplementary Table 3).
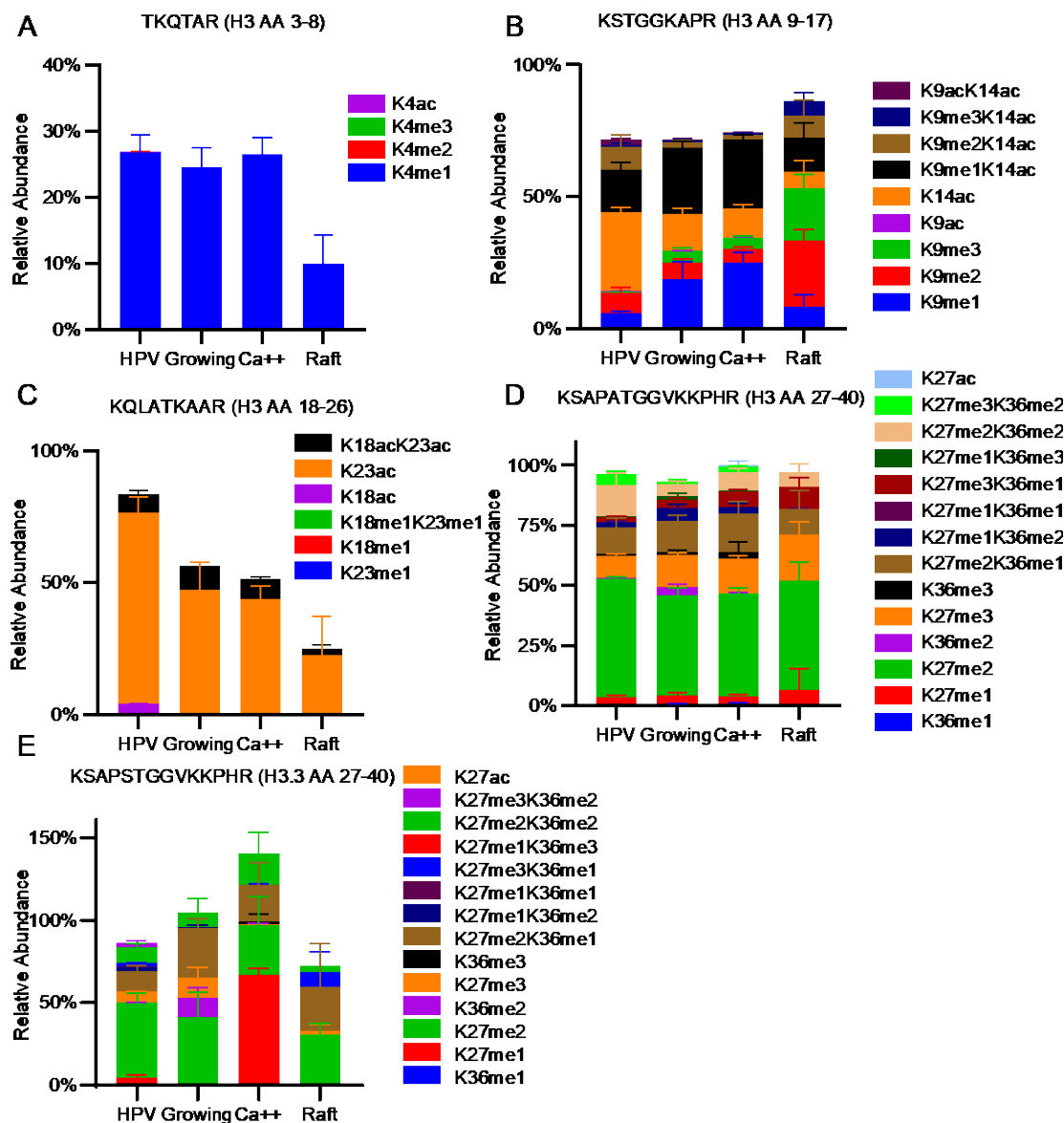
Figure 4.20. Mass spectrometry analysis of PTMs on histone H3 from HPV1 virions and primary HFK control cells. Data are presented as relative abundance of the given modification as a percentage of total detected on that peptide. A) TKQTAR, Histone H3 amino acids 3-8. B) KSTGGKAPR, Histone H3 amino acids 9*17. C) KQLATKAAR histone H3 amino acids 18-26. D) KSAPATGGVKKPHR, histone H3 amino acids 27-40. E) KSAPSTGGVKKPHR histone H3.3 amino acids 27-40. N=2 technical replicates. Error=SD.
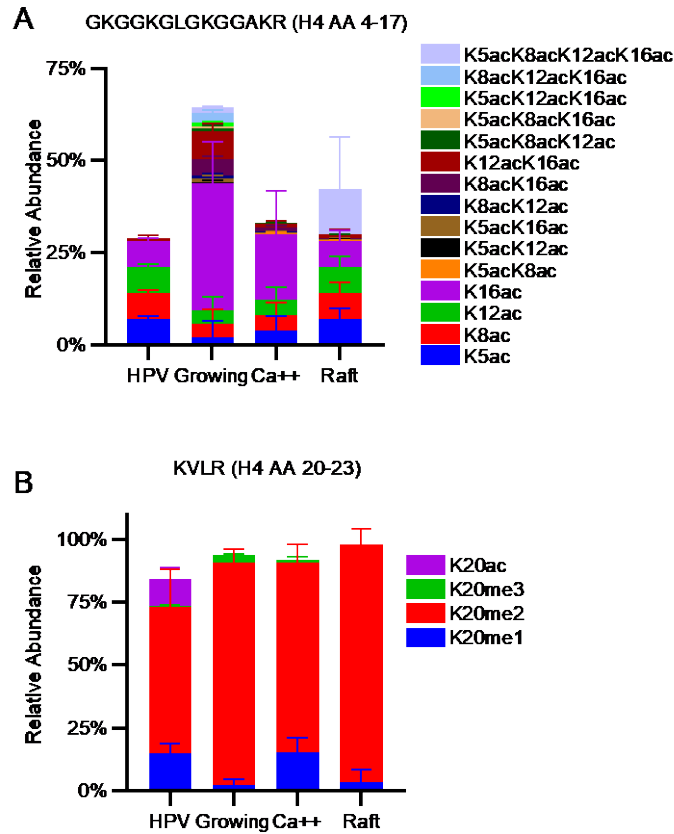
Figure 4.21. Mass spectrometry analysis of PTMs on Histone H4 from HPV1 virions and primary HFK control cells. Data are presented as relative abundance of the given modification as a percentage of total detected on that peptide. A) GKGGKGLGKGGAKR, Histone H4 amino acids 4-17. B) KVLR, histone H4, amino acids 20-23. N=2 technical replicates. Error=SD.

In agreement with the data from BPV1 virions, the HPV1 virions were enriched in acetylated lysines on histone H3, primarily on lysines 9, 14, 18, and 23 (Figure 4.22C, D, F, and G). The combinatorial modification K9acK14ac was also several fold higher in the virus samples compared to cell extracts (Figure 4.22E).
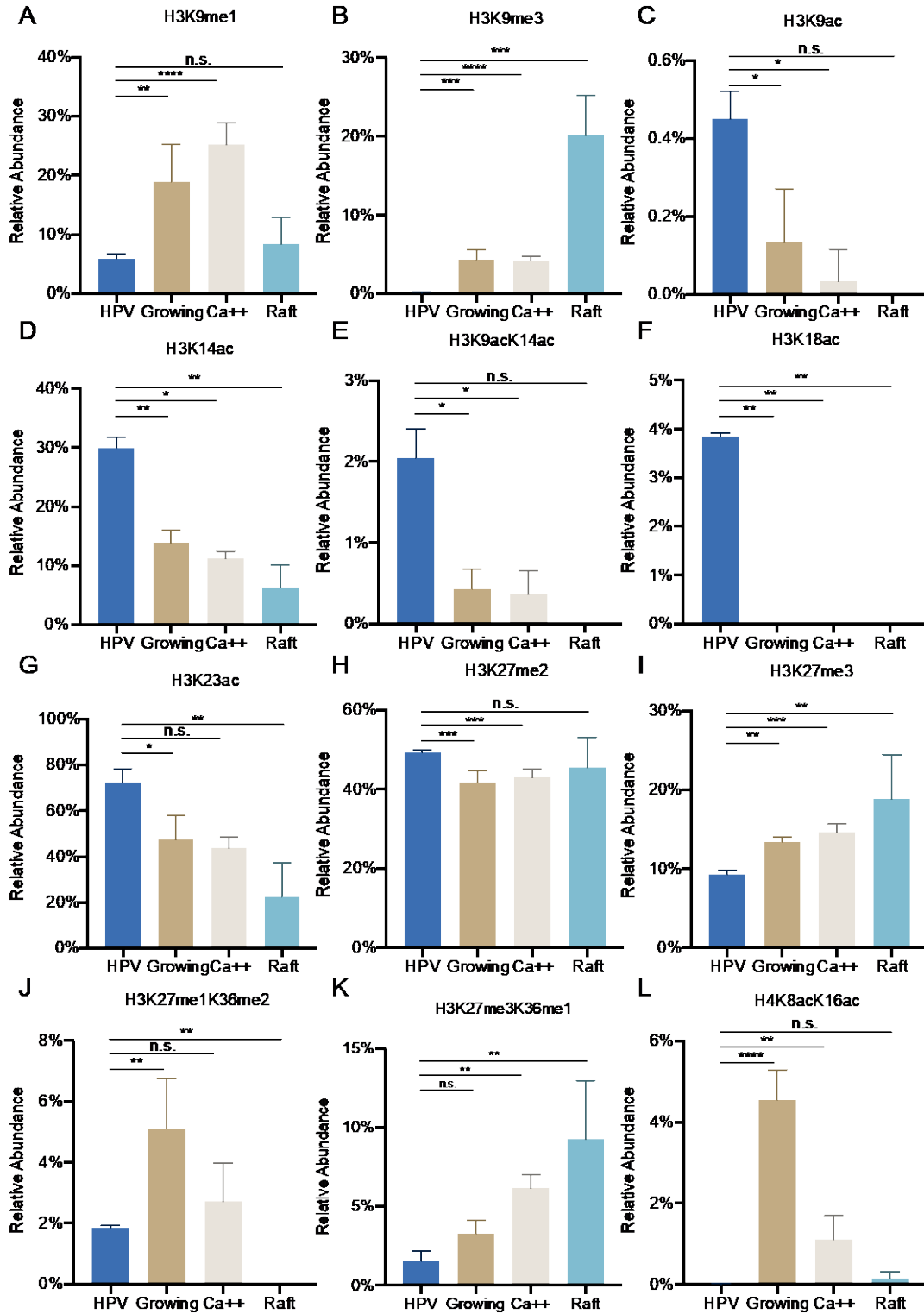
Figure 4.22. Mass spectrometry analysis of PTMs on amino acids histones H3 and H4 of HPV1 virions and primary HFK control cells. Data are presented as relative abundance of the given modification as a percentage of total modified and unmodified peptides. (A-L) Relative abundance of individual modifications. Significance determined by an unpaired t-test. n.s.=not significant. *=p<0.05 **=p<0.01 ***=p<0.001 ****=p<0.0001 N=2 technical replicates. Error=SD.

124

In further agreement, the human virions were depleted for tri-methylation on K9 and tri-methylation K27 of H3 (Figure 4.22B and I). The human virions were enriched for H3K27me2 (Figure 4.22H). There was additional depletion of H3K9me1 (Figure 4.22A), unlike the bovine samples that were depleted for H3K9me2. Another difference between the human and bovine virions is that the former did not show any enrichment in K4 methylation, except in K4me1 when compared to the raft keratinocytes (Supplementary Table 3). We also detected lower levels of the combinatorial modifications K3H27me1K36me2 and H3K27me3K36me1 (Figure 4.22J and K).

The distribution of modifications on histone H4 were more similar between the HPV virions and control cells, though there were still some differences (Figure 4.21A and B, Supplementary Table 3). Most notably, H4K8acK16ac was significantly depleted in the virions compared to the growing and calcium treated HFKs (Figure 4.22L). There were several additional differences that had statistical significance, all compared to the growing cellular samples only; the virion was depleted for H4K16ac, K12acK16ac, and was enriched for K5ac (Supplementary Table 3).

In conclusion, the data show that wart derived human virions are enriched in histone post translational modifications that are associated with transcriptional activation when compared to the primary human foreskin keratinocyte control cells. Correspondingly, the data indicate that these virions are depleted for transcriptionally

repressive histone PTMs. This is in agreement with the data from the wart derived BPV virions.

Histone Variants in Papillomavirus Virions

In addition to histone PTMs and the differences in their relative abundance in the samples, we were also interested to see if there were differences in histone variants. These are histone proteins that have slight differences in amino acid sequence and are expressed from different genes. For example, the histone variant H3.3 has a four amino acid difference from the canonical variant H3.1 (Figure 4.3). Using mass spectrometry, the amount of H3.3 to total H3 was found to be five to eight-fold higher in the native bovine virions than the cellular controls (Figure 4.23A). To confirm this strong enrichment of H3.3, we performed immunoblots with antibodies specific to H3.3 (Figure 4.23D). The BPV virions were the only samples with detectable levels of H3.3 on the blot (Figure 4.23E). Additionally, we separated H3.1 and H3.3 on the basis of hydrophobicity using Triton Acid Urea (TAU) PAGE and immunoblotted using an antibody against all variants of H3 (Figure 4.23F). This confirmed a higher ratio of H3.3:H3.1 in the virion samples compared to the controls, in agreement with the mass spectrometry data (Figure 4.23G). The wart derived HPV virions were also enriched in H3.3 by a factor of 3-5 fold (Figure 4.23B). In comparison, the HPV quasivirions did not shown any enrichment of H3.3; the H3.3 levels were not significantly different from that of the control cells (Figure 4.23C). Overall, the data strongly suggest that wart derived virions are enriched in the histone H3.3.
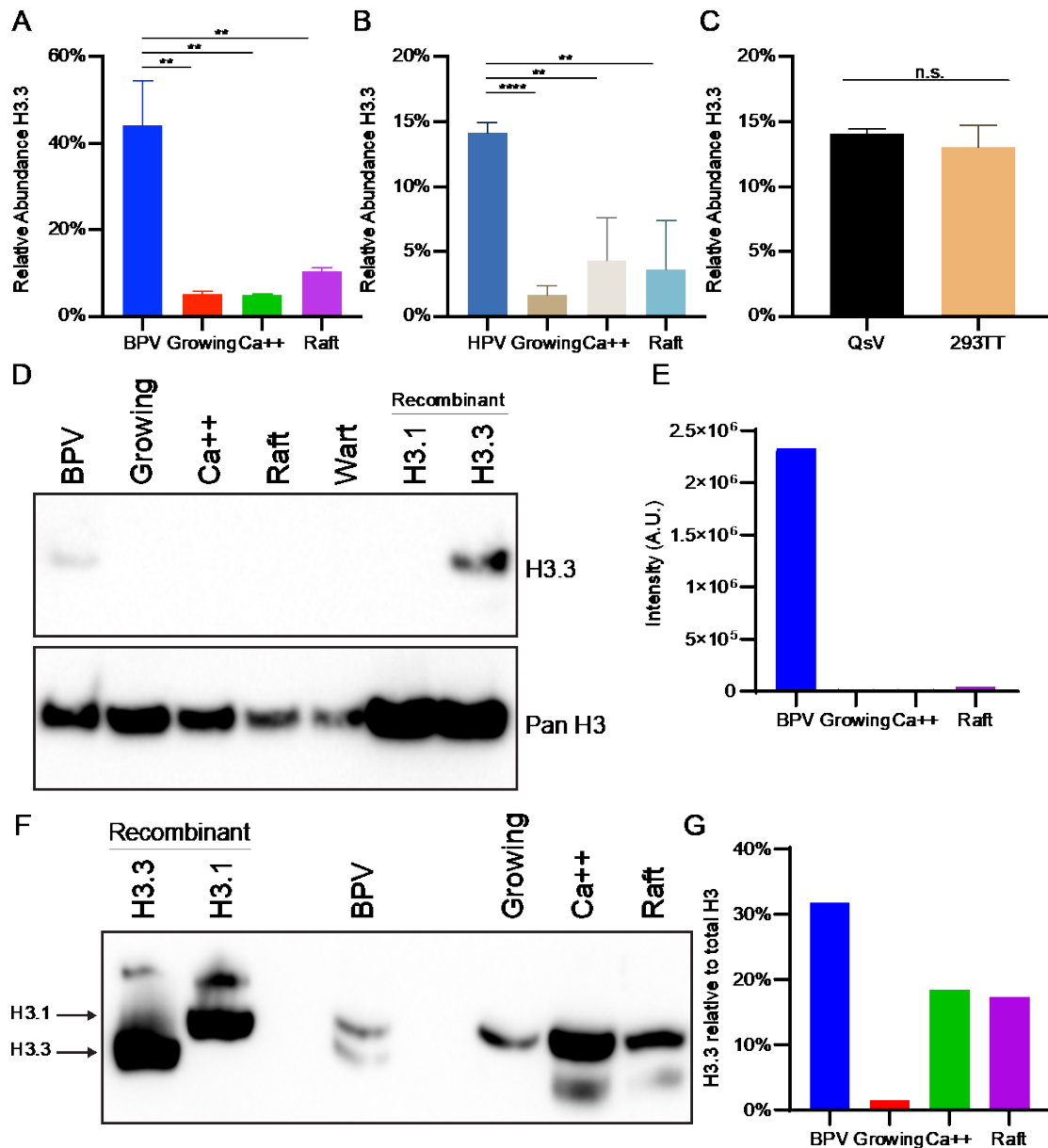
Figure 4.23. Wart derived virions are enriched in the histone H3 variant H3.3. A) Mass spectrometry data of the amount of H3 variant H3.3 relative to total H3 levels of BPV1 virions and bovine control cells. N=3 biological replicates. B) Mass spectrometry analysis of the abundance of H3 variant H3.3 relative to total H3 levels of HPV1 virions and primary human control cells. N=2 technical replicates. C) Mass spectrometry analysis of H3 variant H3.3 in HPV18 quasivirions compared to packaging cells. N=3 technical replicates. Significance was determined by an unpaired t-test. **=$p<0.01$ ****=$p<0.0001$. D) Representative immunoblot of BPV1 and bovine control cells with antibody against H3.3 (top) and all forms of H3 (bottom). N=2. E) Quantification of immunoblot in D. A.U.=arbitrary units. F) Representative H3 immunoblot from TAU PAGE gel of BPV and control keratinocytes. N=2 biological replicates. G) Quantification of blot in F. Data are presented as percent intensity of bottom band compared to sum of both bands. Error=SD.

Discussion

In this study we have used mass spectrometry to profile the chromatin of HPV quasiviruses and showed that they contain nearly all histone modifications found in the cellular controls, indicating that the capsid did not exclude any modifications on the basis of space or chemical compatibility. However, due to the need to extract the histones from an SDS-PAGE gel as part of the mass spectrometry workflow, the data did not include any of the larger histone variants (such as macro H2A) or the larger histones, such as H1. The finding that the quasivirus chromatin profile was very similar to that of the 293TT packaging cells was not surprising; due to the promiscuous nature of L1 and L2 spontaneous self-assembly, the majority of chromatin packaged by quasiviruses is cellular genomic chromatin [220]. We suspect that the vast majority of the signal in these experiments is from histones bound to the cellular genome, not specifically to the viral DNA. However, these findings provide a good control for our methodology by proving that the enhanced histone modifications found in the BPV1 and HPV1 preparations are not artifactual.

Future follow up studies could examine quasivirus preparations made using the "Ripcord" method (described in Chapters 2 and 3) to enrich for particles containing only the viral genome to see whether any trends become more apparent. Despite their many advantages as a model system for early HPV infection (discussed in Chapter 3), these results indicate that quasivirions are not an ideal model for studying the virion packaged chromatin in a physiologically relevant manner. However, this could also be advantageous for future experiments; if the quasivirions essentially mirror the make-up of the 293TT epigenome, the breadth of readily

available small molecule modulators of cellular chromatin modifying enzymes means that manipulating the packaged quasivirus chromatin would be a powerful tool to examine the roles of certain modifications in infection studies.

The data from profiling the chromatin of wart derived virions clearly demonstrate that the viral epigenome is considerably disparate from that of the host cell. Virion chromatin has a unique composition, implying that it is modulated at least semi-independently from processes affecting the cellular chromatin. This is not surprising given that papillomaviruses are well documented in their ability to modulate host cell chromatin. We hypothesize that in the natural papillomavirus virions, the packaged chromatin would enhance immediate early viral transcription, before any viral proteins are synthesized. Unlike some other DNA viruses (such as Herpesviruses), *Papillomaviridae* do not package any tegument proteins so their ability to modulate the host cell environment is relatively limited (L2's displacement of Sp100 being the notable exception) [69]. Thus, packaging chromatin in a state primed for transcription could provide an advantage to the virus.

Tri-methylation of H3 lysine 9 (H3K9me3), in concert with its binding partner Heterochromatin protein 1 (HP1), causes the formation of repressive heterochromatin that results in the strong, constitutive repression of transcription of local genes [244]. Packaging histone H3 loaded with this repressive mark would pose a detriment to the incoming viral genomes in their ability to synthesize replication proteins E1 and E2. In agreement with our hypothesis, wart derived virions from both bovine and human tissue were strongly and significantly depleted for H3K9me3. Similarly, trimethylation of lysine 27 (H3K27me3) is also associated with transcriptional

silencing and compaction of chromatin due to its association with the polycomb

repressive complex (PRC1/2) [244]. BPV1 virions were significantly depleted for the

singular mark H3K27me3 on both H3.1 and H3.3, although to a lesser degree than

H3K9me3. HPV1 virions were depleted for this modification as well, but only on

H3.1. Notably, the bovine virion samples were depleted for H3K27me2, while the

human virions showed an enrichment; this is one of several instances in which the

different host species showed divergent results. The depletion of H3K27me3 could be

explained by E7-mediated activation of KDM6A/B, which decreases the abundance

of H3K27me3 in HPV16 infected cells [151]. Additionally, HPV16 E6/E7 have been

shown to reduce the levels of BMI1, a component of PRC1 that stabilizes H3K27me3

[196].

In addition to repressive methylation, the data also showed enrichment of the

activating methylation modification H3K4me1, known to be enriched at cellular

enhancer regions. H3K4me1 was greatly enriched in the bovine virions compared to

all cell types and slightly in the human virions when compared to the organotypic raft

culture. This is interesting as previous studies report the enrichment of H3K4me1 in

papillomavirus genome replication foci [245]. Notably, other studies have shown that

HPV E6 inhibits the activity of the histone methyltransferase SET7 that catalyzes

monomethylation of H3K4 [199]. BPV1 particles also showed a strong enrichment

for H3K4me3, a hallmark of actively transcribing genomic regions, and H3K4me2

that is associated with permissive euchromatin.

Acetylation of lysine residues in histone proteins can serve to activate

transcription in two ways. Firstly, the acetyl group transferred to the amine group of

the lysine reduces the overall positive charge of the histone, and thus its affinity for the negatively charged DNA, causing the structure of chromatin to become less compact and more accessible to transcription initiation factors. Secondly, the acetylation of specific lysine residues serves as a binding site or scaffold for various transcriptional activators. A dominant trend of the data presented in this chapter is that papillomavirus virions are enriched in acetylated H3 and H4 lysines, sometimes to quite substantial levels. In particular, H3 lysines, 4, 14, 18, and 23 were strongly enriched. The viral E6 and E7 proteins have been known to interact with an array of histone acetyltransferases and modulate their activity. In particular, p300/CBP is a target of several viral proteins and is known to preferentially acetylate H3K14, which was one of the largest enrichments seen in the data. Specifically, E2 uses P300 to activate the early viral promoter [246]. Additionally, E7 binds to and modulates HDAC1 and HDAC2 activity, a function that is important for the maintenance of the viral genome [190, 191, 247]. This binding has biological consequences, as E7 has been shown to globally increase acetylation of Histone H3 [188]. Previous work suggests that the effect of E6 binding to the HAT Tip60 is to destabilize it in order to repress the early viral promoter [186]. It is possible that the increase in acetylation in the virions is a result of a different HAT or that this silencing of the early promoter is reversed prior to packaging. Other studies have shown that the viral chromatin is enriched in acetylated H3 and H4 at both promoter regions at early points in the lifecycle, and that this enrichment becomes more pronounced at later timepoints [174]. Previous work from other labs in cell lines studying integrated copies of the HPV genome indicates that higher levels of histone H3 acetylation are associated

131

with increased transcription of the viral genes [248]. Combined, there is room for speculation that the viral proteins direct the host HATs and HDACs to enrich the histones on the viral genome for acetylation prior to packaging.

This enrichment of acetylation on histones packaged in native papillomavirus particles is especially intriguing when considering recent work showing that the cellular Bromodomain-containing protein 4 (Brd4) serves to activate early viral transcription [203]. The double bromodomains of Brd4 preferentially bind pairs of acetylated lysines on histones, specifically H3K14ac and either H4K5ac or H4K12ac [249]. All three of those modifications were significantly enriched in the native BPV and HPV virion samples. This suggests that papillomaviruses may enrich the viral chromatin with these marks prior to packaging so that the genome is primed for transcriptional activation by Brd4 immediately after infection of the next host keratinocyte [203].

Perhaps the most striking result of our investigation was the dramatic enrichment of histone H3 variant H3.3 in the native virions. As H3.3 has been shown to become incorporated into regions of active transcription, the enrichment could be a natural progression from the enrichment of transcriptionally active histone PTMs. Alternatively, because papillomaviruses replicate outside of S-phase in a recombination-directed manner, there is likely little free H3.1 to load onto the high level of nascently forming viral DNA during the late part of the viral lifecycle, as its expression is under strict cell cycle control. Since H3.3 is expressed throughout the cell cycle, is it is possible that the observed increase in the relative abundance of the

132

variant could be a simple stochastic process due to the unique nature of HPV replication.

An additional unique feature of Papillomavirus DNA replication is that it is dependent on the host DNA damage response (DDR) [250]. Furthermore, several of the modifications found to be enriched in the virions (H3K14ac, H3K18ac, H3K23ac, H4K8ac, H4K16ac, H4K12ac) are known to be linked to DNA damage repair (reviewed in [164]). Acetylation of N-terminal lysines on histones H3 and H4 are found at sites of homologous recombination [251]. Acetyl transferases, including Tip60 (known to be manipulated known to be bound by the viral E6 protein), aid the loading of DNA repair proteins by relaxing the surrounding chromatin [252]. All of this is interesting in the context of a substantial amount of work implicating the DNA damage response (DDR) in HPV replication [250] [192]. In fact, the HAT Tip60 is required for productive viral replication in the late phase of the lifecycle [187]. Other groups have speculated that viral proteins (such as E7) sequester HDACs from the viral chromatin to drive recruitment of homologous recombination (HR) machinery rather than non-homologous end joining (NHEJ) machinery to viral replication factories [193]. Thus, an alternative explanation of the enrichments of acetylated H3 and H4 could be that these modifications are necessary for the unique replication mechanism of papillomaviruses during the late phase.

Beyond priming the incoming genome for transcription of early genes or aiding in DDR-dependent replication, the packaged viral chromatin could confer other advantages to the virus lifecycle. It is possible that, regardless of the composition of chromatin modifications, the organization of the viral genomes into

nucleosomes could reduce the innate immune profile of the incoming viral genome. Relatively long (kilobase) segments of naked DNA are recognized as foreign while DNA organized into nucleosomes inhibits activation of the cGAS-STING pathway [253]. It is well known that the chromatinization of incoming naked DNA of other viruses represents a restriction target. For example, Daxx, a HCMV restriction factor, loads repressive chromatin onto incoming HCMV genomes, forcing the virus to encode a protein, pp71, to counteract it by degradation [254]. It is possible that the HPV skips this potential point of restriction and evades innate immune sensors.

The data presented here also provide another potential insight into the late HPV lifecycle. An alternative explanation for the enrichment in histone modifications associated with active transcription and the depletion of transcriptionally repressive marks is that the L1 and L2 structural proteins assemble selectively around viral genomes that are transcriptionally active. This could happen from a spatial or temporal separation of progeny genomes into two categories: one for replication and another as transcriptional templates.

We were curious as to whether any of the viral particles packaged the linker histone, Histone H1. Total protein stains of both quasiviruses and wart derived virions did not show a band of the expected molecular weight of H1, suggesting that the virion does not contain H1 in the expected ratio of linker histones to nucleosomes.

Combined, these findings show that, upon entering the host cell, the viral genome is relatively euchromatic and readily accessible to the cellular transcription factors it needs to initiate expression of early genes.

Chapter 5: The Role of Histone Acetylation in the Early HPV Lifecycle

Introduction

      To investigate the role of increased acetylation of lysines on viral chromatin, we created a method to manipulate the acetylation status of the viral histones to deduce the biological implications of our observations described in Chapter 4. As outlined in Figure 5.1, we used two strategies to increase the acetylation of the histones bound to the viral genome using small molecule epigenetic modulators, such as inhibitors of histone deacetylases (HDACs).
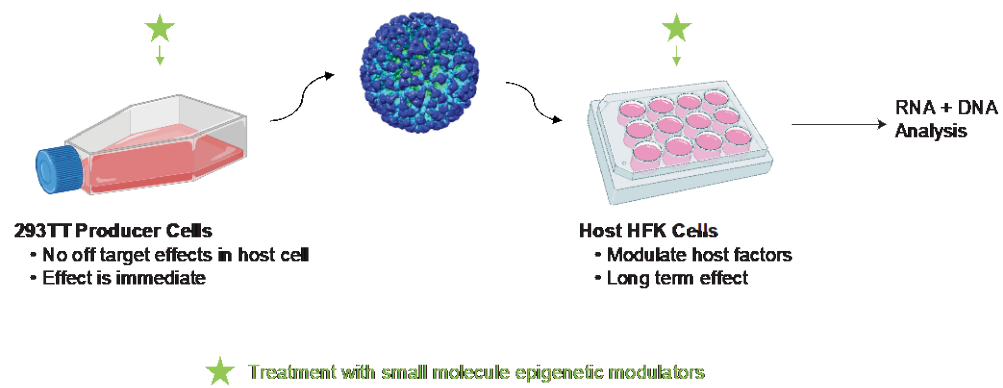
Figure 5.1. Overview of experimental design. Green stars indicate where modulators are added.

For our first strategy, 293TT cells were treated with the HDAC inhibitor sodium butyrate (NaBut) during the production of quasiviruses. There are two main benefits to this strategy. First, treating only the producer cells with the inhibitors means there are no off-target effects on the host cell that would occur if the drug was applied to the keratinocyte. Second, the effect is immediate, the viral chromatin is modified when it is released from the capsid during infection; there is no delay while waiting for host chromatin modifying machinery to act upon it. The drawback for this strategy is that the viral chromatin can be replaced after replication or interaction with various host immune or epigenetic machineries.

Our second strategy was to treat the host keratinocyte with the epigenetic modulators during the infection assay. The strengths of this method are twofold. Primarily, the effect of the treatment is prolonged, possibly increasing the magnitude of the biological readout to detectable levels. Secondly, we can use drugs that target specific processes to get a more precise view of epigenetic processes affecting viral functions. The downsides are the off-target effects created by manipulating the cellular chromatin in addition to the viral chromatin. To induce hyperacetylation of all the histones (including those on the viral genome) the host primary HFKs were treated with trichostatin A (TSA).

Combining the unique strengths of these two strategies with the breadth and versatility of the quasivirus production and infection assays described in Chapter 3 provides us with powerful new ways to study the contribution of packaged viral histone PTMs to early papillomavirus virology.

Sodium butyrate treatment of 293TT packaging cells during quasivirus production results in viral packaging of hyperacetylated histones

To examine the role of histone acetylation in the early phase of the infection cycle, we produced HPV quasiviruses with increased levels of acetylation of the packaged histones (compared to standard quasiviruses). To induce hyper-acetylation of the histones packaged into quasiviruses, we treated the 293TT packaging cells with 3 mM sodium butyrate, which is a potent inhibitor of class I HDACs, during the packaging of HPV18 quasiviruses. To confirm that the treatment resulted in increased acetylation of the virally packaged histones, histones from both the 293TT cells and HPV18 quasiviruses were isolated and separated by charge using acid-urea polyacrylamide gel electrophoresis (AU-PAGE) [255]. An immunoblot using antibodies against all forms of Histones H3 and H4 was performed. Both the quasivirus and cellular samples produced with NaBut treatment had a great increase in the overall acetylation of histone H3 and H4 (Figure 5.2A). To confirm the increase in acetylation, we performed an immunoblot using antibodies specific to acetylated H3 and H4. NaBut treated quasiviruses packaged histones with higher levels of acetylation of lysines 5, 8, 12, and 16 of H4 and lysines 9 and 14 of H3 when compared to control viruses (Figure 5.2B).
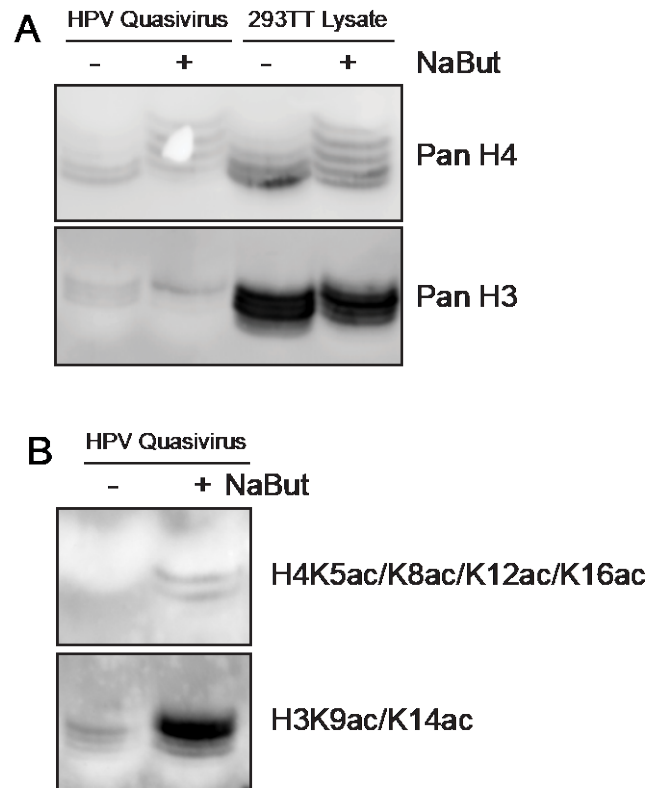
Figure 5.2. Sodium butyrate treatment of 293TT packaging cells induces hyperacetylation of histones in HPV quasiviruses. HPV18 quasiviruses were produced in 293TT cells treated with 3 mM sodium butyrate or vehicle control. Viral and cellular histones were acid extracted, separated by AU-PAGE, and transferred to a membrane. (A) Immunoblot with antibodies against histone H4 (top) and H3 (bottom). (B) Immunoblot with antibodies against acetyl-H4 (top) and acetyl-H3 (bottom). N=1.

To confirm that our sodium butyrate treatment did not alter the packaging or titer of the quasiviruses, we compared the abundance of viral proteins and HPV18 DNA in sodium butyrate treated and control quasiviruses. Sodium butyrate treatment did not significantly affect the concentration of packaged HPV18 genomes, (Figure 5.3A) the titer of HPV virions (Figure 5.3B), or the packaging efficiency (genomes per virion) (Figure 5.3C) of quasivirus preparations. Combined, these results suggest that the NaBut treated quasiviruses package chromatin with increased levels of histone acetylation but do not have other physical differences that could alter infectivity.
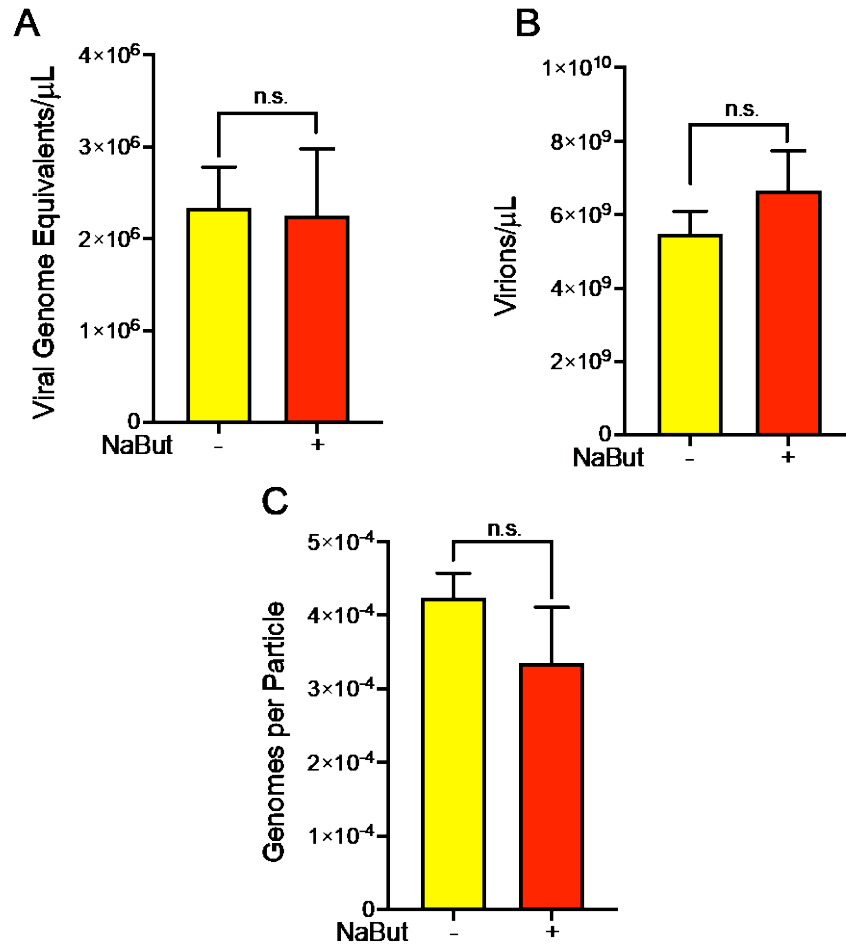
Figure 5.3. Sodium butyrate treatment of 293TT packaging cells does not alter viral titer or packaging. HPV18 quasiviruses were produced in 293TT cells treated with 3 mM sodium butyrate or vehicle control. (A) Viral titer of quasivirus preparations. Viral genomes were extracted from virions and quantitated by qPCR. (B) Quasivirus preparations were separated by SDS-PAGE alongside a standard curve of BSA. Gel was stained with Sypro Ruby and imaged. Standard curve used to calculate quantity of viral L1 protein. (C) Packaging efficiency of quasivirus preparations. Significance determined by an unpaired t-test. n.s.= not significant. N=3 independent preparations. Error=SD.

Quasiviruses with increased histone acetylation have lower levels of viral transcription and replication

To evaluate the effect of the increased acetylation of the packaged viral histones on the early viral lifecycle, the HPV18 quasiviruses produced with NaBut treatment and control quasiviruses were used to infect primary HFKs at an MOI of 100. At 72 hours post infection, RNA was harvested, and viral transcripts were quantified by RT-qPCR. Contrary to expectations, infections with the hyper-acetylated quasiviruses resulted in a significant decrease in the abundance of early viral transcripts E1^E4 and E6*I compared to control infections (Figure 5.4A and B). To assess the effect of the sodium butyrate treatment on viral replication, primary HFKs were infected at an MOI of 100. 72 hours post infection, total DNA was harvested. To distinguish between nascently replicated viral genomes and unreplicated genomes, the DNA was digested with DpnI and MboI, respectively, as well as a mock digest. The resulting DNA was quantified by qPCR. In the cells infected with the hyper-acetylated quasiviruses, the overall HPV18 DNA level was decreased (Figure 5.5A and B). The levels of viral replication from the sodium butyrate-treated quasiviruses were significantly decreased, while the amount of unreplicated viral genomes was not different (Figure 5.5A and B). Combined, these data suggest that the increase in viral chromatin acetylation causes a reduction in early viral transcription and replication.
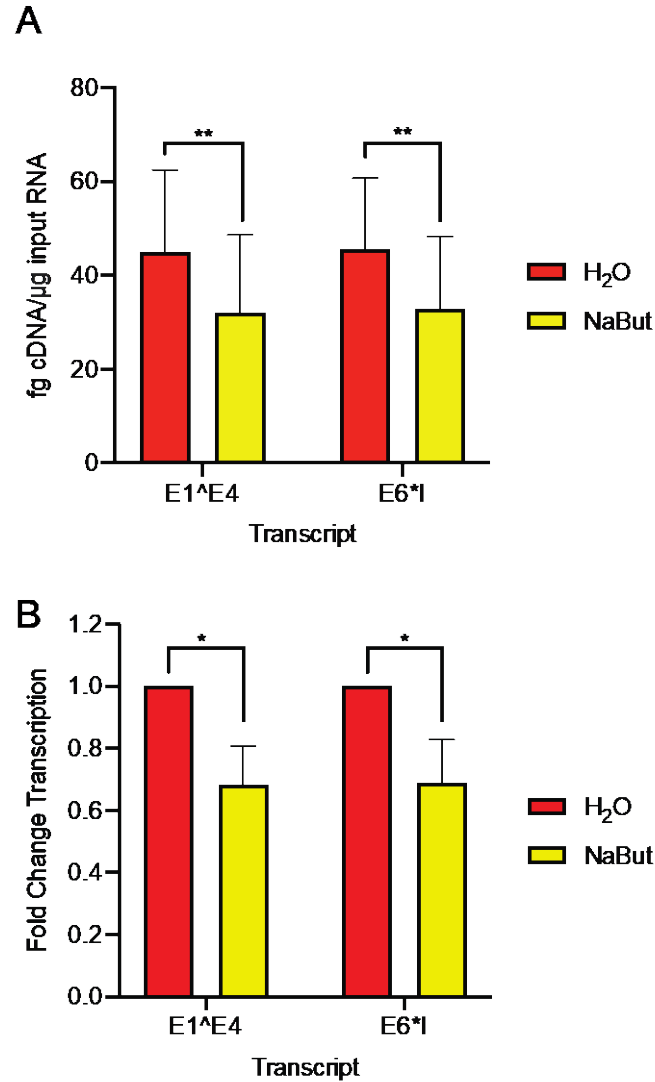
Figure 5.4. HPV early transcription from HPV quasiviruses with hyperacetylated histones.
Primary HFKs were infected at an MOI of 100 with HPV18 quasiviruses with hyperacetylated histones and control viruses. At 72 hpi, total RNA was harvested. Early viral transcripts were quantitated by RT-qPCR and normalized to cellular TBP. (A) Normalized levels of early transcripts. Significance determined by a paired t-test (B) Data presented as fold change from untreated quasivirus infections. Significance determined by an unpaired t-test. *=$p<0.05$ **=$p<0.01$ N=3 biological replicates. Error=SD.
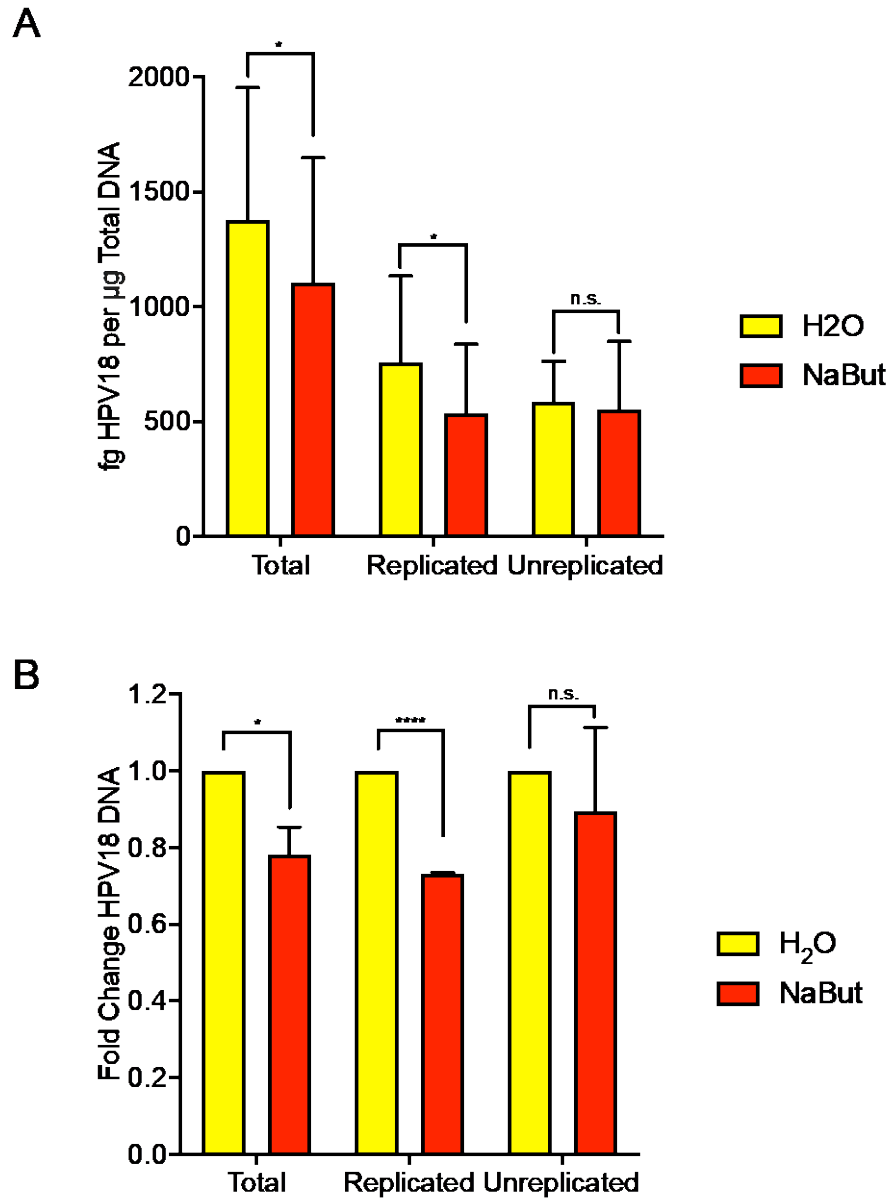
Figure 5.5. HPV replication in cells infected with HPV quasiviruses with hyperacetylated histones is reduced. Primary HFKs were infected at an MOI of 100 with HPV18 quasiviruses with hyperacetylated histones and control viruses. At 72 hpi, total DNA was harvested. DNA was digested with DpnI, MboI or H_2O as a control to distinguish between nascently replicated, unreplicated, and total viral genomes, respectively. Digested viral DNA was quantified by qPCR and normalized to cellular RNase P. (A) Normalized levels of HPV18 DNA. Significance determined by a paired t-test. (B) Data presented as fold change from untreated quasivirus infections. Significance determined by an unpaired t-test. n.s.=not significant *=$p<0.05$ ****=$p<0.0001$ N=3 biological replicates. Error=SD.

To complement the acetylated quasivirus approach, we recapitulated the increase in viral histone acetylation using our second approach described in Figure 5.1. Primary HFKs were infected at an MOI of 100 with untreated HPV18 quasiviruses. At one hour post infection, the HFKs were with treated 400 nM TSA, an inhibitor of class I and II HDACs, thus inducing global hyperacetylation of both cellular and viral histones. At 72 hpi RNA was harvested, and viral transcripts were quantified by RT-qPCR. Early viral transcription in the treated cells was significantly lower than in cells treated with the vehicle control (Figure 5.6A and B). These data suggest that hyperacetylation of viral chromatin has a detrimental effect on the early viral life cycle.
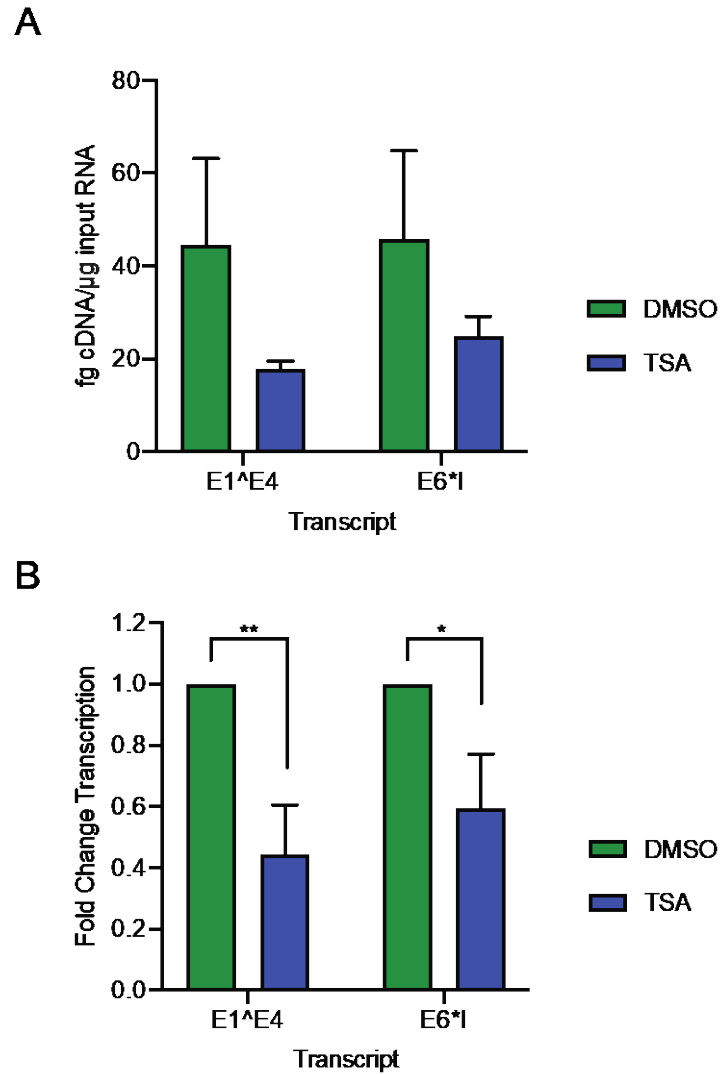
Figure 5.6. HPV early transcription is reduced in cells treated with HDAC inhibitor TSA.
Primary HFKs were infected at an MOI of 100 with wildtype HPV18 quasiviruses. At 1 hpi, cells were treated with 400 nM TSA for 72 hours. At 72 hpi, total RNA was harvested. Early viral transcripts were quantitated by RT-qPCR and normalized to cellular TBP. Significance was determined by an unpaired t-test. *=p<0.05 **=p<0.01 N=3 biological replicates. Error=SD.

To determine the timing of this effect, we infected primary HFKs with HPV18 quasiviruses with hyperacetylated chromatin and untreated controls at 100 MOI and harvested RNA and DNA at 24, 48, 72, and 96 hours post infection. Viral transcripts were quantified by RT-qPCR. Contrary to expectations, the sodium butyrate treated quasiviruses were not decreased in their ability to synthesize early transcripts E1^E4 (Figure 5.7A and B) and E6*I (Figure 5.7C and D) until 72 hours after infection. At earlier timepoints, the transcription from the hyperacetylated quasiviruses was slightly, but not significantly higher. We observed a nearly identical trend with viral replication as well. Total viral genome copy number (Figure 5.8A and B) and the level of nascent viral replication (Figure 5.8C and D) were not significantly different in cells infected with the sodium butyrate treated viruses at immediate early time points (24 and 48 hpi), but differences became more apparent as time since infection progressed. The level of unreplicated DNA was very similar until 96 hours post infection (Figure 5.8E and F). These data suggest that the lack of robust activation of the early viral life cycle of the hyperacetylated quasiviruses does not occur immediately after entry into the host cell.
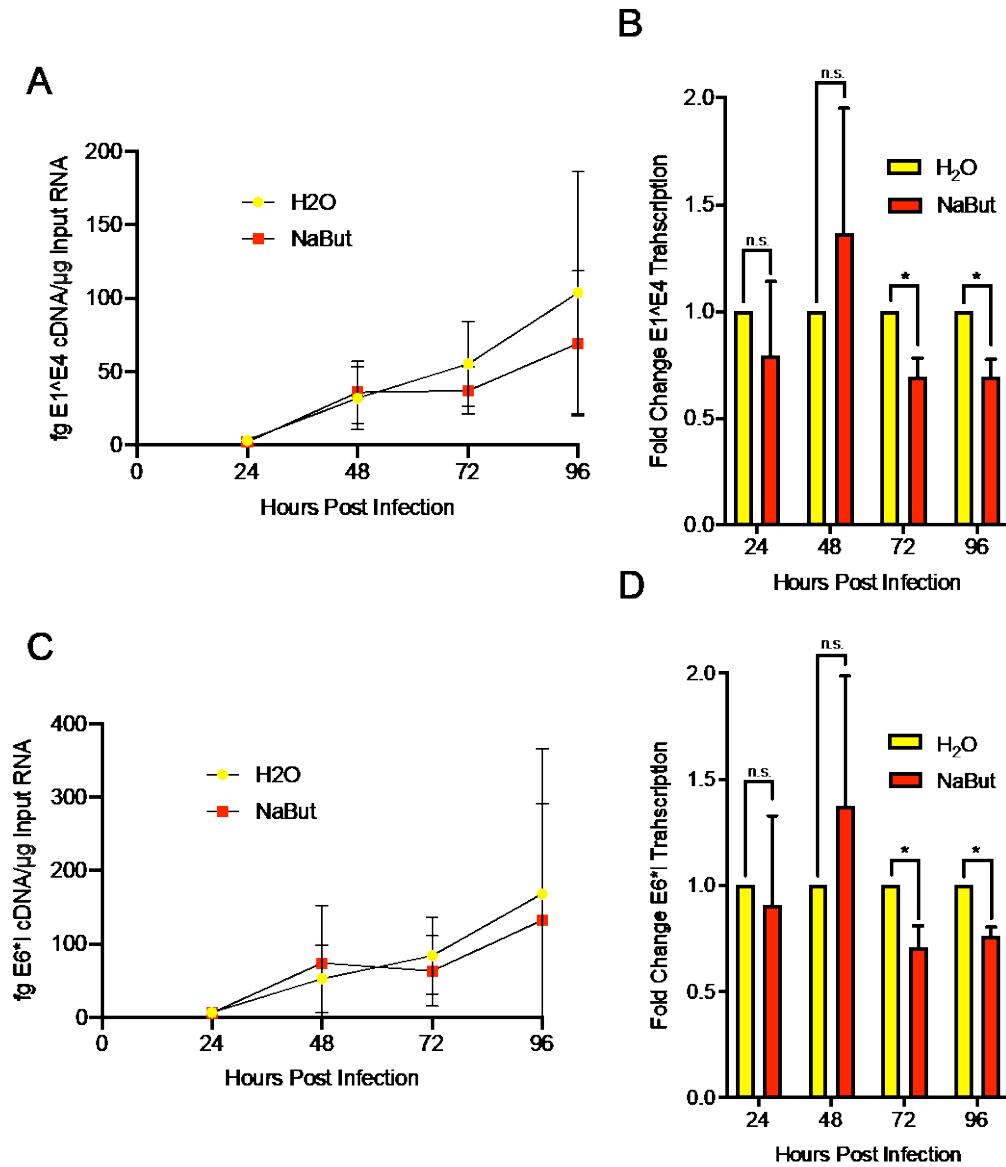
Figure 5.7. HPV quasiviruses with hyperacetylated histones have reduced transcription at later time points. Primary HFKs were infected at an MOI of 100 with HPV18 quasiviruses with hyperacetylated histones and control viruses. At 24, 48, 72, and 96 hpi, total RNA was harvested. Early viral transcripts were quantitated by RT-qPCR and normalized to cellular TBP. (A) Normalized E1^E4 transcription. (B) Data are presented as fold change from untreated control infections at the indicated timepoint. (C) Normalized E6*I transcription. (D) Data are presented as fold change from control infections at the indicated timepoint. Significance was determined by a paired t-test. n.s.= not significant. *=p<0.05 N=3 biological replicates. Error=SD.
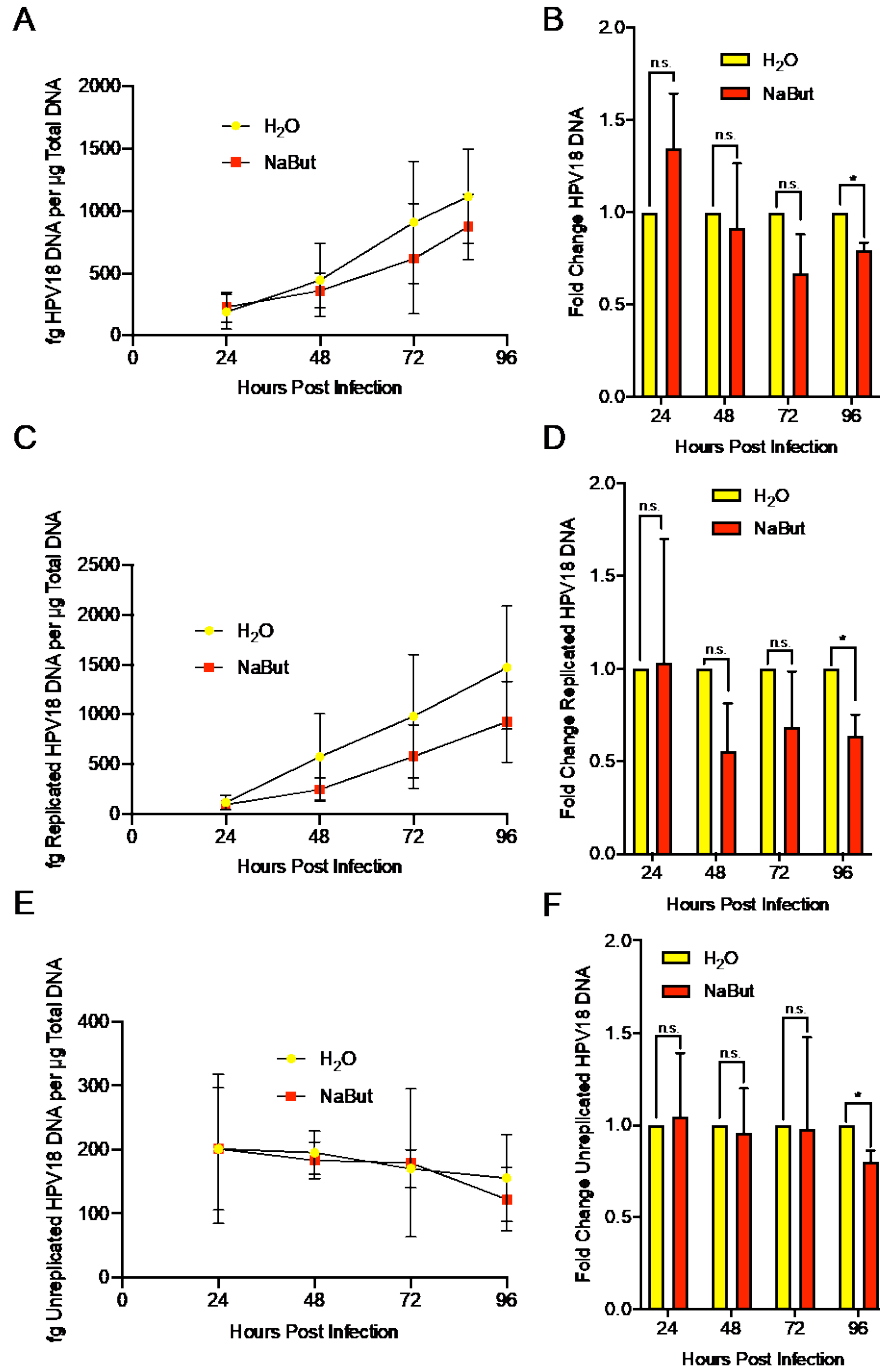
Figure 5.8. HPV quasiviruses with hyperacetylated histones have reduced replication at later time points. Primary HFKs were infected at an MOI of 100 with HPV18 quasiviruses with hyperacetylated histones and control viruses. At 24, 48, 72, and 96 hpi, total DNA was harvested. DNA was digested with DpnI, MboI or H_2O as control to distinguish between nascently replicated, unreplicated, and total viral genomes, respectively. Digested viral DNA was quantified by qPCR and normalized to cellular RNase P. (A) Total HPV18 DNA. (B) Data presented as fold change from control infections at the indicated timepoint. (C) Replicated (DpnI resistant) HPV18 DNA. (D) Data are presented as fold change from control infections at the indicated timepoint. (E) Input (MboI resistant) HPV18 DNA. (F) Data are presented as fold change from control infections at the indicated timepoint. Significance was determined by a paired t-test. n.s.= not significant. *=p<0.05 N=3 biological replicates. Error=SD.

149

"Ripcord" quasiviruses produced with sodium butyrate treatment have reduced viral early transcription

We next investigated the mechanism by which the apparent repression (or lack of activation) occurred. First, we hypothesized that the hyperacetylated cellular chromatin packaged by the quasivirus system (see Chapter 3) could be causing the effect. To test this theory, we generated "ripcord" HPV18 quasiviruses (produced to reduce packaging of cellular chromatin) with and without the sodium butyrate treatment. The quasiviruses were used to infect primary HFKs. At 72 hpi, total RNA was harvested, and viral transcripts were quantified using RT-qPCR. Cells infected with the "ripcord", sodium butyrate treated quasiviruses had significantly lower levels of viral transcripts than untreated controls (Figure 5.9A and B). These data suggest that the introduction of hyperacetylated cellular chromatin by the quasivirus is not responsible for the decrease in early viral functions.
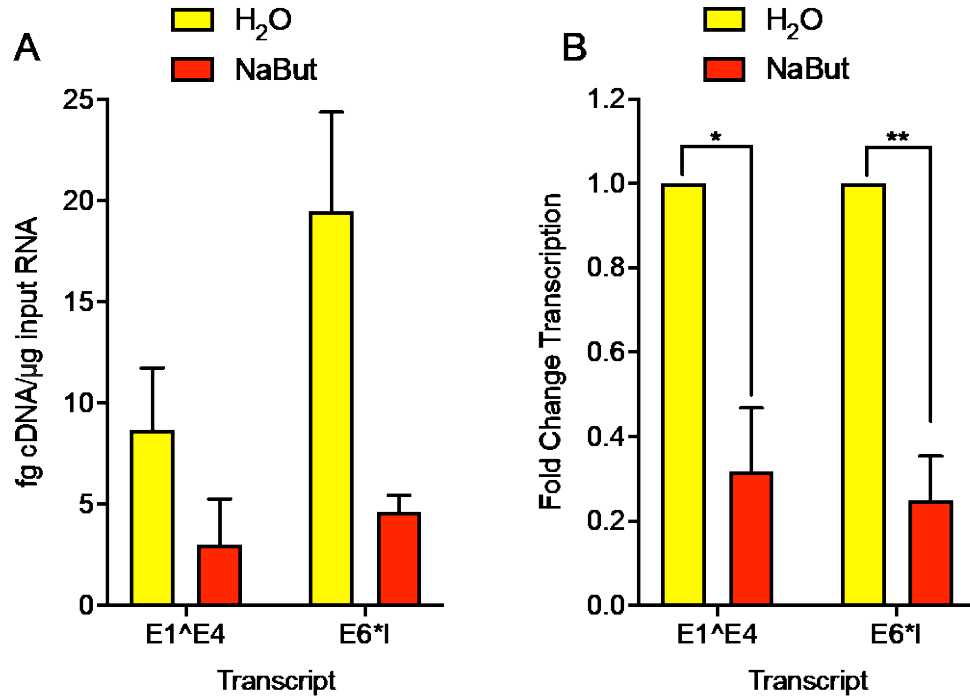
Figure 5.9. HFKs infected with "ripcord", sodium butyrate treated quasiviruses express lower levels of viral early transcripts. Primary HFKs were infected at an MOI of 10 with HPV18 "ripcord" quasiviruses with hyperacetylated histones and control viruses. At 72 hpi, total RNA was harvested, and early viral transcripts were quantified by RT-qPCR and normalized to cellular TBP. (A) Normalized viral transcripts. (B) Data are presented as fold change from untreated quasivirus infections. Significance determined by an unpaired t-test. *=p<0.05 **p<0.01 N=2 biological replicates. Error=SD.

Viral replication is not necessary for decreased transcription from quasiviruses with increased histone acetylation

Additionally, we wanted to determine whether viral DNA replication inside the host keratinocyte was required for the observed reduction in transcription. To test this, we generated HPV quasiviruses containing a translation termination linker (TTL) mutation in the E1 gene (E1mut), rendering them replication incompetent. We used these viruses, produced with and without NaBut treatment in the 293TT cells, to infect primary HFKs at 100 MOI. 72 hours after infection, RNA was extracted and early viral transcription was measured by RT-qPCR. As expected, transcription from the E1 mutant viruses was decreased compared to wildtype controls (Figure 5.10A and C), but the relative difference between the sodium butyrate treated viruses and the untreated controls was very similar (Figure 5.10B and D), implying that decreased transcription is not due to decreased replication of the viral genome.
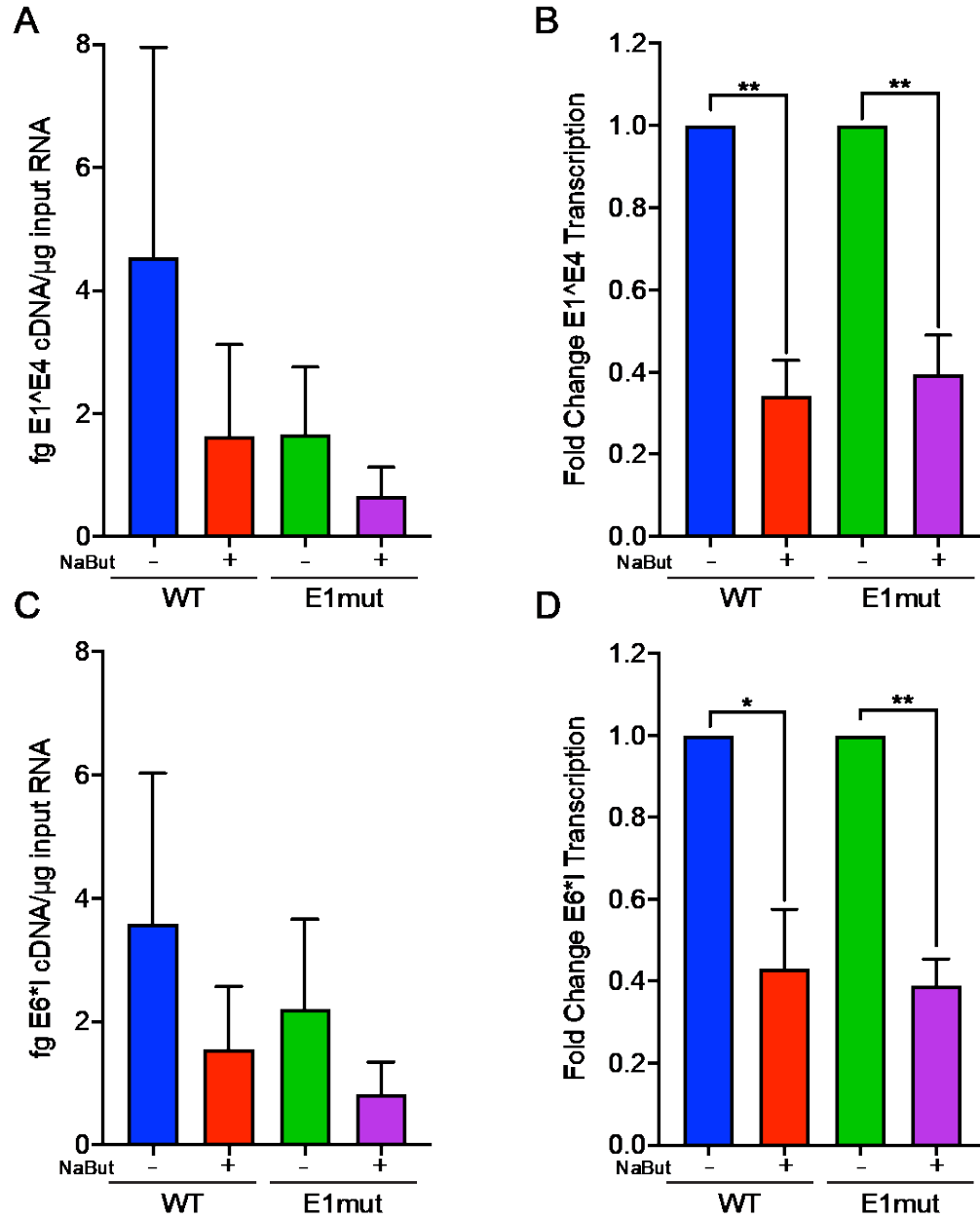
Figure 5.10. Viral replication is not necessary for decreased transcription from hyperacetylated quasiviruses. Primary HFKs were infected at an MOI of 100 with replication incompetent or wildtype HPV18 quasiviruses with hyperacetylated histones and control viruses. At 72 hpi, total RNA was harvested, and early viral transcripts were quantified by RT-qPCR and normalized to cellular TBP. (A) Normalized E1^E4 transcription. (B) Data are presented as fold change from untreated quasivirus infections. (C) Normalized E6*I transcription. (D) Data are presented as fold change from untreated quasivirus infections. Significance determined by a paired t-test. *=p<0.05 **=p<0.01 N=3 biological replicates. Error=SD.

Brd4-E2 complex formation is not necessary for decreased transcription from hyperacetylated quasiviruses

Our next hypothesis was that the decrease in transcriptional activity in quasiviruses with hyperacetylated histones was mediated by increased binding of the E2-Brd4 (Bromodomain containing protein 4) complex to the viral chromatin. Cellular Brd4 contains two bromodomains that bind to the acetylated lysines on the N-terminal histone tails [256]. Brd4 forms a complex with the viral E2 protein that represses viral transcription [125]. To test whether the increased acetylation of the quasiviral histones promoted repressive Brd4-E2 complex binding, we produced HPV18 quasiviruses with a mutation in the E2 protein (I77A) that prevents binding to Brd4 with and without the sodium butyrate treatment [121]. Primary HFKs infected with these quasivirus preparations showed the same phenomena of significantly decreased E1^E4 (Figure 5.11A and B) and E6*I transcription (Figure 5.11C and D) regardless of the ability for E2 and Brd4 to form a complex. These data indicate that the Brd4-E2 complex formation is not the mechanistic driving force behind our observations.
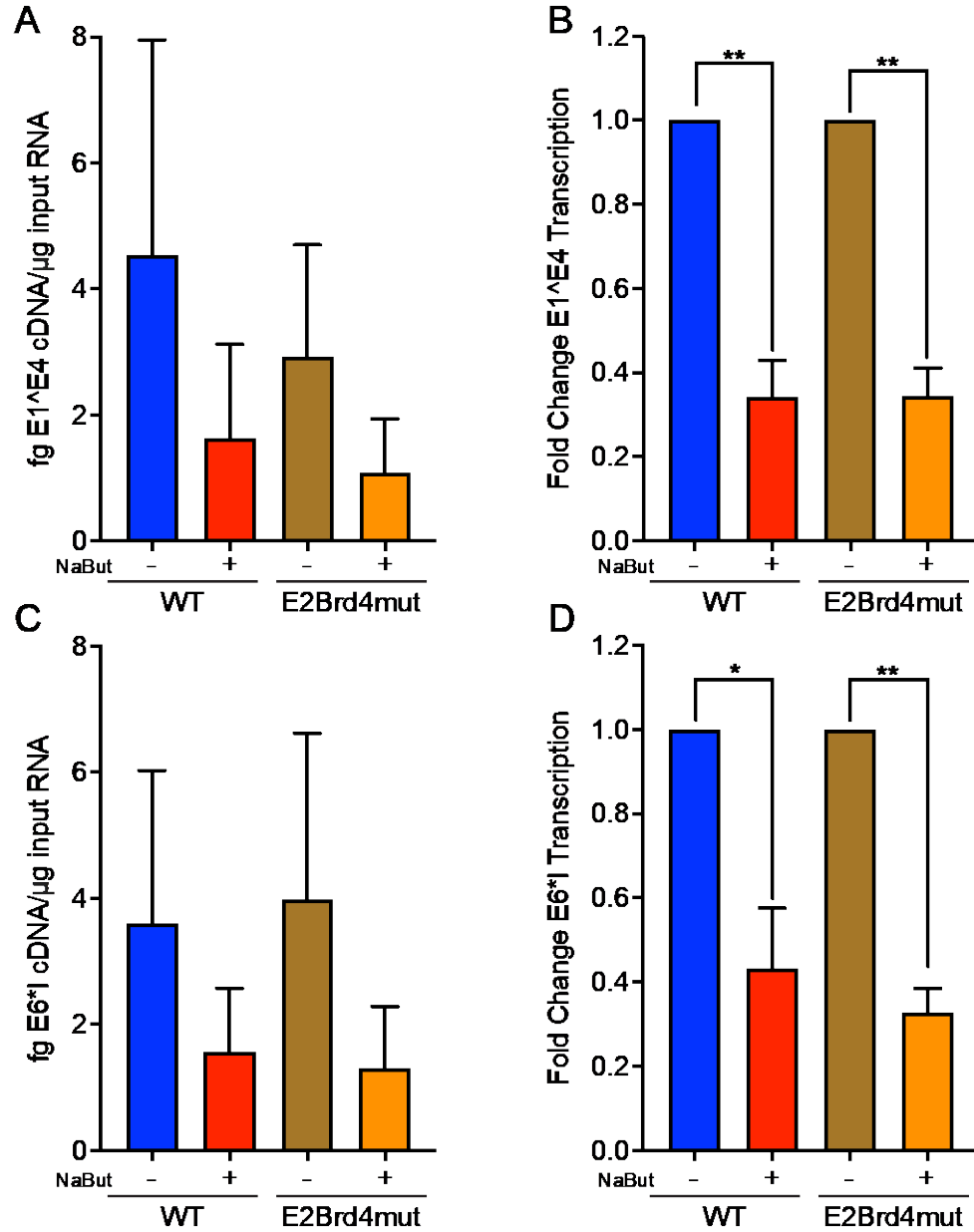
Figure 5.11. Brd4-E2 complex formation is not necessary for decreased transcription from hyperacetylated quasiviruses. HPV18 quasiviruses with either wildtype genomes or mutation I77A in E2 (preventing binding to cellular Brd4) were produced with or without sodium butyrate treatment and used to infect primary HFKs at an MOI of 100. At 72 hpi, total RNA was harvested, and early viral transcripts were quantified by RT-qPCR and normalized to cellular TBP. (A) Normalized E1^E4 transcription. (B) Data presented as fold change from untreated quasivirus infections. (C) Normalized E6*I transcription. (D) Data presented as fold change from untreated quasivirus infections. Significance determined by a paired t-test. *=$p<0.05$ **=$p<0.01$ N=3 biological replicates. Error=SD.

155

Sp100 is not responsible for decreased transcription from hyperacetylated quasiviruses

We next examined an another cellular bromodomain-containing protein, Sp100. Sp100 co-localizes to incoming HPV genomes and has been shown to be a restriction factor for HPV infection, repressing early viral transcription [69, 70]. To determine if increased Sp100 binding to acetylated histones was repressing the early viral lifecycle, we used a series of Near-Diploid Immortalized Human Keratinocyte (NIKS) Sp100 (-/-) cell lines generated in our lab using CRISPR-Cas9. We infected parental and Sp100 (-/-) NIKS cells with the NaBut treated and control quasiviruses. After 72 hours, RNA was collected, and early transcripts quantified were by RT-qPCR. While the overall magnitude of the transcriptional effect was lower than in primary HFKs, there was very little difference between the Sp100 deficient cell lines and the controls in terms of the relative transcription levels from the acetylated and control viruses (Figure 5.12A and B). The data imply that the Sp100 protein is not mediating decreased transcription from hyperacetylated quasivirus chromatin.
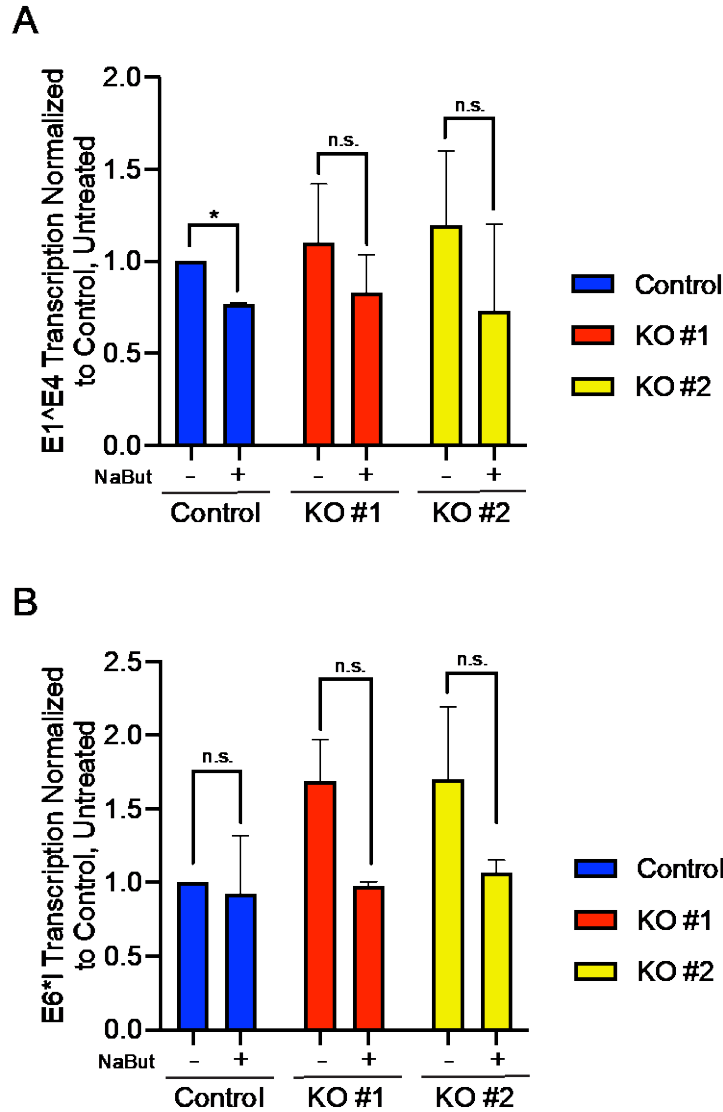
Figure 5.12. Sp100 is not responsible for decreased transcription from hyperacetylated quasiviruses. Sp100 (-/-) NIKS or wildtype control cells were infected at an MOI of 100 with HPV18 quasiviruses with hyperacetylated histones and control viruses. At 72 hpi, total RNA was harvested, and early viral transcripts were quantified by RT-qPCR and normalized to cellular TBP. Data are presented as normalized to control cells with untreated quasivirus. (A) E1^E4 transcription. (B) E6*I transcription. Significance was determined by an unpaired t-test. n.s.=not significant. *=p<0.05 N=2 biological replicates. Error=SD.

Discussion

In Chapter 4 we showed that native papillomavirus virions are enriched in acetylation of lysine tails on the N-terminus of histone H3 and H4. We initially hypothesized that this was to prime the incoming viral genome for immediate early viral transcription. Following this logic, we theorized that keratinocytes infected with quasiviruses packaging hyperacetylated histones would have higher levels of early viral transcripts. However, our experimental data showed the opposite results. Transcription from quasiviruses produced in 293TTs treated with sodium butyrate was significantly lower.

Replication assays showed that cells infected with the NaBut treated and control quasiviruses showed no difference in the levels of unreplicated HPV18 DNA through the first 72 hours of the infection. This suggests that the two quasivirus preparations have no difference in their ability to bind to and enter the host cell, giving increased confidence that this is not a viral entry-mediated phenomenon. However, given that the assay does not distinguish where in the cell the genomes are located, we cannot rule out the possibility that the quasiviruses produced in sodium butyrate-treated 293TT packaging cells are somehow defective in their ability to effectively traffic to the nucleus.

We also speculated that the sodium butyrate treatment to the 293TT cells during packaging could have induced off target effects and induced acetylation of lysines on the viral L1 and L2 proteins. L2 directs the incoming viral particle to the nucleus and is responsible for displacing the restriction factor Sp100 upon arrival [69, 257]. L2 has a number of lysines that could potentially be acylated, possibly affecting

158

these functions. To test this hypothesis, we partnered with the Protein Chemistry Section of NIAID's Research Technologies Branch to detect any differences in acetylation of lysines on the capsid proteins. They attempted to perform mass spectrometry on the viral capsid proteins from quasivirus preparations produced with and without sodium butyrate treatment. However, the amino acid sequence of L1 and L2 made this method technically challenging. They also tried to detect differences in the charge of the capsid proteins by isoelectric focusing and 2D SDS-PAGE, but those results were inconclusive.

Due to the nonspecific packaging by L1/L2 in the 239TT cells, quasiviruses can package and deliver linearized segments of host chromatin to cells upon infection [221]. We theorized that hyperacetylated, linear segments of the cellular genome being introduced to the cell could trigger an innate immune response. Utilizing the "ripcord" method of quasivirus production to reduce the packaged cellular DNA, we observed that the magnitude of the transcriptional effect was in fact larger, ruling out this potential artifact. Combined with our data showing that the quasivirus titer, virion abundance, and packaging were not affected by the sodium butyrate treatment, we postulate that this is a true transcriptional observation.

Our data showing that replication-incompetent, highly acetylated quasiviruses exhibited decreased transcription was important for several reasons. By showing that replication is not necessary for the decrease in transcription from highly acetylated quasiviruses, it is possible that the reduced viral replication is due to lower expression of the viral replication proteins E1 and E2, rather than an alternative scenario in which the decreased replication provides fewer transcriptional templates. In addition,

159

once the virus undergoes replication, the histones that are loaded onto the progeny genomes could be acetylated at reduced levels, removing the effect of the sodium butyrate treatment. Because in this experiment, all transcription occurs from unreplicated genomes, we can have increased confidence that the sodium butyrate-induced acetylation of the viral histones is either directly or indirectly responsible for the transcriptional effects.

Possibly the most perplexing data from the experiments presented above was the time course infection assay. Initially, we expected that any differences would be most pronounced at the earliest timepoints after infection. On the contrary, the transcriptional and replicative effects only became significant at 72 hours after the virus was introduced to the cells. Given that the hyperacetylation of the histones on the viral genome would be removed by displacement of histones from the viral genome during the first round of replication, this result was surprising. There are two explanations for this observation of delayed onset transcriptional repression. First, it is possible that the hyperacetylated quasivirus genomes trigger an antiviral host response that takes place over 24 to 48 hours. Second, because the infections occur when the keratinocytes are only ~5-10% confluent, there are likely quasivirions transiently attached to the J2 feeder cells at early time points. By the later timepoints the keratinocytes cover much of the well, potentially becoming exposed to additional rounds of infection as they divide. It is possible that the NaBut treated quasiviruses are restricted from successful infection during these later viral entry events in a manner that does not occur with the control quasiviruses.

In the work presented here, we were unable to identify a mechanism for the decrease in transcription from highly acetylated quasiviruses. We hypothesized that, if there was a cellular protein involved in this regulation, it would be one with specificity for binding to acetylated histone tails. We speculated that the most likely candidate would be a histone acetylation reader protein containing a bromodomain. We examined the role of two bromodomain-containing proteins that were previously shown to bind to HPV chromatin and regulate viral functions, Brd4 and Sp100 [70, 91, 125, 258]. Our data indicate that these two bromodomain-containing proteins are not solely responsible for transcriptional repression. Future work in this area could use bromodomain inhibitors to see if there are additional, yet to be identified, cellular proteins mediating this response. Alternatively, a newly identified class of histone reader domains called plant homeodomain (PHD) fingers (one is present in Sp100 isoform C) could be involved in this process [259, 260]. Proteins with these domains can bind to histone H3 with acetylated lysines, so it stands to reason they would be likely to bind to the incoming viral chromatin in the sodium-butyrate treated quasivirus infections [261].

It is possible that the hyperacetylated chromatin is somehow more immunogenic, alerting the cell's innate immune system to the virus's presence. Future studies to continue this work should involve looking at the levels of cellular anti-viral proteins in cells infected with the treated and untreated quasiviruses. Alternatively, we could produce hyperacetylated "pseudoviruses" to determine if this phenomenon is specific to papillomavirus genomes or if it would occur for all foreign DNA delivered by papillomavirus capsids.

It is interesting that the alternative strategy of inducing acetylation of the histone bound to the viral genome by treating the host cell with the HDAC inhibitor TSA gave nearly identical results. While it does mirror the observations obtained with hyperacetylated quasiviruses, it is possible that the repressive effects on viral transcription by the sodium butyrate treatment in 293TTs and TSA treatment in the HFKs are caused by two separate mechanisms. As the keratinocytes were continuously cultured in the presence of the drug throughout the infection, the histones bound to the viral genomes would have been hyperacetylated throughout the duration of the experiment, while in the experiments with the NaBut treated quasiviruses, the hyperacetylation may have been lost after the first round of viral replication. In agreement with our results, a previous study showed that cell lines that maintain the HPV31 genome as an extrachromosomal element exhibited a reduction in E2 and E7 transcription following TSA treatment [262]. Another study demonstrated that inducing global hyperacetylation in infected cells with a different HDAC inhibitor, Vorinostat, can reduce productive viral genome replication during the late stage of the lifecycle [263]. One possible explanation for these results is that treatments with these inhibitors epigenetically activates transcription from all of the viral genomes in a cell. Some groups have speculated that in natural infections there exists a small subset of transcriptionally active genomes; it is possible that the TSA treatment throws off this balance [174]. Other studies carried out in cells with integrated HPV genomes have shown that TSA treatment increases the expression of the oncogenes E6 and E7 [248].

A previous study has shown that treating host cells with TSA immediately prior to infection treatment reduces early HSV-1 replication [264]. The authors of this work suggest that the HDAC inhibitor increased expression of cellular antiviral defenses, leading to repression of the HSV lifecycle. Future work using our system should involve examining the transcription of antiviral factors in infected keratinocytes treated with TSA. There is ample additional evidence in the literature to support the use of HDAC inhibitors as a means of pharmaceutical antiviral intervention [265].

While other studies describe a positive a correlation between acetylation of histones on the viral genome and HPV transcription and replication, our results appear to be contradictory. However, it is possible that the methods for inducing hyperacetylation of the viral chromatin were detrimental to the lifecycle because the acetylation was likely evenly distributed across the viral genome, rather than being enriched in certain areas (such as the early and late promoters) as has been seen in work by other groups in untreated cells [174] . This could induce transcription factor binding all over the genome rather than in desired areas. To address this, we could target histone acetylation to the early and late promoter regions by utilizing acetylation transferases (such as p300) complexed to a deactivated Cas9 and targeted to specific regions of the viral genome using gRNAs [266]. Alternatively, future experiments could involve using epigenetic modulators that have more specific targets than TSA or sodium butyrate.

In this chapter we describe a system to selectively modify the PTMs of packaged histones in papillomavirus particles and examine their role in the early

infectious cycle. Future experiments could use epigenetic modulators or siRNAs that target more specific enzymes, such as individual HATs or HDACs or other epigenetic processes such as histone or DNA methylation. Additionally, further work could combine the infection-based colony forming assay developed in Chapter 3 to determine the role of viral histone modifications on the establishment of the viral genome as a persistently maintained episome.

Chapter 6: Discussion

In this dissertation, we use a wide variety of techniques to explore how the HPV infectious cycle is regulated by chromatin modifications. We focus particularly on the early phase of infection, immediately after the incoming virus is delivered to the nucleus. Chapter 3 describes optimization of recombinant HPV quasivirus production. In Chapter 4, these quasiviruses were analyzed for histone modifications by mass spectrometry in comparison to native virions isolated from patients and animals. We showed that native virions have a distinct profile of chromatin modifications when compared to host cells, and that they are enriched in activating chromatin marks (particularly acetylation of histones H3 and H4) and depleted in repressive modifications (certain lysine methylations). Chapter 5 describes experiments that analyze the biological significance of these modifications by modulating the acetylation of histone H3 and H4 in quasiviruses and evaluating the effect on early infection of keratinocytes.

One of the goals we had for improving the preparation of HPV quasiviruses was to improve the particle to infectivity ratio. Pseudovirus preparations have far higher titer and infectivity to particle ratios, in part because of the Large T antigen-directed replication of the packaged reporter plasmid inside the 293TT packaging cells. We described two different ways to induce replication of the viral genome in the 293TT packaging cells: co-expression of the E1/E2 viral replication proteins and the insertion of a native SV40 origin of replication into the late region of the viral genome. Both methods increased yields of quasivirus preparations and improved the

ratio of viral genomes to capsids. However, surprisingly, this did not result in an increase in early viral transcription in infected keratinocytes; transcription was lower at 72 hours post infection. We postulate that replication induces the ordered assembly of nucleosomes on the viral DNA but, in turn, this is repressive for early transcription.

To test this hypothesis, future work could involve isolating chromatin from 293TT-replicated and unreplicated quasivirus virions and performing a nucleosome positioning assay to determine if there is any difference in the ordering of nucleosomes. The ordering of nucleosomes is known to have enormous importance in the initiation of transcription [233]. These assays have been performed using chromatin isolated from other viruses, such as SV40 [267]. Initial studies of the nucleosomes packaged by papillomavirus virions showed that the length of spacer DNA between nucleosomes is variable, suggesting that the nucleosomes are located at specific sites, rather than at regular intervals [29]. Other studies have reported that there are two nucleosomes specifically positioned within the HPV URR in the viral genome in infected cells, one of which overlaps the Sp1 site of the early promoter [268]. This region of the viral genome has a weaker affinity for nucleosomes than the rest, suggesting nucleosomes are likely displaced to initiate viral transcription [269]. We propose that DNA replication of the viral genome in 293TT cells causes nucleosomes to be loaded into the URR in a manner that is suboptimal for the initiation of transcription. E1 and E2 induce changes in nucleosome positioning, however, as the unreplicated genomes are packaged in the absence of the viral replication proteins, it is plausible that their nucleosome positioning differs, resulting

in increased ability for transcription factors to bind immediately upon arrival in the nucleus [269, 270].

Additionally, it is possible that inducing replication in the 293TT cells (outside of the normal context of viral genome replication in keratinocytes and without other viral gene products present) induces repressive modifications in the viral chromatin, causing the decreased transcription. To determine if this is responsible for our effect, we could use the histone modification profiling techniques we described in Chapter 4 to look at the differences in the histone PTMs between quasiviruses with replicated and unreplicated genomes. Lastly, we could perform a time course of infection, to see if the magnitude or direction of our transcriptional effect changes at earlier timepoints, as occurred in the sodium butyrate treated quasiviruses in Chapter 5.

Like the E1/E2-replicated quasiviruses, the "ripcord" virus preparations had an increased percentage of capsids containing viral genomes. However, unlike inducing replication of the viral genome in packaging cells, producing quasiviruses using the "ripcord" maturation method did result in higher transcription of viral early genes in infected cells. Another possibility is that the "ripcord" quasiviruses are more effective in the delivery of viral DNA to the host cell than normal quasiviruses. This could be tested by performing infections at the same MOI and performing our assay to detect unreplicated HPV18 DNA at early timepoints post infection. Additionally, we considered the possibility that the "ripcord" quasiviruses packaged less linearized, digested cellular DNA than traditional quasiviruses preparations. This could help determine if the mechanistic explanation for our observation involved entry or

transcriptional regulation. To determine if this is the case, we could calculate the quantity of non-viral DNA in each type of preparation by extracting all packaged DNA and measure its quantity and then subtracting the amount of viral DNA (determined by qPCR for HPV18 DNA).

In Chapter 4, we describe a quantitative approach to profile the global modifications present on histones in native papillomavirus particles. We demonstrated that quasivirus particles had an overall very similar chromatin modification profile to the 293TT cells in which they are packaged. In the native papillomavirus virion isolated from bovine and human warts, the composition of the virion epigenome differed significantly from that of the uninfected host cell. We detected large enrichments in histone PTMs associated with transcriptional activation, particularly histone H3 acetylation (H3K4ac, H3K14ac, H3K18ac, and H3K23ac) and H4 acetylation (H4K5ac, H4K8ac, and H412ac). We also detected trends in the enrichment of the methylation of the lysines associated with activating transcription (H3K4me1 and H3K4me3) and depletion of transcriptionally repressive methylation (H3K9me3 and H3K27me3). The first study to look at histone modifications packaged in small DNA tumor viruses examined the acetylation of histones packaged in SV40 virions and found that histones H3 and H4 were extensively acetylated [271]. More recent studies conducted similar experiments using BK polyomavirus particles, and they report an enrichment of acetylated and methylated H3 and H4 in the virions compared to host cells (and the presence of many additional modifications), suggesting that the viral chromatin is in a transcriptionally active state while packaged in the polyomavirus capsid, in agreement with our data [272]. Combined

our data, and that in the literature, suggest that amongst small DNA tumor viruses that package chromatinized genomes, there is conservation in the preferential packaging of acetylated histones and that whatever benefit this provides the virus, it is not unique to the *Papillomaviridae*.

To further advance this project, we need to answer the critical question of how these modifications are distributed around the viral genome. Future work could include isolating chromatin from virions and performing ChIP-PCR or ChIP-seq using antibodies against the modifications we identified to be most enriched in the virions (H3K4me1, H3K4me3, H3K9ac, H3K18ac). We predict that there will be a higher level of these histone modifications at the early and late promoter regions, as previous studies have shown that, in viral chromatin isolated from infected cells, both the promoter regions are enriched in acetylated H3 and H4 throughout the productive lifecycle, but that this enrichment is largely increased at the late promoter upon differentiation [174]. The data from these proposed experiments could help determine a model for explaining our observations of increased activating histone PTMs in the virion. If we detect more signal at the late promoter, then this would suggest that the enrichment of the active modifications is likely due to the preferential packaging of genomes actively transcribing the late genes. Alternatively, if the data shows more intense acetylation at sites around the early promoter, this would suggest that the virus selects these modifications to be packaged to better prime the incoming viral genome to initiate transcription upon arrival in the nucleus.

One of the limitations of our study was that the control cells for the native bovine and human papillomavirus virions, while primary, were uninfected. This

prevents us from making strong conclusions about whether the enrichments and depletions of histone PTMs we detected were the result of selective packaging or if the virus induced global changes to the cellular epigenome. We performed the experiments described in Chapter 4 using BPV1 infected wart tissue as controls for the bovine virions in the mass spectrometry and immunoblot experiments, but ultimately decided that the tissue was too heterogeneous; it contained a range of cells at various stages of differentiation and with different viral loads. As packaging occurs only in the most differentiated cells, and previous studies have shown a dramatic change in the viral chromatin modifications once differentiation occurs, it was not an ideal comparison [174]. For the human virions, there was simply not enough excised tissue to both isolate a sufficient quantity of virions and use warts as controls for the same infection. To address this, future work could involve the production of infectious virions from transfected primary HFKs grown in 3D organotypic raft culture. Virions could be isolated from this tissue and, as controls, the upper most layer of the infected raft (where the productive viral replication and virion assembly occurs) could be extracted using laser capture microdissection. This would allow the direct comparison of the chromatin composition of virions to the cells in which they were assembled, allowing us to more confidently determine whether the enrichments and depletions we reported are due to global changes in infected cells (and the enrichments are therefore simply stochastic) or if there is true selective packaging.

After we discovered that native papillomavirus virions were significantly enriched in acetylated H3 and H4, we determined what role this played in the early infection cycle using the quasivirus infection system. We produced HPV quasiviruses

in the presence of the HDAC inhibitor sodium butyrate. This resulted in hyperacetylation of the packaged viral histones. Unexpectedly, after infection we detected a decrease in viral early gene expression from these viruses. We recapitulated the result using TSA treatment of newly infected cells, implying that this was not an artifact of the sodium butyrate treatment. We were unable to determine a specific mechanism to explain the decreased viral transcription that we observed but did rule out several including acetylated 293TT chromatin packaged in quasivirus preparations, viral replication, increased repression by the E2-Brd4 complex, and increased host Sp100 binding. While we did show that these viruses have increased overall levels of histone acetylation we did not check for the presence or absence of repressive methylation. It is possible that the HDAC inhibitor treatment in the packaging cells induced off target effects resulting in a mixture of repressive methylation and activating acetylation on the packaged histones.

We also discovered that native papillomavirus virions were enriched in the histone H3 variant H3.3, and there are several implications for the viral lifecycle that could be explored in future work. First would be the roles of H3.3 chaperones in the HPV lifecycle. H3.3 utilizes different chaperones than the canonical variant H3.1 to be assembled into nucleosomes in a replication independent manner [273, 274]. These chaperones include the Daxx/ATRX complex and the HIRA complex, which load H3.3 into transcriptionally repressive and active regions, respectively [273, 275]. Daxx is found at HPV replication foci [276]. However, the role of Daxx in HPV replication and transcription remains unclear. In studies done in U2OS cells, Daxx depletion was detrimental to transient viral transcription, while in another study

conducted in primary HFKs, Daxx depleted cells do not show significant differences in HPV transcription or replication, suggesting that Daxx is not responsible for the H3.3 enrichment in virion chromatin [70, 276]. Our results show that the viral chromatin appears to be euchromatic, at least immediately prior to packaging, raising the possibility that Daxx is not involved in manipulating the viral chromatin during productive replication. This would implicate HIRA as the factor responsible for directly loading H3.3 onto the viral chromatin during the late viral genome replication prior to packaging.

Furthermore, the chromatin-associated oncoprotein DEK is upregulated by E7 and promotes proliferation of HPV positive cancer cells (although studies exploring its role in productive infections have yet to be performed) [277, 278]. DEK regulates the balance of H3.3 deposition by acting as a "gatekeeper", regulating the access to soluble H3.3 by the different chaperones and has been shown to localize to ND-10 bodies [279]. Given that some ND-10 body components are found associated with late replication foci, it is plausible that DEK and HIRA together play an important role in enriching the late viral chromatin in the histone H3 variant H3.3 [258]. What biological function H3.3 has on viral activities is not known. It is possible that H3.3 enrichment is simply due to the replication of the viral genome outside of S-phase. To explore this idea, we could perform ChIP-qPCR for H3.3 in growing and differentiated cells to determine whether there is an increase in H3.3 binding to the viral genome during late, productive replication.

To examine the role of H3.3 in the early lifecycle, HPV quasiviruses could be produced in 293TT cells that are either depleted for H3.3 using siRNA or have H3.3

over expressed from an expression vector. These viruses would be used to infect cells and look for any differences in early transcription. To examine the role of H3.3 in the late viral lifecycle, we could explore the use of siRNA depletion of histone H3.3 or the chaperones DEK and HIRA in differentiated cells containing the viral genome and assess the impact on productive viral amplification.

The goal of this dissertation was to gain further insight into the manner by which the early HPV lifecycle was regulated by chromatin modifications. We have shown, in agreement with a wide body of previous studies, that HPV infection is extensively regulated in an epigenetic fashion. Our results indicated that the chromatin packaged in papillomavirus virions is extensively modified and has a structure that is overall quite distinct from that of the host cell. Our data lays the foundation for future experiments to uncover crucial mechanisms that govern immediate early viral processes.

Additionally, the work presented in this dissertation could have implications for the development of therapeutics for treating HPV infection. While vaccination is the best prophylactic treatment of HPV infection, there are still hundreds of thousands of new cases each year, in addition to those who have already been infected before vaccination [280]. In Chapter 5, we showed that the treatment of host cells with the HDAC inhibitor TSA substantially restricted the early viral gene expression. Previous studies have shown that the late HPV lifecycle can be abrogated by treatment of HDACs such as Vorinostat [263]. Our findings complement a growing body of work suggesting that HPV's intricate association with the cellular histone acetylation machinery could be a potent target for antiviral development.

Appendices

Supplementary Table 1. Relative abundance of histone PTMs in HPV quasivirus virions and 293TT control cells.

Histone	Peptide	Modification	Mean QsV	Mean 293TT	Fold Change	p value
H3	KSTGGKAPR	K4me1	13.52%	17.00%	0.80	0.5703
		K4me2	1.01%	0.74%	1.36	0.6018
		K4me3	0.32%	0.26%	1.24	0.7137
		K4ac	0.30%	0.06%	5.36	0.0396
	KSTGGKAPR	K9me1	9.55%	9.55%	1.00	0.3366
		K9me2	20.37%	20.55%	0.99	0.8959
		K9me3	10.52%	12.22%	0.86	0.0611
		K9ac	0.15%	0.39%	0.40	0.0748
		K14ac	8.19%	14.14%	0.58	0.0401
		K9me1K14ac	4.47%	7.08%	0.63	0.2237
		K9me2K14ac	14.09%	16.00%	0.88	0.6452
		K9me3K14ac	6.01%	6.20%	0.97	0.9264
		K9acK14ac	0.88%	0.91%	0.96	0.8416
	KQLATKAAR	K23me1	0.06%	0.08%	0.82	0.3143
		K18me1	0.15%	0.12%	1.20	0.0181
		K18me1K23me1	0.01%	0.01%	0.57	0.3912
		K18ac	2.01%	0.91%	2.20	0.0187
		K23ac	40.85%	47.65%	0.86	0.3319
		K18acK23ac	1.93%	1.40%	1.38	0.0150
	KSAPATGGVKKPHR	K36me1	0.94%	1.17%	0.80	0.5999
		K27me1	1.02%	1.01%	1.01	0.1398
		K27me2	28.03%	32.71%	0.86	0.0000

174

		K36me2	15.26%	10.26%	1.49	0.4382
		K27me3	6.31%	3.97%	1.59	0.8047
		K36me3	1.14%	1.23%	0.93	0.8608
		K27me2K36me1	8.05%	5.65%	1.43	0.1995
		K27me1K36me2	4.91%	4.12%	1.19	0.0803
		K27me1K36me1	0.94%	0.66%	1.43	0.0126
		K27me3K36me1	1.79%	1.54%	1.16	0.0257
		K27me1K36me3	1.85%	1.77%	1.04	0.0348
		K27me2K36me2	16.02%	29.38%	0.55	0.0279
		K27me3K36me2	2.90%	4.52%	0.64	0.0444
		K27ac	0.01%	0.00%	2.26	0.0058
	KSAPSTGGVKKPHR	K36me1	1.12%	1.05%	1.06	0.5736
		K27me1	2.18%	1.92%	1.14	0.9247
		K27me2	11.85%	14.99%	0.79	0.2026
		K36me2	3.70%	4.09%	0.90	0.4317
		K27me3	12.44%	12.65%	0.98	0.2054
		K36me3	3.38%	3.28%	1.03	0.7558
		K27me2K36me1	8.71%	9.18%	0.95	0.0862
		K27me1K36me2	10.39%	7.26%	1.43	0.3494
		K27me1K36me1	2.07%	2.63%	0.78	0.0452
		K27me3K36me1	4.02%	3.19%	1.26	0.3926
		K27me1K36me3	2.55%	1.56%	1.64	0.8329
		K27me2K36me2	22.30%	29.85%	0.75	0.0074
		K27me3K36me2	4.55%	5.44%	0.84	0.0156
		K27ac	0.03%	0.01%	2.45	0.4538
H4	GKGGKGLGKGGAKR	K5ac	2.14%	1.09%	1.97	0.0025
		K8ac	2.26%	1.73%	1.31	0.1473
		K12ac	5.35%	5.29%	1.01	0.8731

		K16ac	27.00%	34.30%	0.79	0.0487
		K5acK8ac	0.55%	0.59%	0.94	0.5060
		K5acK12ac	1.98%	1.03%	1.92	0.0045
		K5acK16ac	1.52%	0.82%	1.86	0.0001
		K8acK12ac	0.59%	0.85%	0.70	0.2232
		K8acK16ac	3.77%	2.87%	1.32	0.0223
		K12acK16ac	6.54%	5.85%	1.12	0.0691
		K5acK8acK12ac	0.70%	0.37%	1.87	0.0052
		K5acK8acK16ac	0.58%	0.34%	1.71	0.0271
		K5acK12acK16ac	1.77%	0.73%	2.43	0.0007
		K8acK12acK16ac	2.14%	1.65%	1.30	0.0277
		K5acK8acK12acK16ac	1.62%	1.54%	1.05	0.2181
	KVLR	K20me1	6.47%	7.68%	0.84	0.0382
		K20me2	81.90%	82.69%	0.99	0.4687
		K20me3	1.95%	2.20%	0.89	0.0358
		K20ac	0.02%	0.00%	41.12	0.0055

Supplementary Table 2. Relative abundance of histone PTMs in BPV virions and bovine keratinocyte control cells.

Histone	Peptide	Modification	Mean BPV	Mean Growing	Fold Change	p-value	Mean Ca++	Fold Change	p-value	Mean Raft	Fold Change	p-value
H3	KSTGGKAPR	K4me1	37.31%	6.19%	6.03	0.0029	7.65%	4.88	0.0032	7.30%	5.11	0.0035
		K4me2	8.68%	0.76%	11.42	0.0389	0.69%	12.49	0.0380	0.51%	17.02	0.0367
		K4me3	3.25%	0.30%	10.75	0.0342	0.31%	10.53	0.0336	0.18%	17.88	0.0314
		K4ac	0.61%	0.11%	5.67	0.0408	0.12%	5.03	0.0409	0.11%	5.74	0.0386
	KSTGGKAPR	K9me1	6.32%	5.64%	1.12	0.5406	6.12%	1.03	0.8582	5.28%	1.20	0.4339
		K9me2	6.40%	18.33%	0.35	0.0012	17.76%	0.36	0.0023	19.34%	0.33	0.0008
		K9me3	2.77%	15.87%	0.17	0.0019	17.68%	0.16	0.0005	16.82%	0.16	0.0031
		K9ac	3.46%	0.62%	5.58	0.2275	1.19%	2.92	0.3052	1.26%	2.74	0.3167
		K14ac	31.57%	14.97%	2.11	0.0851	10.95%	2.88	0.0572	8.78%	3.60	0.0438
		K9me1K14ac	13.49%	8.54%	1.58	0.0058	8.34%	1.62	0.0008	8.66%	1.56	0.0008
		K9me2K14ac	11.76%	15.99%	0.74	0.0414	17.76%	0.66	0.0020	21.35%	0.55	0.0003
		K9me3K14ac	2.78%	6.87%	0.40	0.0949	6.73%	0.41	0.1099	8.06%	0.35	0.0450
		K9acK14ac	5.52%	1.16%	4.76	0.0010	1.44%	3.84	0.0053	0.83%	6.66	0.0015
	KQLATKAAR	K23me1	0.23%	0.17%	1.37	0.5533	0.07%	3.28	0.1631	0.18%	1.30	0.5972
		K18me1	0.16%	0.14%	1.21	0.7393	0.11%	1.51	0.2648	0.18%	0.93	0.7904
		K18me1K23me1	0.00%	0.00%	0.00	0.4226	0.00%	N/A	N/A	0.00%	N/A	N/A
		K18ac	8.38%	4.77%	1.76	0.0879	3.19%	2.63	0.0147	3.41%	2.46	0.0126
		K23ac	40.94%	29.18%	1.40	0.2767	23.68%	1.73	0.0517	23.72%	1.73	0.0505
		K18acK23ac	13.29%	3.52%	3.78	0.0037	2.73%	4.87	0.0102	1.90%	6.99	0.0090
	KSAPATGGVKKPHR	K36me1	0.56%	1.55%	0.36	0.0011	1.62%	0.35	0.2277	0.86%	0.65	0.0558
		K27me1	6.27%	9.93%	0.63	0.1220	4.73%	1.33	0.4740	8.47%	0.74	0.2664
		K27me2	17.01%	33.28%	0.51	0.0087	32.51%	0.52	0.0106	30.79%	0.55	0.0255
		K36me2	5.05%	3.10%	1.63	0.6953	1.44%	3.50	0.4903	1.54%	3.27	0.5010
		K27me3	6.89%	11.11%	0.62	0.0086	14.41%	0.48	0.0047	11.50%	0.60	0.0151
		K36me3	4.83%	4.36%	1.11	0.6405	3.76%	1.28	0.5615	1.83%	2.63	0.0079

		K27me2K36me1	14.19%	5.94%	2.39	0.0238	6.67%	2.13	0.0322	8.98%	1.58	0.0780
		K27me1K36me2	3.96%	3.60%	1.10	0.5843	3.55%	1.12	0.5635	3.74%	1.06	0.7259
		K27me1K36me1	1.59%	1.89%	0.84	0.1578	0.98%	1.62	0.0231	1.56%	1.02	0.8158
		K27me3K36me1	7.74%	3.10%	2.50	0.0385	3.71%	2.09	0.0474	4.44%	1.74	0.0775
		K27me1K36me3	1.24%	1.70%	0.73	0.3443	1.98%	0.63	0.1831	1.71%	0.73	0.3382
		K27me2K36me2	12.16%	8.02%	1.52	0.5280	15.04%	0.81	0.6752	12.98%	0.94	0.8957
		K27me3K36me2	10.97%	2.75%	3.99	0.2583	4.27%	2.57	0.3311	5.01%	2.19	0.3749
		K27ac	0.23%	0.17%	1.32	0.8306	0.00%	N/A	0.4226	0.03%	7.21	0.4799
	KSAPSTGGVKKPHR	K36me1	1.69%	4.67%	0.36	0.0029	3.00%	0.56	0.4782	3.26%	0.52	0.0242
		K27me1	1.98%	5.05%	0.39	0.0128	4.31%	0.46	0.0584	5.69%	0.35	0.0141
		K27me2	10.11%	25.70%	0.39	0.0070	17.74%	0.57	0.0100	10.89%	0.93	0.6575
		K36me2	9.97%	6.07%	1.64	0.0399	6.25%	1.60	0.1366	7.10%	1.40	0.0721
		K27me3	3.50%	10.37%	0.34	0.0006	7.35%	0.48	0.0012	4.58%	0.76	0.1001
		K36me3	5.11%	6.99%	0.73	0.1676	9.28%	0.55	0.0258	4.77%	1.07	0.7728
		K27me2K36me1	12.42%	6.34%	1.96	0.0171	7.02%	1.77	0.0398	6.96%	1.78	0.0288
		K27me1K36me2	7.55%	7.20%	1.05	0.7593	6.10%	1.24	0.5341	11.97%	0.63	0.0185
		K27me1K36me1	2.86%	1.76%	1.63	0.1411	0.09%	31.11	0.0011	2.38%	1.20	0.2712
		K27me3K36me1	4.24%	1.82%	2.33	0.0138	0.88%	4.81	0.0012	2.57%	1.65	0.0168
		K27me1K36me3	1.35%	2.64%	0.51	0.1674	2.09%	0.64	0.6042	4.18%	0.32	0.0022
		K27me2K36me2	23.66%	3.06%	7.74	0.0016	13.81%	1.71	0.1890	18.85%	1.26	0.1229
		K27me3K36me2	9.07%	2.08%	4.36	0.0226	2.03%	4.47	0.0204	5.88%	1.54	0.1362
		K27ac	0.85%	0.16%	5.25	0.2557	0.00%	N/A	0.1942	0.34%	2.54	0.3637
H4	GKGGKGLGKGGAKR	K5ac	5.04%	2.50%	2.02	0.0233	2.24%	2.25	0.0104	3.31%	1.52	0.2297
		K8ac	4.75%	1.84%	2.57	0.0563	1.54%	3.07	0.0486	1.28%	3.72	0.0361
		K12ac	4.01%	5.21%	0.77	0.0126	3.30%	1.22	0.0377	3.58%	1.12	0.1265
		K16ac	19.34%	25.60%	0.76	0.1137	29.29%	0.66	0.0528	33.42%	0.58	0.0130
		K5acK8ac	2.31%	0.88%	2.61	0.0080	0.68%	3.38	0.0083	1.23%	1.88	0.1162
		K5acK12ac	1.50%	1.43%	1.05	0.7700	0.90%	1.66	0.0610	1.09%	1.37	0.1611

178

		K5acK16ac	1.08%	0.65%	1.65	0.1085	0.32%	3.37	0.0262	0.31%	3.46	0.0513
		K8acK12ac	0.69%	0.64%	1.08	0.7299	0.25%	2.77	0.0741	0.72%	0.95	0.9462
		K8acK16ac	3.63%	2.32%	1.56	0.0412	1.97%	1.84	0.0151	1.41%	2.57	0.0426
		K12acK16ac	3.33%	6.07%	0.55	0.0000	3.26%	1.02	0.4947	3.82%	0.87	0.1999
		K5acK8acK12ac	1.77%	1.02%	1.73	0.0077	0.60%	2.96	0.0003	0.81%	2.17	0.0017
		K5acK8acK16ac	0.82%	0.13%	6.41	0.0792	0.08%	10.13	0.0704	0.05%	15.90	0.0667
		K5acK12acK16ac	0.64%	0.69%	0.93	0.8103	0.21%	2.99	0.1266	0.13%	4.75	0.0901
		K8acK12acK16ac	2.45%	2.00%	1.22	0.1451	0.98%	2.50	0.0169	1.17%	2.09	0.0106
		K5acK8acK12acK16ac	2.01%	0.78%	2.57	0.0416	0.45%	4.48	0.0321	0.38%	5.31	0.0356
	KVLR	K20me1	38.73%	47.33%	0.82	0.2019	16.54%	2.34	0.0235	40.78%	0.95	0.9228
		K20me2	44.76%	27.95%	1.60	0.1179	60.23%	0.74	0.1654	36.36%	1.23	0.6026
		K20me3	9.37%	2.75%	3.40	0.0929	15.33%	0.61	0.1612	14.35%	0.65	0.3391
		K20ac	1.86%	0.00%	N/A	0.0631	0.89%	2.08	0.2421	0.46%	4.01	0.1078

179

Supplementary Table 3. Relative abundance of histone PTMs in HPV virions and human keratinocyte control cells.

Histone	Peptide	Modification	Mean HPV	Mean Growing	Fold Change	p-value	Mean Ca++	Fold Change	p-value	Mean Raft	Fold Change	p-value
H3	KSTGGKAPR	K4me1	26.82%	24.56%	1.09	0.4227	26.54%	1.01	0.9092	10.07%	2.66	0.0068
		K4me2	0.05%	0.00%	N/A	0.1974	0.00%	N/A	0.1974	0.00%	N/A	0.1974
		K4me3	0.00%	0.00%	N/A	N/A	0.00%	N/A	N/A	0.00%	N/A	N/A
		K4ac	0.08%	0.00%	N/A	0.1921	0.00%	N/A	0.1921	0.00%	N/A	0.1921
	KSTGGKAPR	K9me1	5.95%	18.98%	0.31	0.0034	25.15%	0.24	0.0000	8.36%	0.71	0.2649
		K9me2	7.75%	6.18%	1.26	0.4093	4.98%	1.56	0.2534	24.86%	0.31	0.0005
		K9me3	0.09%	4.34%	0.02	0.0005	4.29%	0.02	0.0000	20.12%	0.00	0.0002
		K9ac	0.43%	0.13%	3.25	0.0182	0.04%	10.56	0.0306	0.00%	204.12	0.0744
		K14ac	29.92%	13.85%	2.16	0.0079	11.26%	2.66	0.0221	6.27%	4.77	0.0002
		K9me1K14ac	15.88%	25.07%	0.63	0.0811	25.90%	0.61	0.0977	12.79%	1.24	0.3863
		K9me2K14ac	8.83%	2.07%	4.26	0.2819	1.64%	5.40	0.2680	8.22%	1.07	0.8922
		K9me3K14ac	0.76%	0.65%	1.17	0.7804	0.71%	1.07	0.8929	5.70%	0.13	0.0094
		K9acK14ac	2.04%	0.42%	4.88	0.0400	0.35%	5.89	0.0281	0.00%	N/A	0.0642
	KQLATKAAR	K23me1	0.00%	0.00%	N/A	N/A	0.00%	N/A	N/A	0.00%	N/A	N/A
		K18me1	0.18%	0.00%	N/A	0.0413	0.00%	N/A	0.0413	0.00%	N/A	0.0413
		K18me1K23me1	0.00%	0.00%	N/A	N/A	0.00%	N/A	N/A	0.00%	N/A	N/A
		K18ac	3.85%	0.00%	N/A	0.0028	0.00%	N/A	0.0028	0.00%	N/A	0.0028
		K23ac	72.42%	47.46%	1.53	0.0200	43.72%	1.66	0.0500	22.66%	3.20	0.0010
		K18acK23ac	7.20%	9.10%	0.79	0.2575	7.73%	0.93	0.6842	2.55%	2.82	0.0647
	KSAPATGGVKKPHR	K36me1	0.00%	0.29%	0.00	0.0774	0.53%	0.00	0.0687	0.00%	N/A	N/A
		K27me1	3.54%	3.92%	0.90	0.6043	3.18%	1.11	0.5906	6.64%	0.53	0.4293
		K27me2	49.40%	41.79%	1.18	0.0010	42.97%	1.15	0.0005	45.54%	1.08	0.2708
		K36me2	0.12%	3.49%	0.03	0.0001	0.09%	1.22	0.8071	0.00%	N/A	0.2253
		K27me3	9.35%	13.39%	0.70	0.0094	14.70%	0.64	0.0008	18.89%	0.50	0.0084
		K36me3	0.52%	0.82%	0.63	0.5388	2.69%	0.19	0.2485	0.00%	N/A	0.2195

Protein	Peptide	Modification										
		K27me2K36me1	11.40%	13.40%	0.85	0.5809	15.99%	0.71	0.2800	10.68%	1.07	0.8683
		K27me1K36me2	1.84%	5.08%	0.36	0.0048	2.73%	0.67	0.1912	0.00%	N/A	0.0073
		K27me1K36me1	0.53%	0.14%	3.85	0.1937	0.00%	N/A	0.1676	0.19%	2.78	0.1785
		K27me3K36me1	1.57%	3.28%	0.48	0.0668	6.16%	0.25	0.0065	9.27%	0.17	0.0031
		K27me1K36me3	0.49%	1.42%	0.35	0.1348	0.51%	0.97	0.9011	0.00%	N/A	0.0617
		K27me2K36me2	13.24%	5.24%	2.53	0.2586	7.87%	1.68	0.3633	6.11%	2.17	0.2529
		K27me3K36me2	4.38%	1.06%	4.12	0.1676	1.86%	2.36	0.2311	1.06%	4.12	0.1153
		K27ac	0.19%	0.02%	8.23	0.0083	0.00%	N/A	0.0727	0.00%	N/A	0.0727
	KSAPSTGGVKKPHR	K36me1	0.00%	0.00%	N/A	N/A	0.01%	0.00	0.3739	0.00%	N/A	N/A
		K27me1	4.66%	0.00%	N/A	0.1485	67.09%	0.07	0.0093	0.00%	N/A	0.1485
		K27me2	45.44%	41.29%	1.10	0.6158	29.60%	1.54	0.1332	31.01%	1.47	0.0963
		K36me2	0.05%	11.65%	0.00	0.0307	0.51%	0.09	0.4161	0.00%	N/A	0.5000
		K27me3	6.53%	12.33%	0.53	0.2374	0.29%	22.67	0.0000	2.23%	2.93	0.0694
		K36me3	0.01%	0.03%	0.50	0.0778	1.96%	0.01	0.3709	0.00%	N/A	0.1129
		K27me2K36me1	12.58%	30.00%	0.42	0.0085	21.97%	0.57	0.2056	26.34%	0.48	0.3136
		K27me1K36me2	1.95%	0.45%	4.31	0.0212	0.00%	N/A	0.0080	0.00%	N/A	0.0080
		K27me1K36me1	0.52%	0.00%	N/A	0.2091	0.00%	N/A	0.2091	0.00%	N/A	0.2091
		K27me3K36me1	2.17%	0.00%	N/A	0.0482	0.19%	11.55	0.0018	9.09%	0.24	0.2735
		K27me1K36me3	0.00%	0.00%	N/A	N/A	0.00%	N/A	N/A	0.00%	N/A	N/A
		K27me2K36me2	9.54%	9.06%	1.05	0.9021	18.63%	0.51	0.1958	3.74%	2.55	0.2143
		K27me3K36me2	3.11%	0.00%	N/A	0.1222	0.00%	N/A	0.1222	0.00%	N/A	0.1222
		K27ac	0.00%	0.00%	N/A	N/A	0.00%	N/A	N/A	0.00%	N/A	N/A
H4	GKGGKGLGKGGAKR	K5ac	7.04%	2.00%	3.52	0.0440	3.95%	1.78	0.1088	7.07%	1.00	0.9877
		K8ac	7.04%	3.75%	1.88	0.1072	4.04%	1.74	0.1092	7.07%	1.00	0.9877
		K12ac	7.04%	3.57%	1.97	0.0845	4.24%	1.66	0.1114	7.07%	1.00	0.9877
		K16ac	7.04%	34.49%	0.20	0.0019	17.86%	0.39	0.0731	7.07%	1.00	0.9877
		K5acK8ac	0.00%	0.00%	N/A	N/A	0.15%	0.00	0.1869	0.14%	0.00	0.1092
		K5acK12ac	0.00%	0.43%	0.00	0.0346	0.15%	0.00	0.1869	0.14%	0.00	0.1092

		K5acK16ac	0.00%	1.01%	0.00	0.0261	0.15%	0.00	0.1869	0.14%	0.00	0.1092
		K8acK12ac	0.00%	0.68%	0.00	0.0132	0.15%	0.00	0.1869	0.14%	0.00	0.1092
		K8acK16ac	0.01%	4.54%	0.00	0.0000	1.11%	0.01	0.0058	0.15%	0.05	0.0913
		K12acK16ac	0.70%	7.52%	0.09	0.0029	1.19%	0.59	0.6098	1.09%	0.64	0.6984
		K5acK8acK12ac	0.00%	0.84%	0.00	0.0203	0.10%	0.00	0.1346	0.01%	0.00	0.3632
		K5acK8acK16ac	0.00%	0.37%	0.00	0.0658	0.00%	0.00	0.1334	0.01%	0.00	0.3632
		K5acK12acK16ac	0.00%	1.12%	0.00	0.0009	0.00%	N/A	N/A	0.01%	0.00	0.3632
		K8acK12acK16ac	0.00%	2.66%	0.00	0.0004	0.17%	0.00	0.0720	0.01%	0.00	0.3632
		K5acK8acK12acK16ac	0.00%	1.55%	0.00	0.0002	0.02%	0.00	0.3632	12.30%	0.00	0.0834
	KVLR	K20me1	14.67%	2.30%	6.37	0.1238	15.32%	0.96	0.8758	3.50%	4.19	0.0857
		K20me2	58.49%	88.58%	0.66	0.2005	75.28%	0.78	0.3384	94.48%	0.62	0.1619
		K20me3	0.26%	2.93%	0.09	0.0052	1.22%	0.21	0.1100	0.00%	N/A	0.5000
		K20ac	10.83%	0.00%	N/A	0.1952	0.00%	N/A	0.1952	0.00%	N/A	0.1952

Bibliography

1.   Herbst, L.H., et al., *Genomic characterization of two novel reptilian papillomaviruses, Chelonia mydas papillomavirus 1 and Caretta caretta papillomavirus 1.* Virology, 2009. **383**(1): p. 131-135.

2.   de Villiers, E.M., et al., *Classification of papillomaviruses.* Virology, 2004. **324**(1): p. 17-27.

3.   Bernard, H.-U., et al., *Classification of papillomaviruses (PVs) based on 189 PV types and proposal of taxonomic amendments.* Virology, 2010. **401**(1): p. 70-79.

4.   Doorslaer, K.V., et al., *ICTV virus taxonomy profile: Papillomaviridae.* Journal of General Virology, 2018.

5.   Van Doorslaer, K., et al., *The Papillomavirus Episteme: a central resource for papillomavirus sequence data and analysis.* Nucleic acids research, 2012. **41**(D1): p. D571-D578.

6.   Van Doorslaer, K., et al., *The Papillomavirus Episteme: a major update to the papillomavirus sequence database.* Nucleic acids research, 2017. **45**(D1): p. D499-D506.

7.   Prevention, C.f.D.C.a., *Genital HPV infection fact sheet.* Rockville: MD: CDC National Prevention Information Network, 2014.

8.   Moscicki, A.-B., et al., *Persistence of human papillomavirus infection in HIV-infected and-uninfected adolescent girls: risk factors and differences, by phylogenetic type.* The Journal of infectious diseases, 2004. **190**(1): p. 37-45.

9.   Castle, P.E., et al., *A prospective study of age trends in cervical human papillomavirus acquisition and persistence in Guanacaste, Costa Rica.* The Journal of infectious diseases, 2005. **191**(11): p. 1808-1816.

10.   Cubie, H.A., *Diseases associated with human papillomavirus infection.* Virology, 2013. **445**(1-2): p. 21-34.

11.   Cogliano, V., et al., *Carcinogenicity of human papillomaviruses.* The lancet oncology, 2005. **6**(4): p. 204.

12.   Saraiya, M., et al., *US assessment of HPV types in cancers: implications for current and 9-valent HPV vaccines.* J Natl Cancer Inst, 2015. **107**(6): p. djv086.

13.   Marur, S., et al., *HPV-associated head and neck cancer: a virus-related cancer epidemic.* Lancet Oncol, 2010. **11**(8): p. 781-9.

14.   Ljubojevic, S. and M. Skerlev, *HPV-associated diseases.* Clinics in dermatology, 2014. **32**(2): p. 227-234.

15.   Stanley, M., D.R. Lowy, and I. Frazer, *Prophylactic HPV vaccines: underlying mechanisms.* Vaccine, 2006. **24**: p. S106-S113.

16.   De Vincenzo, R., et al., *Long-term efficacy and safety of human papillomavirus vaccination.* International journal of women's health, 2014. **6**: p. 999.

17. Giuliano, A.R., et al., *Efficacy of quadrivalent HPV vaccine against HPV Infection and disease in males.* New England Journal of Medicine, 2011. **364**(5): p. 401-411.

18. Leval, A., et al., *Quadrivalent human papillomavirus vaccine effectiveness: a Swedish national cohort study.* Journal of the National Cancer Institute, 2013. **105**(7): p. 469-474.

19. Pollock, K.G., et al., *Reduction of low-and high-grade cervical abnormalities associated with high uptake of the HPV bivalent vaccine in Scotland.* British journal of cancer, 2014. **111**(9): p. 1824-1830.

20. Walker, T.Y., et al., *National, regional, state, and selected local area vaccination coverage among adolescents aged 13–17 years—United States, 2018.* Morbidity and Mortality Weekly Report, 2019. **68**(33): p. 718.

21. McCave, E.L., *Influential factors in HPV vaccination uptake among providers in four states.* Journal of community health, 2010. **35**(6): p. 645-652.

22. Agosti, J.M. and S.J. Goldie, *Introducing HPV vaccine in developing countries—key challenges and issues.* New England Journal of Medicine, 2007. **356**(19): p. 1908-1910.

23. Baker, T., et al., *Structures of bovine and human papillomaviruses. Analysis by cryoelectron microscopy and three-dimensional image reconstruction.* Biophysical journal, 1991. **60**(6): p. 1445-1456.

24. Buck, C.B., et al., *Arrangement of L2 within the papillomavirus capsid.* Journal of Virology, 2008. **82**(11): p. 5190-5197.

25. Buck, C.B. and B.L. Trus, *The papillomavirus virion: a machine built to hide molecular Achilles' heels*, in *Viral Molecular Machines*. 2012, Springer. p. 403-422.

26. Sapp, M., et al., *Organization of the major and minor capsid proteins in human papillomavirus type 33 virus-like particles.* Journal of General Virology, 1995. **76**(9): p. 2407-2412.

27. Modis, Y., B.L. Trus, and S.C. Harrison, *Atomic model of the papillomavirus capsid.* The EMBO journal, 2002. **21**(18): p. 4754-4762.

28. Roden, R.B., D.R. Lowy, and J.T. Schiller, *Papillomavirus is resistant to desiccation.* Journal of Infectious Diseases, 1997. **176**(4): p. 1076-1079.

29. Favre, M., et al., *Chromatin-like structures obtained after alkaline disruption of bovine and human papillomaviruses.* Journal of Virology, 1977. **21**(3): p. 1205-1209.

30. Frearson, P. and L. Crawford, *Polyoma virus basic proteins.* Journal of General Virology, 1972. **14**(2): p. 141-155.

31. Cardone, G., et al., *Maturation of the human papillomavirus 16 capsid.* MBio, 2014. **5**(4): p. e01104-14.

32. Porter, S. and A. McBride, *Human Papillomaviruses*, in *Encyclopedia of Virology*. 2021, Academic Press.

33. Porter, S.S., et al., *Host cell restriction factors that limit transcription and replication of human papillomavirus.* Virus research, 2017. **231**: p. 10-20.

34. Zheng, Z.-M. and C.C. Baker, *Papillomavirus genome structure, expression, and post-transcriptional regulation.* Frontiers in bioscience: a journal and virtual library, 2006. **11**: p. 2286.

35. Chow, L., et al., *Human papillomavirus types 6 and 11 mRNAs from genital condylomata acuminata.* Journal of Virology, 1987. **61**(8): p. 2581-2588.

36. Chow, L.T., et al., *Identification and mapping of human papillomavirus type 1 RNA transcripts recovered from plantar warts and infected epithelial cell cultures.* Journal of virology, 1987. **61**(6): p. 1913-1918.

37. Milligan, S.G., et al., *Analysis of novel human papillomavirus type 16 late mRNAs in differentiated W12 cervical epithelial cells.* Virology, 2007. **360**(1): p. 172-181.

38. Mack, D.H. and L.A. Laimins, *A keratinocyte-specific transcription factor, KRF-1, interacts with AP-1 to activate expression of human papillomavirus type 18 in squamous epithelial cells.* Proceedings of the National Academy of Sciences, 1991. **88**(20): p. 9102-9106.

39. Cripe, T., et al., *Transcriptional regulation of the human papillomavirus-16 E6-E7 promoter by a keratinocyte-dependent enhancer, and by viral E2 trans-activator and repressor gene products: implications for cervical carcinogenesis.* The EMBO journal, 1987. **6**(12): p. 3745-3753.

40. Lechler, T. and E. Fuchs, *Asymmetric cell divisions promote stratification and differentiation of mammalian skin.* Nature, 2005. **437**(7056): p. 275-280.

41. Williams, S.E., et al., *Asymmetric cell divisions promote Notch-dependent epidermal differentiation.* Nature, 2011. **470**(7334): p. 353-358.

42. Coursey, T.L. and A.A. McBride, *Hitchhiking of Viral Genomes on Cellular Chromosomes.* Annual review of virology, 2019. **6**: p. 275-296.

43. Porter, S., et al., *Host Cell Restriction Factors that Limit Transcription and Replication of Human Papillomavirus.* Virus Research, 2016. **submitted**.

44. Aydin, I., et al., *Large scale RNAi reveals the requirement of nuclear envelope breakdown for nuclear import of human papillomaviruses.* PLoS Pathog, 2014. **10**(5): p. e1004162.

45. Shafti-Keramat, S., et al., *Different heparan sulfate proteoglycans serve as cellular receptors for human papillomaviruses.* Journal of virology, 2003. **77**(24): p. 13125-13135.

46. Culp, T.D., L.R. Budgeon, and N.D. Christensen, *Human papillomaviruses bind a basal extracellular matrix component secreted by keratinocytes which is distinct from a membrane-associated receptor.* Virology, 2006. **347**(1): p. 147-159.

47. Cerqueira, C., et al., *Kallikrein-8 proteolytically processes human papillomaviruses in the extracellular space to facilitate entry into host cells.* Journal of virology, 2015. **89**(14): p. 7038-7052.

48. Day, P.M., D.R. Lowy, and J.T. Schiller, *Heparan sulfate-independent cell binding and infection with furin-precleaved papillomavirus capsids.* Journal of virology, 2008. **82**(24): p. 12565-12568.

49. Day, P.M., et al., *Mechanisms of human papillomavirus type 16 neutralization by l2 cross-neutralizing and l1 type-specific antibodies.* Journal of virology, 2008. **82**(9): p. 4638-4646.

50. Richards, R.M., et al., *Cleavage of the papillomavirus minor capsid protein, L2, at a furin consensus site is necessary for infection.* Proc.Natl.Acad.Sci.U.S.A, 2006. **103**(5): p. 1522-1527.

51.   Bienkowska-Haba, M., H.D. Patel, and M. Sapp, *Target cell cyclophilins facilitate human papillomavirus type 16 infection.* PLoS pathogens, 2009. **5**(7).

52.   Selinka, H.C., et al., *Inhibition of transfer to secondary receptors by heparan sulfate-binding drug or antibody induces noninfectious uptake of human papillomavirus.* J.Virol., 2007. **81**(20): p. 10970-10980.

53.   Becker, M., et al., *Extracellular conformational changes in the capsid of human papillomaviruses contribute to asynchronous uptake into host cells.* Journal of virology, 2018. **92**(11): p. e02106-17.

54.   Aksoy, P., E.Y. Gottschalk, and P.I. Meneses, *HPV entry into cells.* Mutation Research/Reviews in Mutation Research, 2017. **772**: p. 13-22.

55.   Bannach, C., et al., *Epidermal Growth Factor Receptor and Abl2 Kinase Regulate Distinct Steps of Human Papillomavirus 16 Endocytosis.* Journal of Virology, 2020. **94**(11).

56.   Popa, A., et al., *Entry of human papillomavirus type 16 by actin-dependent, clathrin- and lipid raft-independent endocytosis.* PLoS Pathog, 2012. **8**(4): p. e1002657.

57.   Inoue, T., et al., *γ-Secretase promotes membrane insertion of the human papillomavirus L2 capsid protein during virus infection.* Journal of Cell Biology, 2018. **217**(10): p. 3545-3559.

58.   Day, P.M., et al., *Identification of a role for the trans-Golgi network in human papillomavirus 16 pseudovirus infection.* J Virol, 2013. **87**(7): p. 3862-70.

59.   Lipovsky, A., et al., *Genome-wide siRNA screen identifies the retromer as a cellular entry factor for human papillomavirus.* Proceedings of the National Academy of Sciences, 2013. **110**(18): p. 7452-7457.

60.   Zhang, W., et al., *Vesicular trafficking of incoming human papillomavirus 16 to the Golgi apparatus and endoplasmic reticulum requires γ-secretase activity.* MBio, 2014. **5**(5): p. e01777-14.

61.   Bergant Marusic, M., et al., *Human papillomavirus L2 facilitates viral escape from late endosomes via sorting nexin 17.* Traffic, 2012. **13**(3): p. 455-67.

62.   Pim, D., et al., *A novel PDZ domain interaction mediates the binding between human papillomavirus 16 L2 and sorting nexin 27 and modulates virion trafficking.* Journal of virology, 2015. **89**(20): p. 10145-10155.

63.   Calton, C.M., et al., *Translocation of the papillomavirus L2/vDNA complex across the limiting membrane requires the onset of mitosis.* PLoS pathogens, 2017. **13**(5).

64.   Pyeon, D., et al., *Establishment of human papillomavirus infection requires cell cycle progression.* PLoS Pathog, 2009. **5**(2): p. e1000318.

65.   DiGiuseppe, S., et al., *Human Papillomavirus Major Capsid Protein L1 Remains Associated with the Incoming Viral Genome throughout the Entry Process.* Journal of Virology, 2017. **91**(16): p. e00537-17.

66.   DiGiuseppe, S., et al., *Incoming human papillomavirus type 16 genome resides in a vesicular compartment throughout mitosis.* Proc Natl Acad Sci U S A, 2016. **113**(22): p. 6289-94.

67.   Day, P.M., et al., *Establishment of papillomavirus infection is enhanced by promyelocytic leukemia protein (PML) expression.* Proceedings of the

National Academy of Sciences of the United States of America, 2004. **101**(39): p. 14252-14257.

68.   Becker, K.A., et al., *Dissection of human papillomavirus type 33 L2 domains involved in nuclear domains (ND) 10 homing and reorganization.* Virology, 2003. **314**(1): p. 161-167.

69.   Florin, L., et al., *Reorganization of nuclear domain 10 induced by papillomavirus capsid protein l2.* Virology, 2002. **295**(1): p. 97-107.

70.   Stepp, W.H., J.M. Meyers, and A.A. McBride, *Sp100 provides intrinsic immunity against human papillomavirus infection.* MBio, 2013. **4**(6): p. e00845-13.

71.   Yang, L., et al., *The E1 protein of bovine papilloma virus 1 is an ATP-dependent DNA helicase.* Proceedings of the National Academy of Sciences, 1993. **90**(11): p. 5086-5090.

72.   Frattini, M.G. and L.A. Laimins, *Binding of the human papillomavirus E1 origin-recognition protein is regulated through complex formation with the E2 enhancer-binding protein.* Proceedings of the National Academy of Sciences, 1994. **91**(26): p. 12398-12402.

73.   Ustav, M., et al., *Identification of the origin of replication of bovine papillomavirus and characterization of the viral origin recognition factor E1.* The EMBO journal, 1991. **10**(13): p. 4321-4329.

74.   Sedman, T., J. Sedman, and A. Stenlund, *Binding of the E1 and E2 proteins to the origin of replication of bovine papillomavirus.* Journal of Virology, 1997. **71**(4): p. 2887-2896.

75.   Sedman, J. and A. Stenlund, *The papillomavirus E1 protein forms a DNA-dependent hexameric complex with ATPase and DNA helicase activities.* Journal of virology, 1998. **72**(8): p. 6893-6897.

76.   Enemark, E.J. and L. Joshua-Tor, *Mechanism of DNA translocation in a replicative hexameric helicase.* Nature, 2006. **442**(7100): p. 270-275.

77.   Melendy, T., J. Sedman, and A. Stenlund, *Cellular factors required for papillomavirus DNA replication.* Journal of virology, 1995. **69**(12): p. 7857-7867.

78.   Loo, Y.-M. and T. Melendy, *Recruitment of replication protein A by the papillomavirus E1 protein and modulation by single-stranded DNA.* Journal of virology, 2004. **78**(4): p. 1605-1615.

79.   Clower, R.V., J.C. Fisk, and T. Melendy, *Papillomavirus E1 protein binds to and stimulates human topoisomerase I.* Journal of virology, 2006. **80**(3): p. 1584-1587.

80.   Stubenrauch, F. and L.A. Laimins. *Human papillomavirus life cycle: active and latent phases.* in *Seminars in cancer biology.* 1999. Elsevier.

81.   Ilves, I., S. Kivi, and M. Ustav, *Long-term episomal maintenance of bovine papillomavirus type 1 plasmids is determined by attachment to host chromosomes, which is mediated by the viral E2 protein and its binding sites.* Journal of Virology, 1999. **73**(5): p. 4404-4412.

82.   Skiadopoulos, M.H. and A.A. McBride, *Bovine papillomavirus type 1 genomes and the E2 transactivator protein are closely associated with mitotic chromatin.* J Virol, 1998. **72**(3): p. 2079-88.

83. Bastien, N. and A.A. McBride, *Interaction of the papillomavirus E2 protein with mitotic chromosomes.* Virology, 2000. **270**(1): p. 124-34.

84. Lehman, C.W. and M.R. Botchan, *Segregation of viral plasmids depends on tethering to chromosomes and is regulated by phosphorylation.* Proc.Natl.Acad.Sci U.S.A, 1998. **95**(8): p. 4338-4343.

85. Oliveira, J.G., L.A. Colf, and A.A. McBride, *Variations in the association of papillomavirus E2 proteins with mitotic chromosomes.* Proceedings of the National Academy of Sciences, 2006. **103**(4): p. 1047-1052.

86. Banerjee, N.S., et al., *Human papillomavirus (HPV) E7 induces prolonged G2 following S phase reentry in differentiated human keratinocytes.* Journal of Biological Chemistry, 2011. **286**(17): p. 15473-15482.

87. Reinson, T., et al., *The cell cycle timing of human papillomavirus DNA replication.* PLoS One, 2015. **10**(7).

88. Flores, E.R. and P.F. Lambert, *Evidence for a switch in the mode of human papillomavirus type 16 DNA replication during the viral life cycle.* Journal of virology, 1997. **71**(10): p. 7167-7179.

89. Ozbun, M.A. and C. Meyers, *Human papillomavirus type 31b E1 and E2 transcript expression correlates with vegetative viral genome amplification.* Virology, 1998. **248**(2): p. 218.

90. Hummel, M., J.B. Hudson, and L.A. Laimins, *Differentiation-induced and constitutive transcription of human papillomavirus type 31b in cell lines containing viral episomes.* Journal of virology, 1992. **66**(10): p. 6070-6080.

91. Jang, M.K., K. Shen, and A.A. McBride, *Papillomavirus genomes associate with BRD4 to replicate at fragile sites in the host genome.* PLoS Pathog, 2014. **10**(5): p. e1004117.

92. Swindle, C.S., et al., *Human papillomavirus DNA replication compartments in a transient DNA replication system.* Journal of virology, 1999. **73**(2): p. 1001-1009.

93. Anacker, D.C., et al., *Productive replication of human papillomavirus 31 requires DNA repair factor Nbs1.* Journal of virology, 2014. **88**(15): p. 8528-8544.

94. Moody, C.A. and L.A. Laimins, *Human Papillomaviruses Activate the ATM DNA Damage Pathway for Viral Genome Amplification upon Differentiation.* Plos Pathogens, 2009. **5**(10): p. e1000605.

95. Anacker, D.C. and C.A. Moody, *Modulation of the DNA damage response during the life cycle of human papillomaviruses.* Virus research, 2017. **231**: p. 41-49.

96. Howley, P. and D. Lowy, *Papillomaviruses and their replication. In "Virology"(Fields, BN, Knipe, DM, Howley, PM, eds).* 2001, Lippincott-Raven Publishers, Philadelphia.

97. Meyers, C., et al., *Biosynthesis of human papillomavirus from a continuous cell line upon epithelial differentiation.* Science, 1992. **257**(5072): p. 971-973.

98. Zhou, J., et al., *Identification of the nuclear localization signal of human papillomavirus type 16 L1 protein.* Virology, 1991. **185**(2): p. 625-632.

99. Darshan, M.S., et al., *The l2 minor capsid protein of human papillomavirus type 16 interacts with a network of nuclear import receptors.* Journal of virology, 2004. **78**(22): p. 12179-12188.

100. Day, P.M., et al., *The papillomavirus minor capsid protein, L2, induces localization of the major capsid protein, L1, and the viral transcription/replication protein, E2, to PML oncogenic domains.* Journal of virology, 1998. **72**(1): p. 142-150.

101. Heino, P., J. Zhou, and P.F. Lambert, *Interaction of the papillomavirus transcription/replication factor, E2, and the viral capsid protein, L2.* Virology, 2000. **276**(2): p. 304-314.

102. Holmgren, S.C., et al., *The minor capsid protein L2 contributes to two steps in the human papillomavirus type 31 life cycle.* J Virol, 2005. **79**(7): p. 3938-48.

103. Cerqueira, C. and J.T. Schiller, *Papillomavirus assembly: an overview and perspectives.* Virus research, 2017. **231**: p. 103-107.

104. Cerqueira, C., et al., *A Cell-Free Assembly System for Generating Infectious Human Papillomavirus 16 Capsids Implicates a Size Discrimination Mechanism for Preferential Viral Genome Packaging.* J Virol, 2016. **90**(2): p. 1096-107.

105. Buck, C.B., et al., *Efficient intracellular assembly of papillomaviral vectors.* J Virol, 2004. **78**(2): p. 751-7.

106. Kawana, K., et al., *In vitro construction of pseudovirions of human papillomavirus type 16: incorporation of plasmid DNA into reassembled L1/L2 capsids.* Journal of virology, 1998. **72**(12): p. 10298-10300.

107. Conway, M.J., et al., *Tissue-spanning redox gradient-dependent assembly of native human papillomavirus type 16 virions.* Journal of virology, 2009. **83**(20): p. 10515-10526.

108. Matsui, T. and M. Amagai, *Dissecting the formation, structure and barrier function of the stratum corneum.* International Immunology, 2015. **27**(6): p. 269-280.

109. Reinson, T., et al., *Engagement of the ATR-dependent DNA damage response at the human papillomavirus 18 replication centers during the initial amplification.* J Virol, 2013. **87**(2): p. 951-64.

110. Sakakibara, N., R. Mitra, and A.A. McBride, *The papillomavirus E1 helicase activates a cellular DNA damage response in viral replication foci.* J Virol, 2011. **85**(17): p. 8981-95.

111. McKinney, C.C., K.L. Hussmann, and A.A. McBride, *The Role of the DNA Damage Response throughout the Papillomavirus Life Cycle.* Viruses, 2015. **7**(5): p. 2450-69.

112. Fradet-Turcotte, A., et al., *Nuclear export of human papillomavirus type 31 E1 is regulated by Cdk2 phosphorylation and required for viral genome maintenance.* Journal of virology, 2010. **84**(22): p. 11747-11760.

113. Mohr, I.J., et al., *Targeting the E1 replication protein to the papillomavirus origin of replication by complex formation with the E2 transactivator.* Science, 1990. **250**(4988): p. 1694-1699.

114. Sanders, C.M. and A. Stenlund, *Recruitment and loading of the E1 initiator protein: an ATP-dependent process catalysed by a transcription factor.* The EMBO journal, 1998. **17**(23): p. 7044-7055.

115. Spalholz, B.A., et al., *Binding of bovine papillomavirus E1 to the origin is not sufficient for DNA replication.* Virology, 1993. **193**(1): p. 201-212.

116. Li, R. and M.R. Botchan, *Acidic transcription factors alleviate nucleosome-mediated repression of DNA replication of bovine papillomavirus type 1.* Proceedings of the National Academy of Sciences, 1994. **91**(15): p. 7051-7055.

117. Androphy, E.J., D.R. Lowy, and J.T. Schiller, *Bovine papillomavirus E2 trans-activating gene product binds to specific sites in papillomavirus DNA.* Nature, 1987. **325**(6099): p. 70-73.

118. Hawley-Nelson, P., et al., *The specific DNA recognition sequence of the bovine papillomavirus E2 protein is an E2-dependent enhancer.* The EMBO journal, 1988. **7**(2): p. 525-531.

119. Baker, C.C. and P. Howley, *Differential promoter utilization by the bovine papillomavirus in transformed cells and productively infected wart tissues.* The EMBO journal, 1987. **6**(4): p. 1027-1035.

120. Chin, M.T., et al., *Regulation of human papillomavirus type 11 enhancer and E6 promoter by activating and repressing proteins from the E2 open reading frame: functional and biochemical studies.* Journal of virology, 1988. **62**(8): p. 2994-3002.

121. McKinney, C.C., et al., *Brd4 Activates Early Viral Transcription upon Human Papillomavirus 18 Infection of Primary Keratinocytes.* MBio, 2016. **7**(6).

122. Stubenrauch, F., I. Leigh, and H. Pfister, *E2 represses the late gene promoter of human papillomavirus type 8 at high concentrations by interfering with cellular factors.* Journal of virology, 1996. **70**(1): p. 119-126.

123. Dong, G., T.R. Broker, and L.T. Chow, *Human papillomavirus type 11 E2 proteins repress the homologous E6 promoter by interfering with the binding of host transcription factors to adjacent elements.* Journal of Virology, 1994. **68**(2): p. 1115-1127.

124. Fujii, T., et al., *High and low levels of cottontail rabbit papillomavirus E2 protein generate opposite effects on gene expression.* Journal of Biological Chemistry, 2001. **276**(2): p. 867-874.

125. Wu, S.Y., et al., *Brd4 links chromatin targeting to HPV transcriptional silencing.* Genes Dev, 2006. **20**(17): p. 2383-96.

126. Nasseri, M., et al., *A human papilloma virus type 11 transcript encoding an E1^ E4 protein.* Virology, 1987. **159**(2): p. 433-439.

127. Doorbar, J., et al., *Characterization of Events during the Late Stages of HPV16 Infectionin VivoUsing High-Affinity Synthetic Fabs to E4.* Virology, 1997. **238**(1): p. 40-52.

128. Doorbar, J., et al., *Identification of the human papilloma virus-1a E4 gene products.* The EMBO journal, 1986. **5**(2): p. 355-362.

129. Davy, C.E., et al., *Identification of a G2 arrest domain in the E1∧E4 protein of human papillomavirus type 16.* Journal of virology, 2002. **76**(19): p. 9806-9818.

130. Davy, C.E., et al., *Human papillomavirus type 16 E1ʌE4-induced G2 arrest is associated with cytoplasmic retention of active Cdk1/cyclin B1 complexes.* Journal of virology, 2005. **79**(7): p. 3998-4011.

131. Doorbar, J., et al., *Specific interaction between HPV-16 E1–E4 and cytokeratins results in collapse of the epithelial cell intermediate filament network.* Nature, 1991. **352**(6338): p. 824-827.

132. Pim, D., M. Collins, and L. Banks, *Human papillomavirus type 16 E5 gene stimulates the transforming activity of the epidermal growth factor receptor.* Oncogene, 1992. **7**(1): p. 27-32.

133. Straight, S.W., et al., *The E5 oncoprotein of human papillomavirus type 16 transforms fibroblasts and effects the downregulation of the epidermal growth factor receptor in keratinocytes.* Journal of virology, 1993. **67**(8): p. 4521-4532.

134. Ashrafi, G.H., et al., *E5 protein of human papillomavirus type 16 selectively downregulates surface HLA class I.* International journal of cancer, 2005. **113**(2): p. 276-283.

135. Ashrafi, G.H., et al., *E5 protein of human papillomavirus 16 downregulates HLA class I and interacts with the heavy chain via its first hydrophobic domain.* International journal of cancer, 2006. **119**(9): p. 2105-2112.

136. Zhang, B., et al., *The E5 protein of human papillomavirus type 16 perturbs MHC class II antigen maturation in human foreskin keratinocytes treated with interferon-γ.* Virology, 2003. **310**(1): p. 100-108.

137. Goldstein, D.J., et al., *Bovine papillomavirus E5 oncoprotein binds to the 16K component of vacuolar H+-ATPases.* Nature, 1991. **352**(6333): p. 347-349.

138. Faccini, A.M., et al., *The bovine papillomavirus type 4 E8 protein binds to ductin and causes loss of gap junctional intercellular communication in primary fibroblasts.* Journal of virology, 1996. **70**(12): p. 9041-9045.

139. Krawczyk, E., et al., *Koilocytosis: a cooperative interaction between the human papillomavirus E5 and E6 oncoproteins.* The American journal of pathology, 2008. **173**(3): p. 682-688.

140. Chen, J.J., et al., *Identification of an α helical motif sufficient for association with papillomavirus E6.* Journal of Biological Chemistry, 1998. **273**(22): p. 13537-13544.

141. Scheffner, M., et al., *The E6 oncoprotein encoded by human papillomavirus types 16 and 18 promotes the degradation of p53.* Cell, 1990. **63**(6): p. 1129-1136.

142. Huibregtse, J.M., M. Scheffner, and P.M. Howley, *Cloning and expression of the cDNA for E6-AP, a protein that mediates the interaction of the human papillomavirus E6 oncoprotein with p53.* Molecular and cellular biology, 1993. **13**(2): p. 775-784.

143. Park, R.B. and E.J. Androphy, *Genetic Analysis of High-Risk E6 in Episomal Maintenance of Human Papillomavirus Genomes in Primary Human Keratinocytes.* Journal of Virology, 2002. **76**(22): p. 11359-11364.

144. Klingelhutz, A.J., S.A. Foster, and J.K. McDougall, *Telomerase activation by the E6 gene product of human papillomavirus type 16.* Nature, 1996. **380**(6569): p. 79-82.

145. Brimer, N., et al., *Cutaneous papillomavirus E6 oncoproteins associate with MAML1 to repress transactivation and NOTCH signaling.* Oncogene, 2012. **31**(43): p. 4639-4646.

146. Nees, M., et al., *Papillomavirus type 16 oncogenes downregulate expression of interferon-responsive genes and upregulate proliferation-associated and NF-κB-responsive genes in cervical keratinocytes.* Journal of virology, 2001. **75**(9): p. 4283-4296.

147. Ronco, L.V., et al., *Human papillomavirus 16 E6 oncoprotein binds to interferon regulatory factor-3 and inhibits its transcriptional activity.* Genes & development, 1998. **12**(13): p. 2061-2072.

148. Roman, A. and K. Munger, *The papillomavirus E7 proteins.* Virology, 2013. **445**(1-2): p. 138-68.

149. Boyer, S.N., D.E. Wazer, and V. Band, *E7 protein of human papilloma virus-16 induces degradation of retinoblastoma protein through the ubiquitin-proteasome pathway.* Cancer research, 1996. **56**(20): p. 4620-4624.

150. Dyson, N., et al., *The human papilloma virus-16 E7 oncoprotein is able to bind to the retinoblastoma gene product.* Science, 1989. **243**(4893): p. 934-937.

151. McLaughlin-Drubin, M.E., C.P. Crum, and K. Münger, *Human papillomavirus E7 oncoprotein induces KDM6A and KDM6B histone demethylase expression and causes epigenetic reprogramming.* Proceedings of the National Academy of Sciences, 2011. **108**(5): p. 2130-2135.

152. Dreer, M., et al., *Interaction of NCOR/SMRT repressor complexes with papillomavirus E8^ E2C proteins inhibits viral replication.* PLoS pathogens, 2016. **12**(4).

153. Powell, M.L., et al., *NCoR1 mediates papillomavirus E8^ E2C transcriptional repression.* Journal of virology, 2010. **84**(9): p. 4451-4460.

154. Stubenrauch, F., et al., *The E8^ E2C protein, a negative regulator of viral transcription and replication, is required for extrachromosomal maintenance of human papillomavirus type 31 in keratinocytes.* Journal of virology, 2000. **74**(3): p. 1178-1186.

155. Lace, M.J., et al., *The E8∧E2 gene product of human papillomavirus type 16 represses early transcription and replication but is dispensable for viral plasmid persistence in keratinocytes.* Journal of virology, 2008. **82**(21): p. 10841-10853.

156. Bannister, A.J. and T. Kouzarides, *Regulation of chromatin by histone modifications.* Cell research, 2011. **21**(3): p. 381-395.

157. Kornberg, R.D. and J.O. Thomas, *Chromatin structure: oligomers of the histones.* Science, 1974. **184**(4139): p. 865-868.

158. Luger, K., et al., *Crystal structure of the nucleosome core particle at 2.8 Å resolution.* Nature, 1997. **389**(6648): p. 251-260.

159. Davey, C.A., et al., *Solvent mediated interactions in the structure of the nucleosome core particle at 1.9 Å resolution.* Journal of molecular biology, 2002. **319**(5): p. 1097-1113.

160. Mavrich, T.N., et al., *A barrier nucleosome model for statistical positioning of nucleosomes throughout the yeast genome.* Genome research, 2008. **18**(7): p. 1073-1083.

161. Struhl, K. and E. Segal, *Determinants of nucleosome positioning.* Nature structural & molecular biology, 2013. **20**(3): p. 267.

162. Workman, J. and R. Kingston, *Alteration of nucleosome structure as a mechanism of transcriptional regulation.* 1998, Annual Reviews 4139 El Camino Way, PO Box 10139, Palo Alto, CA 94303-0139, USA.

163. Kouzarides, T., *Chromatin modifications and their function.* Cell, 2007. **128**(4): p. 693-705.

164. Lawrence, M., S. Daujat, and R. Schneider, *Lateral Thinking: How Histone Modifications Regulate Gene Expression.* Trends Genet, 2016. **32**(1): p. 42-56.

165. Shogren-Knaak, M., et al., *Histone H4-K16 acetylation controls chromatin structure and protein interactions.* Science, 2006. **311**(5762): p. 844-847.

166. Akhtar, A. and P.B. Becker, *Activation of transcription through histone H4 acetylation by MOF, an acetyltransferase essential for dosage compensation in Drosophila.* Molecular cell, 2000. **5**(2): p. 367-375.

167. Marmorstein, R. and M.-M. Zhou, *Writers and readers of histone acetylation: structure, mechanism, and inhibition.* Cold Spring Harbor perspectives in biology, 2014. **6**(7): p. a018762.

168. Li, B., M. Carey, and J.L. Workman, *The role of chromatin during transcription.* Cell, 2007. **128**(4): p. 707-719.

169. Yi, X., et al., *Histone methyltransferases: novel targets for tumor and developmental defects.* American journal of translational research, 2015. **7**(11): p. 2159.

170. Knipe, D.M., et al., *Snapshots: chromatin control of viral infection.* Virology, 2013. **435**(1): p. 141-56.

171. Balakrishnan, L. and B. Milavetz, *Epigenetic regulation of viral biological processes.* Viruses, 2017. **9**(11): p. 346.

172. Durzynska, J., K. Lesniewicz, and E. Poreba, *Human papillomaviruses in epigenetic regulations.* Mutation Research/Reviews in Mutation Research, 2017. **772**: p. 36-50.

173. del Mar Peña, L. and L.A. Laimins, *Differentiation-dependent chromatin rearrangement coincides with activation of human papillomavirus type 31 late gene expression.* Journal of virology, 2001. **75**(20): p. 10005-10013.

174. Wooldridge, T.R. and L.A. Laimins, *Regulation of human papillomavirus type 31 gene expression during the differentiation-dependent life cycle through histone modifications and transcription factor binding.* Virology, 2008. **374**(2): p. 371-380.

175. Griffin, L.M., et al., *Human keratinocyte cultures in the investigation of early steps of human papillomavirus infection.* Methods Mol Biol, 2014. **1195**: p. 219-38.

176. Patel, D., et al., *The E6 protein of human papillomavirus type 16 binds to and inhibits co-activation by CBP and p300.* The EMBO journal, 1999. **18**(18): p. 5061-5072.

193

177. Bernat, A., et al., *Interaction between the HPV E7 oncoprotein and the transcriptional coactivator p300.* Oncogene, 2003. **22**(39): p. 7871.

178. Ogryzko, V.V., et al., *The transcriptional coactivators p300 and CBP are histone acetyltransferases.* Cell, 1996. **87**(5): p. 953-959.

179. Goodman, R.H. and S. Smolik, *CBP/p300 in cell growth, transformation, and development.* Genes & development, 2000. **14**(13): p. 1553-1577.

180. Kwok, R.P., et al., *Nuclear protein CBP is a coactivator for the transcription factor CREB.* Nature, 1994. **370**(6486): p. 223-226.

181. Krüppel, U., et al., *E2 and the co-activator p300 can cooperate in activation of the human papillomavirus type 16 early promoter.* Virology, 2008. **377**(1): p. 151-159.

182. Valencia-Hernandez, A., C. Cuevas-Bennett, and E. Garrido, *Transcriptional regulation of human papillomavirus type 18 P105 promoter by the co-activator CBP.* Intervirology, 2007. **50**(6): p. 418-425.

183. Bouallaga, I., et al., *HMG-I (Y) and the CBP/p300 coactivator are essential for human papillomavirus type 18 enhanceosome transcriptional activity.* Molecular and cellular biology, 2003. **23**(7): p. 2329-2340.

184. Smith, J.A., et al., *SMCX and components of the TIP60 complex contribute to E2 regulation of the HPV E6/E7 promoter.* Virology, 2014. **468**: p. 311-321.

185. Smith, J.A., et al., *Genome-wide siRNA screen identifies SMCX, EP400, and Brd4 as E2-dependent regulators of human papillomavirus oncogene expression.* Proc Natl Acad Sci U S A, 2010. **107**(8): p. 3752-7.

186. Jha, S., et al., *Destabilization of TIP60 by human papillomavirus E6 results in attenuation of TIP60-dependent transcriptional regulation and apoptotic pathway.* Molecular cell, 2010. **38**(5): p. 700-711.

187. Hong, S., A. Dutta, and L.A. Laimins, *The acetyltransferase Tip60 is a critical regulator of the differentiation-dependent amplification of human papillomaviruses.* Journal of virology, 2015. **89**(8): p. 4668-4675.

188. Zhang, B., et al., *Human papillomavirus type 16 E7 protein increases acetylation of histone H3 in human foreskin keratinocytes.* Virology, 2004. **329**(1): p. 189-198.

189. Ammermann, I., et al., *Inhibition of transcription and DNA replication by the papillomavirus E8-E2C protein is mediated by interaction with corepressor molecules.* J.Virol., 2008. **82**(11): p. 5127-5136.

190. Longworth, M.S., R. Wilson, and L.A. Laimins, *HPV31 E7 facilitates replication by activating E2F2 transcription through its interaction with HDACs.* The EMBO journal, 2005. **24**(10): p. 1821-1830.

191. Longworth, M.S. and L.A. Laimins, *The binding of histone deacetylases and the integrity of zinc finger-like motifs of the E7 protein are essential for the life cycle of human papillomavirus type 31.* Journal of virology, 2004. **78**(7): p. 3533-3541.

192. Gillespie, K.A., et al., *Human papillomaviruses recruit cellular DNA repair and homologous recombination factors to viral replication centers.* Journal of virology, 2012. **86**(17): p. 9520-9526.

193. Gautam, D. and C.A. Moody, *Impact of the DNA Damage Response on Human Papillomavirus Chromatin.* PLoS Pathog, 2016. **12**(6): p. e1005613.

194. Pentland, I., et al., *Disruption of CTCF-YY1–dependent looping of the human papillomavirus genome activates differentiation-induced viral oncogene transcription.* PLoS biology, 2018. **16**(10): p. e2005752.

195. Holland, D., et al., *Activation of the enhancer of zeste homologue 2 gene by the human papillomavirus E7 oncoprotein.* Cancer research, 2008. **68**(23): p. 9964-9972.

196. Hyland, P.L., et al., *Evidence for alteration of EZH2, BMI1, and KDM6A and epigenetic reprogramming in human papillomavirus type 16 E6/E7-expressing keratinocytes.* Journal of virology, 2011. **85**(21): p. 10999-11006.

197. Soto, D.R., et al., *KDM6A addiction of cervical carcinoma cell lines is triggered by E7 and mediated by p21CIP1 suppression of replication stress.* PLOS Pathogens, 2017. **13**(10): p. e1006661.

198. Gautam, D., et al., *SETD2-dependent H3K36me3 plays a critical role in epigenetic regulation of the HPV31 life cycle.* PLoS pathogens, 2018. **14**(10): p. e1007367.

199. Hsu, C.-H., et al., *The HPV E6 oncoprotein targets histone methyltransferases for modulating specific gene transcription.* Oncogene, 2012. **31**(18): p. 2335-2349.

200. Orav, M., et al., *Recombination-dependent oligomerization of human papillomavirus genomes upon transient DNA replication.* J Virol, 2013. **87**(22): p. 12051-68.

201. Cole, S. and O. Danos, *Nucleotide sequence and comparative analysis of the human papillomavirus type 18 genome: phylogeny of papillomaviruses and repeated structure of the E6 and E7 gene products.* Journal of molecular biology, 1987. **193**(4): p. 599-608.

202. Romanczuk, H. and P.M. Howley, *Disruption of Either the E1-Regulatory or the E2-Regulatory Gene of Human Papillomavirus Type-16 Increases Viral Immortalization Capacity.* Proceedings of the National Academy of Sciences of the United States of America, 1992. **89**(7): p. 3159-3163.

203. McKinney, C., et al., *Brd4 activates early viral transcription upon HPV18 infection of primary keratinocytes.* mBio, 2016. **in press**.

204. Van Doorslaer, K., et al., *Novel recombinant papillomavirus genomes expressing selectable genes.* Scientific Reports, 2016. **6**(37782): p. 37782.

205. Roberts, J.N., et al., *Genital transmission of HPV in a mouse model is potentiated by nonoxynol-9 and inhibited by carrageenan.* Nature Medicine, 2007. **13**(7): p. 857-861.

206. Sarver, N., J.C. Byrne, and P.M. Howley, *Transformation and replication in mouse cells of a bovine papillomavirus--pML2 plasmid vector that can be rescued in bacteria.* Proceedings of the National Academy of Sciences, 1982. **79**(23): p. 7147-7151.

207. Porter, S.S. and A.A. McBride, *Human Papillomavirus Quasivirus Production and Infection of Primary Human Keratinocytes.* Current Protocols in Microbiology, 2020. **57**(1): p. e101.

208. Pastrana, D.V., et al., *Metagenomic discovery of 83 new human papillomavirus types in patients with immunodeficiency.* mSphere, 2018. **3**(6): p. e00645-18.

209. Yuan, Z.-F., et al., *EpiProfile 2.0: a computational platform for processing epi-proteomics mass spectrometry data.* Journal of proteome research, 2018. **17**(7): p. 2533-2541.

210. Dunne, E.F., et al., *Human papilloma virions in the laboratory.* Journal of clinical virology, 2014. **61**(2): p. 196-198.

211. Favre, M., *Structural polypeptides of rabbit, bovine, and human papillomaviruses.* Journal of virology, 1975. **15**(5): p. 1239-1247.

212. Orth, G., M. Favre, and O. Croissant, *Characterization of a new type of human papillomavirus that causes skin warts.* Journal of virology, 1977. **24**(1): p. 108-120.

213. Kirnbauer, R., et al., *Efficient self-assembly of human papillomavirus type 16 L1 and L1-L2 into virus-like particles.* Journal of virology, 1993. **67**(12): p. 6929-6936.

214. Rose, R., et al., *Expression of human papillomavirus type 11 L1 protein in insect cells: in vivo and in vitro assembly of viruslike particles.* Journal of virology, 1993. **67**(4): p. 1936-1944.

215. Cook, J.C., et al., *Purification of virus-like particles of recombinant human papillomavirus type 11 major capsid protein L1 from Saccharomyces cerevisiae.* Protein expression and purification, 1999. **17**(3): p. 477-484.

216. Kirnbauer, R., et al., *Papillomavirus L1 major capsid protein self-assembles into virus-like particles that are highly immunogenic.* Proceedings of the National Academy of Sciences, 1992. **89**(24): p. 12180-12184.

217. Suzich, J.A., et al., *Systemic immunization with papillomavirus L1 protein completely prevents the development of viral mucosal papillomas.* Proceedings of the National Academy of Sciences, 1995. **92**(25): p. 11553-11557.

218. Ozbun, M.A., *Infectious human papillomavirus type 31b: purification and infection of an immortalized human keratinocyte cell line.* Journal of general virology, 2002. **83**(11): p. 2753-2763.

219. Ozbun, M.A. and N.A. Patterson, *Using organotypic (raft) epithelial tissue cultures for the biosynthesis and isolation of infectious human papillomaviruses.* Current protocols in microbiology, 2014. **34**(1): p. 14B. 3.1-14B. 3.18.

220. Buck, C.B., et al., *Maturation of papillomavirus capsids.* J Virol, 2005. **79**(5): p. 2839-46.

221. Buck, C.B. and C.D. Thompson, *Production of papillomavirus-based gene transfer vectors.* Curr Protoc Cell Biol, 2007. **Chapter 26**: p. Unit 26 1.

222. Pyeon, D., P.F. Lambert, and P. Ahlquist, *Production of infectious human papillomavirus independently of viral replication and epithelial cell differentiation.* Proc Natl Acad Sci U S A, 2005. **102**(26): p. 9311-6.

223. Culp, T.D., et al., *Papillomavirus particles assembled in 293TT cells are infectious in vivo.* Journal of virology, 2006. **80**(22): p. 11381-11384.

224. Lace, M.J., et al., *Human papillomavirus (HPV) type 18 induces extended growth in primary human cervical, tonsillar, or foreskin keratinocytes more effectively than other high-risk mucosal HPVs.* J Virol, 2009. **83**(22): p. 11784-94.

225. Romanczuk, H., et al., *The Viral Transcriptional Regulatory Region Upstream of the E6 and E7 Genes Is a Major Determinant of the Differential Immortalization Activities of Human Papillomavirus Type-16 and Type-18.* Journal of Virology, 1991. **65**(5): p. 2739-2744.

226. Kay, M.A., C.-Y. He, and Z.-Y. Chen, *A robust system for production of minicircle DNA vectors.* Nature biotechnology, 2010. **28**(12): p. 1287.

227. Worcel, A., S. Han, and M. Wong, *Assembly of newly replicated chromatin.* Cell, 1978. **15**(3): p. 969-977.

228. Senshu, T., M. Fukuda, and M. Ohashi, *Preferential association of newly synthesized H3 and H4 histones with newly replicated DNA.* The Journal of Biochemistry, 1978. **84**(4): p. 985-988.

229. Crémisi, C., A. Chestier, and M. Yaniv, *Preferential association of newly synthesized histones with replicating SV40 DNA.* Cell, 1977. **12**(4): p. 947-951.

230. Hodges, B.L., et al., *Long-term transgene expression from plasmid DNA gene therapy vectors is negatively affected by CpG dinucleotides.* Molecular Therapy, 2004. **10**(2): p. 269-278.

231. Hyde, S.C., et al., *CpG-free plasmids confer reduced inflammation and sustained pulmonary gene expression.* Nature biotechnology, 2008. **26**(5): p. 549-551.

232. Cereghini, S. and M. Yaniv, *Assembly of transfected DNA into chromatin: structural changes in the origin-promoter-enhancer region upon replication.* The EMBO journal, 1984. **3**(6): p. 1243-1253.

233. Jiang, C. and B.F. Pugh, *Nucleosome positioning and gene regulation: advances through genomics.* Nature Reviews Genetics, 2009. **10**(3): p. 161-172.

234. Knipe, D.M., et al., *Snapshots: chromatin control of viral infection.* Virology, 2013. **435**(1): p. 141-156.

235. Burley, M., S. Roberts, and J.L. Parish. *Epigenetic regulation of human papillomavirus transcription in the productive virus life cycle.* in *Seminars in Immunopathology.* 2020. Springer.

236. Jang, M.K., D. Kwon, and A.A. McBride, *Papillomavirus E2 proteins and the host BRD4 protein associate with transcriptionally active cellular chromatin.* J Virol, 2009. **83**(6): p. 2592-600.

237. Favre, M., et al., *Chromatin-like structures obtained after alkaline disruption of bovine and human papillomaviruses.* J.Virol., 1977. **21**: p. 1205-1209.

238. Johnson, J.S., et al., *Adenovirus protein VII condenses DNA, represses transcription, and associates with transcriptional activator E1A.* Journal of virology, 2004. **78**(12): p. 6459-6468.

239. Pignatti, P. and E. Cassai, *Analysis of herpes simplex virus nucleoprotein complexes extracted from infected cells.* Journal of Virology, 1980. **36**(3): p. 816-828.

240. Deshmane, S.L. and N.W. Fraser, *During latency, herpes simplex virus type 1 DNA is associated with nucleosomes in a chromatin structure.* Journal of virology, 1989. **63**(2): p. 943-947.

241. Nevels, M., A. Nitzsche, and C. Paulus, *How to control an infectious bead string: nucleosome-based regulation and targeting of herpesvirus chromatin.* Reviews in Medical Virology, 2011. **21**(3).

242. Nitzsche, A., C. Paulus, and M. Nevels, *Temporal Dynamics of Cytomegalovirus Chromatin Assembly in Productively Infected Human Cells.* Journal of Virology, 2008. **82**(22): p. 11167-11180.

243. Cliffe, A.R. and D.M. Knipe, *Herpes Simplex Virus ICP0 Promotes both Histone Removal and Acetylation on Viral DNA during Lytic Infection.* Journal of Virology, 2008. **82**(24): p. 12030-12038.

244. Beisel, C. and R. Paro, *Silencing chromatin: comparing modes and mechanisms.* Nature Reviews Genetics, 2011. **12**(2): p. 123-135.

245. Sakakibara, N., et al., *Brd4 is displaced from HPV replication factories as they expand and amplify viral DNA.* PLoS Pathog, 2013. **9**(11): p. e1003777.

246. Müller, A., A. Ritzkowsky, and G. Steger, *Cooperative activation of human papillomavirus type 8 gene expression by the E2 protein and the cellular coactivator p300.* Journal of virology, 2002. **76**(21): p. 11042-11053.

247. Brehm, A., et al., *The E7 oncoprotein associates with Mi2 and histone deacetylase activity to promote cell growth.* The EMBO journal, 1999. **18**(9): p. 2449-2458.

248. Groves, I.J., et al., *HPV16 oncogene expression levels during early cervical carcinogenesis are determined by the balance of epigenetic chromatin modifications at the integrated virus genome.* Oncogene, 2016. **35**(36): p. 4773-86.

249. Dey, A., et al., *The double bromodomain protein Brd4 binds to acetylated chromatin during interphase and mitosis.* Proceedings of the National Academy of Sciences, 2003. **100**(15): p. 8758-8763.

250. Moody, C.A. and L.A. Laimins, *Human papillomaviruses activate the ATM DNA damage pathway for viral genome amplification upon differentiation.* PLoS Pathog, 2009. **5**(10): p. e1000605.

251. Tamburini, B.A. and J.K. Tyler, *Localized histone acetylation and deacetylation triggered by the homologous recombination pathway of double-strand DNA repair.* Mol Cell Biol, 2005. **25**(12): p. 4903-13.

252. Murr, R., et al., *Histone acetylation by Trrap–Tip60 modulates loading of repair proteins and repair of DNA double-strand breaks.* Nature cell biology, 2006. **8**(1): p. 91-99.

253. Zierhut, C., et al., *The cytoplasmic DNA sensor cGAS promotes mitotic cell death.* Cell, 2019. **178**(2): p. 302-315. e23.

254. Saffert, R.T. and R.F. Kalejta, *Inactivating a cellular intrinsic immune defense mediated by Daxx is the mechanism through which the human cytomegalovirus pp71 protein stimulates viral immediate-early gene expression.* J Virol, 2006. **80**(8): p. 3863-71.

255. Shechter, D., et al., *Extraction, purification and analysis of histones.* Nature protocols, 2007. **2**(6): p. 1445-1457.

256. Dey, A., et al., *The double bromodomain protein Brd4 binds to acetylated chromatin during interphase and mitosis.* Proc Natl Acad Sci U S A, 2003. **100**(15): p. 8758-63.

257. Xue, Y., et al., *The ATRX syndrome protein forms a chromatin-remodeling complex with Daxx and localizes in promyelocytic leukemia nuclear bodies.* Proceedings of the National Academy of Sciences, 2003. **100**(19): p. 10635-10640.

258. Stepp, W.H., et al., *Sp100 colocalizes with HPV replication foci and restricts the productive stage of the infectious cycle.* PLoS pathogens, 2017. **13**(10): p. e1006660.

259. Lange, M., et al., *Regulation of muscle development by DPF3, a novel histone acetylation and methylation reader of the BAF chromatin remodeling complex.* Genes & development, 2008. **22**(17): p. 2370-2384.

260. Seeler, J.S., et al., *Common properties of nuclear body protein SP100 and TIF1alpha chromatin factor: role of SUMO modification.* Mol Cell Biol, 2001. **21**(10): p. 3314-24.

261. Zeng, L., et al., *Mechanism and regulation of acetylated histone binding by the tandem PHD finger of DPF3b.* Nature, 2010. **466**(7303): p. 258-262.

262. Gray, E., et al., *In vitro progression of human papillomavirus 16 episome-associated cervical neoplasia displays fundamental similarities to integrant-associated carcinogenesis.* Cancer research, 2010. **70**(10): p. 4081-4091.

263. Banerjee, N.S., et al., *Vorinostat, a pan-HDAC inhibitor, abrogates productive HPV-18 DNA amplification.* Proceedings of the National Academy of Sciences, 2018. **115**(47): p. E11138-E11147.

264. Shapira, L., et al., *Histone deacetylase inhibitors reduce the number of herpes simplex virus-1 genomes initiating expression in individual cells.* Frontiers in microbiology, 2016. **7**: p. 1970.

265. Nehme, Z., S. Pasquereau, and G. Herbein, *Control of viral infections by epigenetic-targeted therapy.* Clinical epigenetics, 2019. **11**(1): p. 55.

266. Hilton, I.B., et al., *Epigenome editing by a CRISPR-Cas9-based acetyltransferase activates genes from promoters and enhancers.* Nature biotechnology, 2015. **33**(5): p. 510-517.

267. Kumar, M.A., et al., *Nucleosome positioning in the regulatory region of SV40 chromatin correlates with the activation and repression of early and late transcription during infection.* Virology, 2017. **503**: p. 62-69.

268. Stünkel, W. and H.-U. Bernard, *The chromatin structure of the long control region of human papillomavirus type 16 represses viral oncoprotein expression.* Journal of virology, 1999. **73**(3): p. 1918-1930.

269. Swindle, C.S. and J.A. Engler, *Association of the human papillomavirus type 11 E1 protein with histone H1.* Journal of virology, 1998. **72**(3): p. 1994-2001.

270. Lefebvre, O., G. Steger, and M. Yaniv, *Synergistic transcriptional-activation by the papillomavirus E2 protein occurs after DNA binding and correlates with a change in chromatin structure.* Journal of molecular biology, 1997. **266**(3): p. 465-478.

271. Schaffhausen, B.S. and T.L. Benjamin, *Deficiency in histone acetylation in nontransforming host range mutants of polyoma virus.* Proceedings of the National Academy of Sciences, 1976. **73**(4).

272.   Fang, C.-Y., et al., *Global profiling of histone modifications in the polyomavirus BK virion minichromosome.* Virology, 2015. **483**(Chromosoma 105 1997).

273.   Goldberg, A.D., et al., *Distinct factors control histone variant H3. 3 localization at specific genomic regions.* Cell, 2010. **140**(5): p. 678-691.

274.   Ahmad, K. and S. Henikoff, *The histone variant H3. 3 marks active chromatin by replication-independent nucleosome assembly.* Molecular cell, 2002. **9**(6): p. 1191-1200.

275.   Lewis, P.W., et al., *Daxx is an H3.3-specific histone chaperone and cooperates with ATRX in replication-independent chromatin assembly at telomeres.* Proc Natl Acad Sci U S A, 2010. **107**(32): p. 14075-80.

276.   Kivipold, P., et al., *DAXX modulates human papillomavirus early gene expression and genome replication in U2OS cells.* Virol J, 2015. **12**: p. 104.

277.   Wise-Draper, T.M., et al., *The human DEK proto-oncogene is a senescence inhibitor and an upregulated target of high-risk human papillomavirus E7.* Journal of virology, 2005. **79**(22): p. 14309-14317.

278.   Adams, A.K., et al., *DEK promotes HPV-positive and-negative head and neck cancer cell proliferation.* Oncogene, 2015. **34**(7): p. 868-877.

279.   Ivanauskiene, K., et al., *The PML-associated protein DEK regulates the balance of H3.3 loading on chromatin and is important for telomere integrity.* Genome Research, 2014. **24**(10).

280.   Organization, W.H. *Human papillomavirus (HPV) and cervical cancer*. 2019 [cited 2020 June 7]; Available from: https://www.who.int/en/news-room/fact-sheets/detail/human-papillomavirus-(hpv)-and-cervical-cancer.